PREDICTION OF SLIPPING ACCIDENTS USING BIOMECHANICAL AND TRACTION ANALYSIS OF FOOTWEAR OUTSOLE DESIGN

by

Arian Iraqi

B.S. in Mechanical Engineering (Honors), Multimedia University, Melaka, Malaysia, 2011

M.S. in Mechanical Engineering, Blekinge Institute of Technology, Karlskrona, Sweden, 2014

Submitted to the Graduate Faculty of

Swanson School of Engineering in partial fulfillment

of the requirements for the degree of

Doctor of Philosophy

University of Pittsburgh

2018

UNIVERSITY OF PITTSBURGH

SWANSON SCHOOL OF ENGINEERING

This dissertation was presented

by

Arian Iraqi

It was defended on

November 27, 2018

and approved by

Mark S. Redfern, Ph.D., Professor, Department of Bioengineering

Rakié Cham, Ph.D., Associate Professor, Department of Bioengineering

Natasa S. Vidic, Ph.D., Assistant Professor, Department of Industrial Engineering

Dissertation Director: Kurt E. Beschorner, Ph.D., Associate Professor, Department of Bioengineering

PREDICTION OF SLIPPING ACCIDENTS USING BIOMECHANICAL AND TRACTION ANALYSIS OF FOOTWEAR OUTSOLE DESIGN

Arian Iraqi, Ph.D.

University of Pittsburgh, 2018

Slip-initiated falls due to insufficient traction are a major contributor to occupational injuries. Footwear interventions have a significant potential to mitigate slipping accidents. Unfortunately, performance of the footwear used in these interventions is variable and there is a paucity of empirical evidence supporting the validity of current methods for assessing footwear traction. Furthermore, footwear traction testing methods are expensive and require expertise, which may limit their use. These limitations may guide footwear designers toward suboptimal footwear and create barriers for safety managers to assess and identify appropriate footwear. The goal of this dissertation was to (1) guide the development of valid traction testing methods and (2) create tread assessment methods that are inexpensive and require minimal expertise. The ability of footwear traction tests under different biomechanical parameters (normal force, shoe-floor angle, and sliding speed) to predict slip outcomes were assessed based on human exposures to slippery surfaces. The combination of 250 N normal force and 17° shoe-floor angle best predicted slip risk during gait experiments. Biomechanical analysis of various shoes during human slipping events were performed to guide shoe traction measurements for additional improvements. The findings revealed that the normal force (26.7 %BW, 179 N), shoe-floor angle (22.1°) and contact time (0.02

s) at slip initiation were significantly different from current footwear traction testing standard methods (400 and 500 N, 7º, 0.10-0.30 s). Thus, current methods may need to utilize lower normal forces, larger shoe-floor angles and shorter contact duration to further improve slip risk prediction by mimicking the shoe dynamics at slip initiation. A tread assessment model was developed to predict footwear traction based on outsole design features. The statistical model predicted 88% of variation in traction using contact area, heel shape, shape factor and material hardness while controlling for the floor surface in the presence of canola oil. Safety practitioners can use this information to select shoes with high slip-resistant performance in cases where footwear traction testing apparatuses are not readily available. The findings from this dissertation may reduce slipping accidents by improving the quality and accessibility of shoe traction assessment methods.

TABLE OF CONTENTS

LIST OF TABLES

LIST OF FIGURES

PREFACE

I would like to express my gratitude to the people who supported my career aspirations. I would like to thank my committee members, Rakié Cham, Natasa Vidic, Mark Redfern, and Kurt Beschorner, for their scholarly contribution to this dissertation. Their knowledgeable insight, experience and enthusiasm improved my research experience and the quality of my education. I would like to thank my advisor, Kurt Beschorner, for his patience and optimism in my work as a graduate student. I would like to thank my current and former colleagues at the Human Movement and Balance Laboratory for their help and collaborative spirit, as well as for creating a wonderful work atmosphere. I have always been blessed with an amazing family and friends. I am grateful for my wonderful parents, Nahid and Shakir, who provided me with the best education and are always present. I would like to express my appreciation for my older siblings, Ali and Nastaran, who supported me and strongly believed in my abilities to pursue higher education. I would like to express my gratitude to my twin brother, Armin, who always bolsters my confidence and provides positive input on many of my life decisions. I would especially like to thank my wife, Kristen, who constantly makes me happy and gave me the motivation to accomplish this degree. Finally, I would like to thank all of my friends and family in the U.S. and abroad who helped me in both my personal life and education.

NOMENCLATURE

For section 2.3.1

P_i : Highest peak in each cut-off length

R_a : Arithmetic average

R_q : Root means square

R_{tm} : Average peak to valley height

R_z : Average peak to valley height

V_i : Lowest valley in each cut-off length

z_i : Discretized height value

For section 2.3.2

COF : Coefficient of friction

F_{Normal} : Normal applied load

F_{Shear} : Shear force

h : Fluid film thickness

h_{min} : Minimum fluid film thickness

p : Fluid pressure

R : Effective radius

R_q : Root means square

$R_{q,a}$: Root means square of surface ‘a’

$R_{q,b}$: Root means square of surface ‘b’

$\tilde{u}$: Mean surface velocity in x-direction

v : Speed of the interacting surfaces

v_{Lower} : Velocity of the lower surface

η : Liquid viscosity

η_0 : Absolute viscosity at p = 0 and constant temperature

Λ : Dimensionless film parameter

ρ : Density of the lubricant

For section 2.3.3

$F_{Adhesion}$: Adhesion friction

$F_{Friction}$: Friction force

$F_{Hysteresis}$: Hysteresis friction

For section 2.5

$F_{Horizontal}$: Horizontal force

$F_{Longitudinal\ shear}$: Longitudinal shear force

F_{Normal} : Normal force

$F_{Vertical}$: Vertical force

$V_{Horizontal}$: Horizontal sliding speed

θ : Shoe-floor angle

For section 2.7

ACOF : Available coefficient of friction

ACOF-RCOF: Available coefficient of friction minus required coefficient of friction

RCOF : Required coefficient of friction

Slip_Risk : Probability of slip

β_0 : Regression coefficient of the intercept term

β_1 : Regression coefficient of the first or only predictor

For section 3.3.5

ACOF : Available coefficient of friction

$F_{Longitudinal\ shear}$: Longitudinal shear force

F_{Normal} : Normal force

$F_{Transverse\ shear}$: Transverse shear force

Slip_Risk : Probability of slip

β_0 : Regression coefficient of the intercept term

β_1 : Regression coefficient of the first or only predictor

For section 5.3.3

S : Shape factor

1.0 INTRODUCTION

Slip-initiated falls are a significant contributor of occupational injuries. Prevention of falls due to slippery conditions is achievable through the use of footwear interventions. Footwear interventions reduce slip-related injuries primarily by increasing the traction between the shoe outsole and floor surface in the presence of liquid contamination. Shoe-floor-contaminant traction is affected by the testing methods (especially the dynamics of the tribosystem), and the properties of the outsole, floor and lubricant. Shoe traction is generally evaluated using mechanical friction measurement devices that can be operated under different biomechanical testing conditions. A lack of consensus exists in the test methods used to evaluate shoe traction. Using inappropriate test methods may lead to inaccurate inference on the slip-performance of footwear. Thus, poor test methods may guide footwear designers toward suboptimal footwear. Comparing test methods to human-centered outcome (i.e., occurrence of slipping) may guide the prediction of human slips. Furthermore, biomechanical assessment of human slips could guide traction testing methods that mimic shoe dynamics during slipping. Another concern regarding footwear traction measurement methods is the required expense of experimental apparatuses which may inhibit certain stakeholders (e.g., occupational health and safety managers) to utilize this technology. A cost-effective assessment tool that is simple and accurate to predict shoe traction could increase assessment among these stakeholders. Thus, there is potential to improve methods that design out slipping hazards and improve occupational safety.

The long-term goal of this dissertation is to reduce slip-initiated fall accidents due to liquid contamination by improving traction testing methods and creating accessible (based on cost and expertise) tread assessments as an alternative to these methods. First, the current state of biomechanical parameters utilized for footwear traction testing will be assessed using human gait experiments. Second, shoe dynamics during human slipping events will be quantified to further improve traction testing methods. Third, an alternative tread assessment method will be developed to predict footwear traction for safety practitioners that have no or limited access to footwear traction testing methods. The rationale of this dissertation is that new developments in assessment methods will enable better tread design and increase the use of shoe traction assessments.

1.1 SPECIFIC AIMS

1.1.1 Specific Aim 1

Identify the set of biomechanical parameters that best predict human slipping incidents.

1.1.2 Specific Aim 2

Quantify the kinetics and kinematics of footwear during human slipping.

1.1.3 Specific Aim 3

Develop a statistical model to predict footwear traction based on outsole tread design features.

1.2 SUMMARY OF CHAPTERS

This dissertation includes 6 chapters. Chapter 1 summarizes the specific aims of the dissertation. Chapter 2 provides background on epidemiology of slip-related injuries, biomechanics of gait, tribology theory relevant to slipping, methods for shoe traction testing, and predictive modelling applied to slips and falls. Chapter 3 is a study that evaluates the ability of shoe traction tests operated under different biomechanical testing parameters to predict slip outcomes. Chapter 4 is the quantification of kinematics and kinetics of footwear during human slips to guide shoe traction measurement. Chapter 5 is a development of a cost-effective and simple statistical model to predict shoe traction based on its outsole design. Chapter 6 summarizes the findings from Chapter 3-5 and their potential implications for the improvement of shoe traction measurement methods and the prevention of slips.

2.0 BACKGROUND

2.1 EPIDEMIOLOGY OF SLIP AND FALL INJUIRES

Falls on the same level have been ranked consistently among the top two disabling occupational injuries in the U.S. from 1998 to 2010 (Marucci-Wellman et al., 2015). Falls on the same level have followed an increasing trend recently. For instance, fatal falls on the same level have increased from 111 cases in 2011 to 134 cases in 2016, which is about 20.7 % increase (U.S. Department of Labor- Bureau of Labor Statistics, 2017) (Figure 2-1). Costs due to occupational falls on the same level in the United States have also grown from $4.2 billion in 1998 to $8.6 billion in 2010 (about $6.0 billion in 1998 dollars) (Marucci-Wellman et al., 2015). Falls on the same level commonly cause injuries to the lower extremities, upper extremities, trunk and head (Yeoh et al., 2013). A variety of industries are affected by falls on the same level including accommodation and food services, construction, agriculture, healthcare, manufacturing, mining, transportation and ware housing (Yeoh et al., 2013).

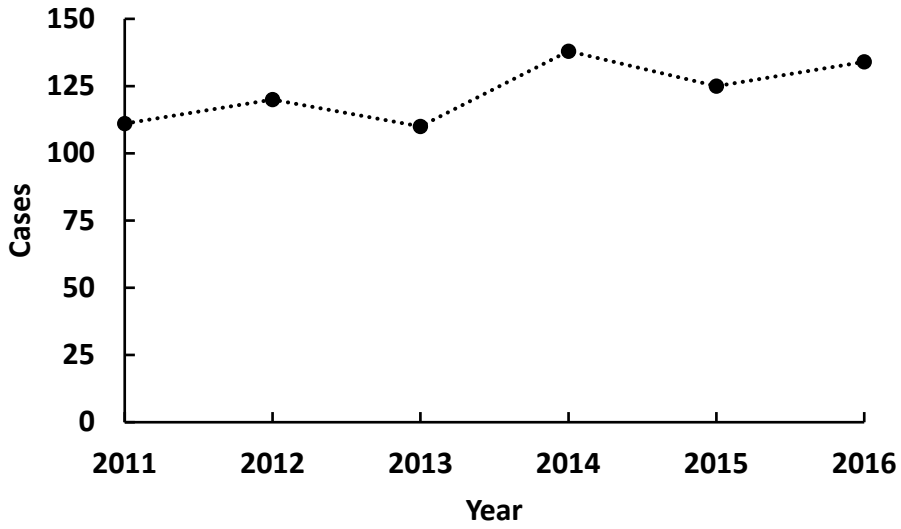

Figure 2-1. Fatal occupational injuries due to falls on same level [Data was taken from U.S. Department of Labor- Bureau of Labor Statistics (2017)]

Falls on the same level are often due to slipperiness or slippery conditions. Across 10 years of surveillance, liquid contamination was identified as the leading cause (23.6%) of slips, trips, and falls in hospital environments (Bell et al., 2008). Heijnen and Rietdyk (2016) indicated in a survey among young adults that about 48% falling accidents are caused by slips. Courtney et al. (2001) also reported that slips contributed to 40-50% of occupational fall injuries.

Slips, trips, and falls prevention programs have shown to be effective to reduce fall-related injuries. Bell et al. (2008) demonstrated that comprehensive fall prevention programs reduced the slips, trips and falls compensation claim rate by 58% from pre-intervention to post-intervention. These programs included (1) change of flooring, (2) use of slip-resistant footwear, (3) floor cleaning and drying procedures, (4) preventing entry to areas that are contaminated, and (5) ice

and snow removal. Verma et al. (2011) found that the use of footwear that are labeled as slip-resistant were associated with decreased rate of slipping accidents. Shoes that are labeled as slip-resistant generally have higher traction compared to shoes with no slip-resistant label (Beschorner et al., 2017). This reduction in slipping accidents may be explained due to an increase in the traction between shoe and floor in the presence of surface contaminants (Burnfield & Powers, 2006; Siegmund et al., 2006). Thus, footwear can be a promising form of personal protective equipment to be used as an intervention.

2.2 BIOMECHANICS OF GAIT

Fundamental knowledge on gait patterns is needed to identify the causes of slips from a human-centered perspective. The underfoot ground reaction forces (GRF) and foot kinematics during the stance phase of gait cycle are critical biomechanical factors relevant to slips. Biomechanical analyses may provide insight on gait strategies that lessen slip risk and provide supplemental information that guides traction measurement.

The stance phase is crucial to maintaining balance since it is the phase that supports the body weight (Figure 2-2). The stance phase begins with heel strike and ends with toe-off. After heel strike, weight acceptance occurs, followed by mid-stance, and push-off. The weight acceptance is between heel strike and maximum knee flexion of the support limb (Winter, 1987). Push-off occurs when the lower limb generates a force against the ground to accelerate the body forward and ankle plantar flexion happens (Winter, 1987). Mid-stance is the duration between the weight acceptance and push-off (Winter, 1987). Slipping can negatively affect the body's ability to support weight or propel the body and its effect is dependent on the phase where is occurs.

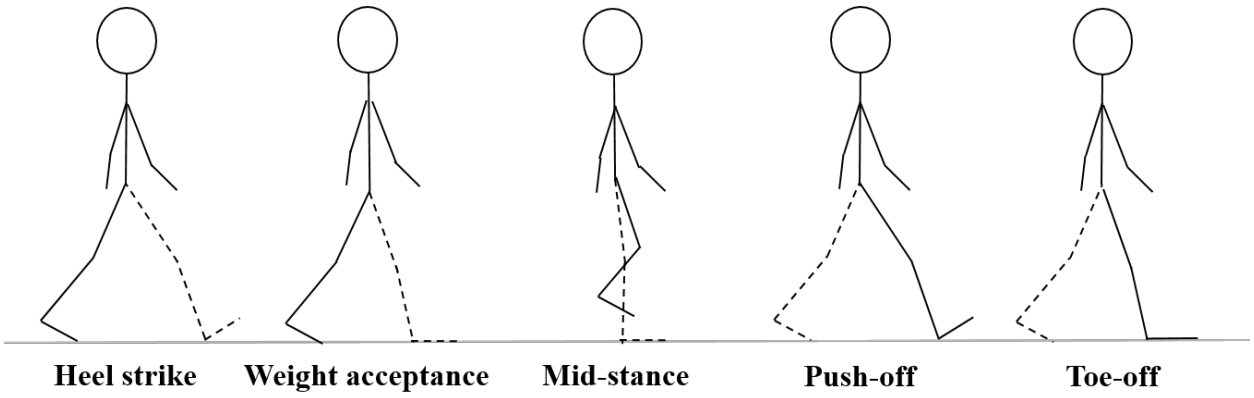

Figure 2-2. A schematic example of a foot (dashed line) in the **s**tance phase of a gait cycle during level walking. The gait cycle starts at heel strike of the foot (dashed line) and ends with toe-off.

The GRF during the stance phase of a normal gait on linear walkway (Figure 2-3) are used to quantify the frictional demand of an individual that is required to prevent a slip (Burnfield & Powers, 2006; Hanson et al., 1999; Perkins, 1978; Siegmund et al., 2006). The vertical force has two distinct peaks. Peak one occurs about 25% of the stance phase and biomechanically corresponds to weight acceptance. The second peak happens at about 75% of the stance phase and corresponds to the push-off period. The longitudinal shear (friction in the gait direction) has two peaks, i.e. the first peak (about 15% of stance phase) in the anterior direction exerted by the foot on floor and the second peak (about 85% of stance phase) in the posterior direction. The first and second peak correspond to braking and propulsion phase, respectively. The ratio of shear to vertical forces are used to calculate the frictional demand for an individual during gait to avoid slipping and is termed as the required coefficient of friction (RCOF) (Eq. 2-1) (Figure 2-3)

(Burnfield & Powers, 2006; Hanson et al., 1999; Perkins, 1978; Siegmund et al., 2006). The peak RCOF during the weight acceptance period (Table 2-1), which occurs at about the same time as the peak longitudinal shear force in the anterior direction, is a significant predictor of slips with higher RCOF values being associated with increased risk of slipping (Beschorner et al., 2016).

$$RCOF = \frac{\sqrt{F^2_{Longitudinal\ Shear} + F^2_{Transverse\ Shear}}}{F_{Normal}} \quad \text{Eq. 2-1}$$

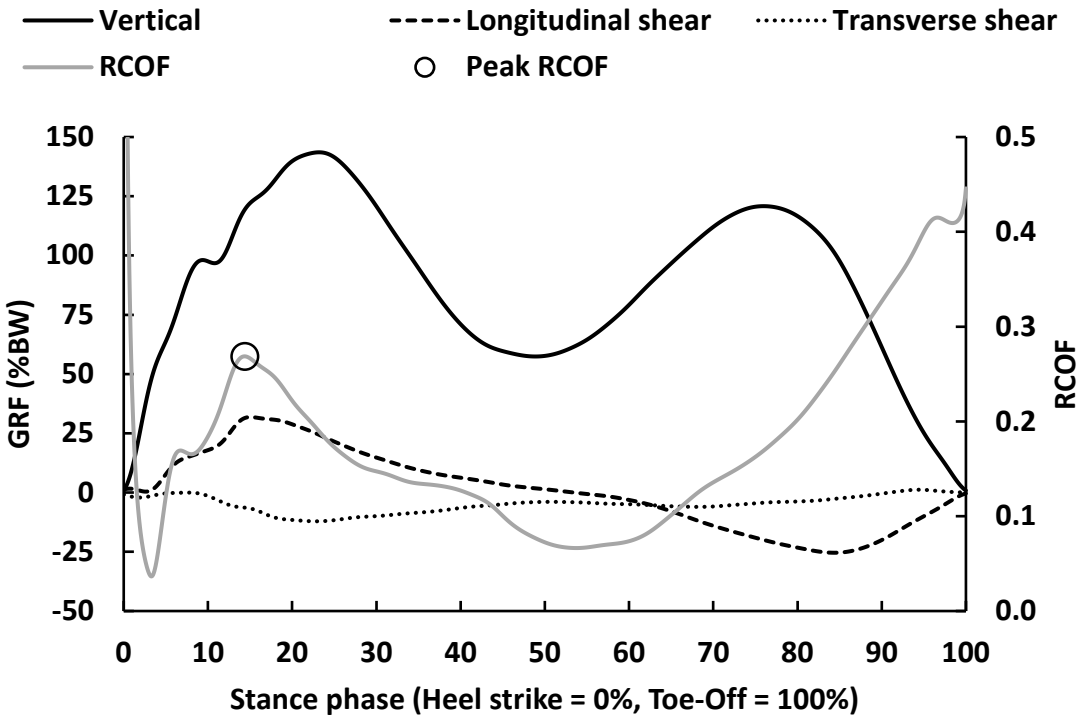

Figure 2-3. A representative GRF and RCOF during level walking. The positive and negative longitudinal shear represent anterior and posterior direction, respectively. The positive and negative transverse shear represent medial and lateral direction, respectively.

The kinematics of walking including gait speed, step length, and shoe-floor angle, also affect slip propensity. Table 2-1 summarizes kinematic values during typical level walking in previous studies. Gait speed (Powers et al., 2002) and step length (Moyer et al., 2006) are associated with changes in slipping risk. Powers et al. (2002) showed that increase in gait speed is associated with an increase in peak RCOF. However, gait speed and step length are coupled, i.e. faster gait speed is generally accompanied with longer step lengths (Powers et al., 2002). Anderson et al. (2014) decoupled the effect of gait speed and step length on RCOF. This study found that increased step length had a strong positive effect on RCOF, whereas gait speed independent of step length had a weak negative effect on RCOF. This might be due to longer step length positively impacting shear forces and increasing the individual frictional demand whereas increasing gait speed (when step length is controlled) leads to modest increases of vertical GRF (Anderson et al., 2014). Additionally, the decoupling of step length and gait speed showed that shorter step length and faster gait speed improved stability following a slip onset (Espy et al., 2010). Other kinematic factors like shoe-floor angle (Moyer et al., 2006) and anterior heel acceleration (Beschorner & Cham, 2008) at heel strike have been demonstrated to impact the severity of slips. Higher shoe-floor angles increases slip severity (Moyer et al., 2006) and higher heel deceleration (negative acceleration) reduces the occurrence of severe slips (Beschorner & Cham, 2008). Thus, several gait parameters that are based on human factors influence the risk of slip-initiated falls.

Table 2-1. Peak RCOF, shoe-floor angle, gait speed, and step length reported by biomechanical studies during level walking under dry conditions. Values are reported as mean ± standard deviations.

Study	Peak RCOF	Shoe-floor angle at HS (°)	Gait speed (m/s)	Step length (mm)
(Perkins & Wilson, 1983)	0.22	NA	NA	NA
(Redfern & DiPasquale, 1997)	0.20	NA	0.57±0.13§	0.32±0.06§
(Cham & Redfern, 2002a)Ψ	0.18±0.05P, 0.19±0.04V	23.5±3.7 P, 24.1±4.3V	NA	NA
(Lockhart et al., 2003)*	0.18±0.02Y, 0.19±0.02O	NA	NA	NA
(Menant et al., 2009)	NA	21.4±3.3	1.17±0.18	638±64
(Beschorner et al., 2016)	0.21±0.03	NA	NA	NA

§ normalized to height
Ψ reported for two separate floor conditions [vinyl tile (**V)** vs. rough, silicate impregnated, painted plywood floor (**P)**]
***** reported for two separate age groups [young (**Y)** vs. old (**O**)]
NA indicates that this variable was not reported for this study
HS Heel strike

Another important factor to consider that may potentially affect slip outcome is subject's mindset including anticipation. Subjects tend to lower gait speed, step length and shoe-floor angle at heel strike when they are aware of a slippery surface (Menant et al., 2009). Additionally, subjects reduce their peak RCOF when anticipating a slippery surface (Cham & Redfern, 2002a). These adaptions are likely intended to reduce the risk of slipping accidents (Menant et al., 2009). Moreover, this anticipation of a slippery surface may underestimate the actual slipping risk (Siegmund et al., 2006). Thus, the mindset or anticipation factor needs to be considered when evaluating slipping risk.

The gait biomechanics is an important determinant of slip outcome and changes in gait strategies may decrease slipping accidents. Thus, biomechanical information about individual's

gait pattern should be considered during the development of shoe traction testing and when considering an individual's overall slipping risk.

2.3 FRICTION AND LUBRICATION OF ELASTOMERS

Previous research has supported the relevance of certain tribology principles to the shoe-floor interface during a slipping incident. This section provides an overview of the lubrication mechanisms relevant to shoe-floor interface during traction testing and human slipping. In addition, the friction of elastomers in boundary lubrication will be discussed. The lubrication mechanisms explain the dependency of coefficient of friction on the state of fluid film and the friction of elastomer-hard contact surfaces address the contribution of shoe outsole material properties, liquid contaminant, and floor surface to the adhesion and hysteresis friction forces.

2.3.1 Surface topography

Surfaces of solid materials often have rough surface or protuberances at micrometer and nanometer scale due to manufacturing process. These features are even present on surfaces that appear to be smooth. The protuberances on the surface are termed as asperities (Hamrock, 1994). Floor surfaces with high roughness often have a positive impact on coefficient of friction (Chang et al., 2001c). The geometry of the surface is broadly divided into three main categories: (1) error of form (deviation from a well-defined pattern), (2) waviness (relatively long waves), and (3) roughness (irregularities) (Hamrock, 1994). Roughness is generally the geometric characteristic of interest (Hamrock, 1994) and measured using stylus technique (e.g., stylus profilometer) or non-contacting

methods (e.g., optical and electron devices) (Chang et al., 2001c; Hamrock, 1994). The height of the roughness profile is quantified relative to a defined reference line (e.g., average height, centroid of the profile) and this reference line is used to measure roughness parameters (Hamrock, 1994). Some commonly used surface parameters are arithmetic average (R_a, Eq. 2-2) (Hamrock, 1994), root mean square (R_q, Eq. 2-3) (Hamrock, 1994), and average peak to valley height (R_{tm} or R_z, Eq. 2-4) (Chang et al., 2001c). In Eq. 2-2 and Eq. 2-3, z_i is the discretized height value, i = 1, 2, …, N. In Eq. 2-4, P_i and V_i are the highest peak and lowest valley in each cut-off length, respectively.

$$R_a = \frac{1}{N}\sum_{i=1}^{N}|z_i| \qquad \text{Eq. 2-2}$$

$$R_q = \left(\frac{1}{N}\sum_{i=1}^{N} z_i^2\right)^{1/2} \qquad \text{Eq. 2-3}$$

$$R_{tm} \text{ or } R_z = \frac{\sum_{i=1}^{5}(P_i+V_i)}{5} \qquad \text{Eq. 2-4}$$

2.3.2 Lubrication mechanism of shoe-floor interface

The response of shoe-floor friction to lubricating fluid during slips can be explained by lubrication theory and tribology principles (Figure 2-4). The Stribeck curve depicts the variation in coefficient of friction (COF, Eq. 2-5) as a function of liquid viscosity (η), speed of the interacting surfaces (v) and normal force exerted on the interface (F_{Normal}) (Eq. 2-6) (Khonsari & Booser, 2017). In Eq. 2-5, F_{Shear} is the shear or tangential force. The coefficient of friction varies as the lubrication regime transitions from the boundary to hydrodynamic lubrication. This variation in coefficient of friction is primarily caused by changes to the fluid film thickness. The minimum fluid film thickness (h_{min}) is a function of normal applied load (F_{Normal}), relative velocity of the surfaces (v), lubricant viscosity (η) and the geometry (R) in a hydrodynamically lubricated bearing assuming conformal

surfaces and no elastic effect (Eq. 2-7). Researchers have established thresholds, known as dimensionless film parameter (Λ) (Eq. 2-8), for differentiating across the lubrication regimes based on the ratio of the minimum fluid film thickness to the surface roughness, root mean square (R_q), of the interacting surfaces (Hamrock, 1994). At boundary lubrication ($\Lambda < 1$) (Figure 2-5), the surface asperities are in contact. Hence, the coefficient of friction is significantly higher compared to the other lubrication regimes. At mixed lubrication ($1 \leq \Lambda < 5$) (Figure 2-5), the asperities are partially in contact due to fluid pressure buildup, which results in the reduction of coefficient of friction. As the fluid pressure continues to buildup ($\Lambda > 5$), the interacting surfaces are fully separated and the coefficient of friction further increases from drag forces within the fluid. This separation (as measured by film thickness) of the interacting surfaces is characterized as hydrodynamic or thin-fluid film lubrication ($5 \leq \Lambda < 100$) (Figure 2-5). In the case of hydrodynamic lubrication, if the fluid pressure deforms the interacting surface(s), then the regime is characterized as elastohydrodynamic lubrication (EHL) (Khonsari & Booser, 2017). The EHL ($3 \leq \Lambda < 10$) is further categorized into hard and soft EHL (Khonsari & Booser, 2017). The hard EHL is applicable to rolling or combined rolling and sliding in ball bearings, roller bearings, and gear teeth, whereas soft EHL is relevant to rubber seals, human joints, and tire traction (Khonsari & Booser, 2017).

$$COF = \frac{F_{Shear}}{F_{Normal}} \quad \text{Eq. 2-5}$$

$$COF = f\left(\frac{\eta \times v}{F_{Normal}}\right) \quad \text{Eq. 2-6}$$

$$h_{min} = f(F_{Normal}, v, \eta, R) \quad \text{Eq. 2-7}$$

$$\Lambda = \frac{h_{min}}{(R_{q,a}^2 + R_{q,b}^2)^{1/2}} \quad \text{Eq. 2-8}$$

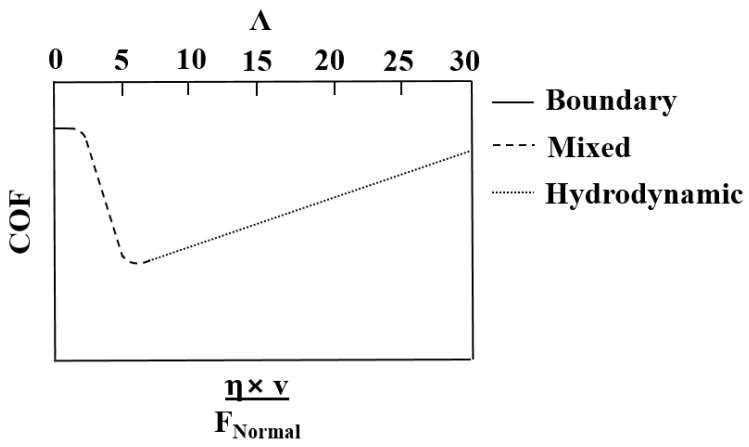

Figure 2-4. Stribeck curve

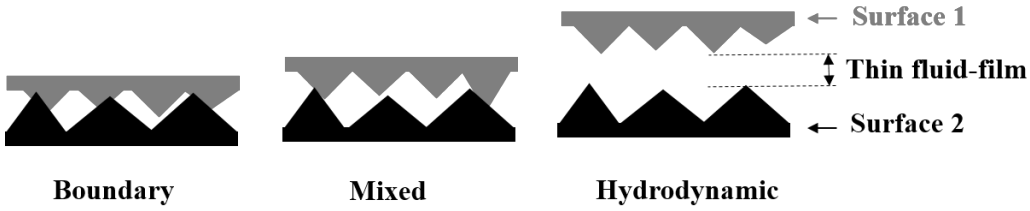

Figure 2-5. Interacting surfaces demonstrated using different lubrication mechanism

In the mixed and hydrodynamic lubrication, the fluid film thickness (h) is related to the fluid pressure (p) by the Reynolds equation (Eq. 2-9) (Hamrock, 1994), which describes the fluid pressure distribution across the contact. Eq. 2-9 is under the assumptions of pure sliding and the fluid properties (viscosity, density) do not change significantly throughout the contact. In Eq. 2-9, η_0 is the absolute viscosity at p = 0 and constant temperature, ρ is the density of the lubricant, and $\tilde{u}$ is the mean surface velocity in x-direction.

$$\frac{\partial}{\partial x}\left(h^3\frac{\partial p}{\partial x}\right)+\frac{\partial}{\partial y}\left(h^3\frac{\partial p}{\partial y}\right)=12\,\tilde{u}\eta_0\frac{\partial(\rho h)}{\partial x} \qquad \text{Eq. 2-9}$$

Different lubrication regimes have been thought to be important to describe slipping dynamics (Chang et al., 2001b; Leclercq et al., 1995; Proctor & Coleman, 1988) but experimental methods have only been recently developed to better characterize the regimes (Beschorner et al., 2014; Moore et al., 2012; Singh & Beschorner, 2014; Strobel et al., 2012). Mixed or hydrodynamic lubrication have been found to apply to high viscous liquid combined with shoes that have no outsole tread (Beschorner et al., 2014; Singh & Beschorner, 2014), whereas boundary lubrication generally applies to shoe outsole with intact tread (Figure 2-6). For instance, shoes with the absence of outsole tread have high interfacial fluid pressures (> 200 kPa) during mechanical friction-testing when combined with glycerol aqueous (9:1) solution (Singh & Beschorner, 2014). These hydrodynamic pressures (124 ± 75 kPa) were also documented during human slip experiments on glycerol aqueous (9:1) solution when subjects wore shoes with no outsole tread (Beschorner et al., 2014). In contrast, the presence of outsole tread significantly reduced hydrodynamic pressures under high viscous liquid contaminant (Beschorner et al., 2014; Singh & Beschorner, 2014) most likely due to the drainage capability, which may suggest that boundary lubrication is applicable to shoe-floor friction in the presence of outsole tread. Thus, compelling experimental data from previous research supports the existence of different lubrication mechanisms at the shoe-floor interface during slipping incidents.

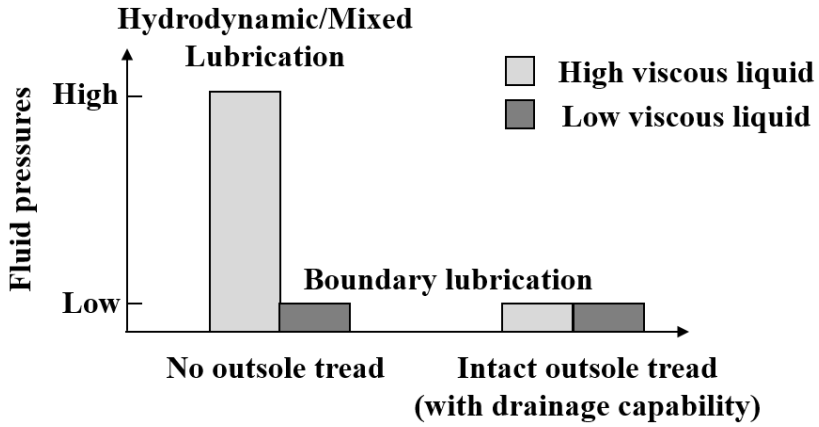

Figure 2-6. Conceptual diagram for how fluid pressure and lubrication regimes vary across contaminants and shoe outsoles.

2.3.3 Friction of elastomers-hard contact surfaces

The outsoles of footwear are commonly made of elastomers and their friction against hard surfaces is primarily explained by adhesion and hysteresis friction theory (Eq. 2-10) (Figure 2-7) (Moore, 1975). Adhesion occurs due to inter-molecular forces developed between the asperities in contact whereas hysteresis friction is due to deformation within the elastomer caused by the surface asperities of the hard surface (Moore, 1975). Adhesion is caused due to the formation and breaking of the molecular junctions between elastomer and hard base, which is characterized as a dissipative molecular stick-slip process (Moore, 1975). Hysteresis is caused by the asymmetrical pressure distribution of the elastomer due to asperity penetration of the rigid surface during sliding (Moore, 1975). Adhesion friction can be minimized in the presence of lubricant (boundary lubrication) whereas hysteresis friction is reduced on smooth and dry surfaces (Moore, 1975). Both adhesion and hysteresis components of friction are applicable to the footwear-floor traction (Cowap et al., 2015; Strobel et al., 2012).

$$F_{Friction} = F_{Adhesion} + F_{Hysteresis}$$ Eq. 2-10

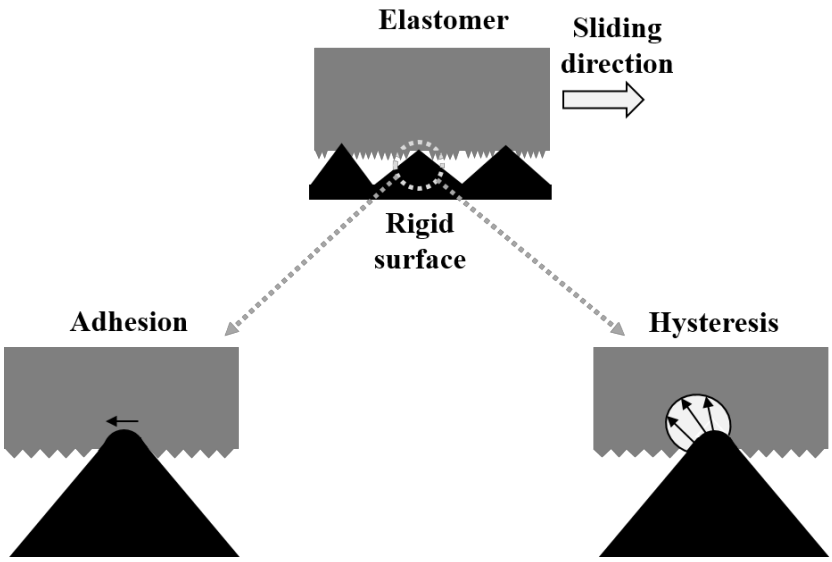

Figure 2-7. Adhesion and hysteresis friction

Adhesion and hysteresis components of friction have been conceptually linked to shoe-floor traction (Leclercq et al., 1995). Leclercq et al. (1995) suggested that the properties of elastomer, lubricant amount and floor roughness explains the changes in adhesion and hysteresis friction forces. Additionally, tribological studies have demonstrated the role of adhesion and hysteresis friction with respect to lubrication, shoe outsole material and floor roughness (Cowap et al., 2015; Strobel et al., 2012). Adhesion friction is substantially minimized between a footwear outsole material and floor surface in the presence of liquid contaminants (Cowap et al., 2015; Strobel et al., 2012). Adhesion friction further reduces as the liquid viscosity increases (Cowap et al., 2015). Hysteresis friction is positively impacted by increase in the floor roughness (Cowap et al., 2015; Moghaddam et al., 2018; Moghaddam et al., 2015). In addition, softer and rougher elastomers have

higher hysteresis friction compared to harder and smoother elastomers (Cowap et al., 2015). Thus, adhesion and hysteresis mechanisms can be used to describe the impact of designing on shoe-floor friction.

Theory on lubrication and friction of elastomers provide a useful framework to contextualize and interpret factors influencing shoe-floor coefficient of friction. Lubrication theory provides an insight on how the hydrodynamic pressures can be reduced by the presence of outsole tread and enhance coefficient of friction. Then the friction of elastomers at boundary lubrication can further help to inform researchers and footwear manufacturers on how shoe material properties and floor surface/type can affect coefficient of friction in different adverse environmental conditions.

2.4 OCCUPATIONAL ASSESSMENT

Occupational injuries are often mitigated through ergonomic interventions. The tasks that are prioritized for interventions are typically identified by ergonomic assessments. Ergonomic assessment tools generally include direct measurement techniques, observational methods, and questionnaires (Dempsey et al., 2005). Direct measurement techniques like the lumbar motion monitor (LMM) system, electromyography (EMG), a motion capture camera system, a force plate, and a mechanical friction measurement device are used by researchers or occupational health and safety practitioners to objectively evaluate risk factors. In contrast, the observational methods like revised NIOSH lifting equation (Waters et al., 1993), Rapid Upper Limb Assessment (McAtamney & Corlett, 1993) and Strain Index (Steven Moore & Garg, 1995), requires the practitioner or ergonomist to assess worker's workload in order to identify hazards (Takala et al., 2010).

The choice of ergonomic tool depends on the problem, ergonomist's preference (e.g., expertise, experience) and practicality (e.g., cost, availability, time) (Dempsey et al., 2005). Ideally, an ergonomic assessment tool should be predictive, robust, inexpensive, non-invasive, quick to administer and easy-to-use (Marras & Karwowski, 2006). For instance, the lumbar motion monitor helps to quantify the dynamic trunk motion and assess low back injuries during manual material handling (Marras et al., 1993). This is beneficial to the practitioner to acquire biomechanical information under *in vivo* conditions (Marras et al., 1993). On the other hand, the NIOSH lifting equation can be used to assess the lifting task that may contribute to low back injuries, which is relatively inexpensive, readily available and often require simple mode of recording (e.g., pen and paper) by the ergonomists. The choice between lumbar motion monitor and NIOSH lifting equation may depend on the trade-off between cost, availability, time, experience, and accuracy. Lumbar motion monitor is more expensive but provides an accurate estimate of trunk motion. However, NIOSH lifting equation is relatively inexpensive and readily available but may be time intensive to assess all of the tasks relevant to a job (Dempsey, 2002). A survey of ergonomic assessment tools used by professional ergonomists indicated that over 80% of the practitioners utilized NIOSH lifting equation to address manual material handling, whereas lumbar motor motion was used by only 16.6% (Dempsey et al., 2005). Thus, differences in the tool's attributes can lead to variations in usage.

Injuries due to overexertion and falls on the same level are consistently among the top two disabling workplace injuries (Marucci-Wellman et al., 2015). Assessments based on direct measurements are utilized to address both overexertion injuries due to manual material handling and fall injuries due to slipperiness. For example, the lumbar motion monitor is a candidate tool for manual material handling and mechanical friction measurement devices for evaluation of slip

risk. As far as observational assessment tools are concerned, NIOSH lifting equation is one of the tools that is widely used for manual material handling (Dempsey et al., 2005). A comparable observational method like NIOSH lifting equation does not exist to assess footwear or floor traction performance. The ergonomic tools for slip risk assessment are often hardware based. An alternative assessment tool based on observational techniques may increase the use of ergonomic tools by safety practitioners to evaluate slip hazards.

Development of the NIOSH lifting equation can be used as a case to inform the development of observational methods to assess slip risk. The NIOSH lifting equation was developed to facilitate occupational health and safety practitioners with an assessment tool to evaluate the lifting demand of a task in order to prevent low back injuries (Eq. 2-11 and Eq. 2-12) (NIOSH, 1981). The NIOSH lifting equation was established based on research in the areas of epidemiology, biomechanics, physiology, and psychophysics (NIOSH, 1981). This interdisciplinary research led to the selection of five variables to evaluate lifting tasks: horizontal location (H), vertical location (V), vertical travel distance (D), average frequency of lift (F), and maximum frequency of lift (Fmax) (NIOSH, 1981). The analyzed lifting task is categorized based on two thresholds: the action limit (AL) and the maximum permissible limit (MPL) (NIOSH, 1981). However, this equation was limited to the lifting tasks performed in the sagittal plane and assumed a good hand-object coupling (NIOSH, 1981). Therefore, the NIOSH lifting equation was revised to incorporate asymmetrical lifting tasks and suboptimal hand-object coupling (Eq. 2-13 and Eq. 2-14) (Waters et al., 1993). In addition, the load constant was changed from 40 kg to 23 kg partially due to change of the horizontal displacement of 15 cm to 25 cm in the revised NIOSH lifting equation (Waters et al., 1993). A load constant of 23 kg was chosen based on the biomechanical and psychophysical criteria such that this lift would be achievable by 75% of female

and about 90% of male workers. Also, this load constant ensures that the compression force on the L5/S1 disc would be less than 3.4 kN (Waters et al., 1993). Six coefficients (multipliers) were used to decrease the load constant to account for suboptimal conditions like twisting (AM), frequent lifting (FM), poor couplings (CM), vertical distance moved (DM), vertical (VM) and horizontal (HM) location of the object. The lifting task is analyzed based on the recommended weight limit (RWL) and lifting index (LI) (Waters et al., 1993). The changes in the revised NIOSH lifting equation was intended to apply this assessment tool to a larger number of lifting tasks.

$$AL\ (kg) = 40 \times \left(\frac{15}{H}\right) \times (1\text{-}0.004|V\text{-}75|) \times \left(0.7+\frac{7.5}{D}\right) \times \left(1-\frac{F}{F_{max}}\right) \quad \text{Eq. 2-11}$$

$$MPL = 3 \times AL \quad \text{Eq. 2-12}$$

$$RWL = 23\ kg \times \left(\frac{25}{H}\right) \times (1\text{-}0.003|V\text{-}75|) \times \left(0.82+\frac{4.5}{D}\right) \times FM \times (1\text{-}0.0032 \times A) \times CM \quad \text{Eq. 2-13}$$

$$LI = \frac{L}{RWL} \quad \text{Eq. 2-14}$$

Ergonomic tools are infrequently utilized for footwear or floor safety, which is surprising given the prevalence of slipping accidents. A survey by Dempsey et al. (2005) indicated that only 21.4% of the professional ergonomists used slipmeters as an assessment tool to assess slip risk. One reason that might explain the low utilization of slipmeters might be due to their cost and expertise required to perform shoe or floor traction testing. In addition, a lack of observational assessment tools exists available to assess slip risk. For example, Takala et al. (2010) identified 30 observational methods to assess biomechanical exposures in the workplace, but no observational assessment tool exists in the literature to assess slip risk. This may cause a barrier for the occupational health and safety practitioners to implement Prevention through Design (PtD)

process. Thus, development of observational assessment tools to assess shoe traction performance are necessary, specifically given the scale of slips and falls injuries.

2.5 FOOTWEAR TRACTION TESTING

Experimental traction testing of footwear or flooring have been performed using human-centered approaches and mechanical friction measurement devices. Human-centered approaches generally expose participants to a slippery surface. Subjects are typically first exposed to a dry pathway to quantify RCOF of the given shoe-floor-individual combination and then exposed to a slippery condition to determine whether the person experiences a slip (Hanson et al., 1999; Siegmund et al., 2006). Slip-resistant properties of the shoe-floor-contaminant conditions are compared using the rate of slipping (ratio of number of trials that lead to a slip to the total number of liquid contaminated exposure trials) across each condition (Powers et al., 2007). The outcome of a walking trial (slip or no slip) is determined based on the heel slip distance (Beschorner et al., 2016; Cham & Redfern, 2002b; Powers et al., 2007) or rating scales of personal perception of slipperiness (DiDomenico et al., 2007; Powers et al., 2007). The other commonly used method to assess the slip-resistant properties of a shoe or flooring is mechanical friction measurement devices (also known as mechanical slip/friction-testing devices, slipmeters, and tribometers) (Blanchette & Powers, 2015b; Powers et al., 2007; Redfern & Bidanda, 1994). These devices often use either a sample of shoe outsole material or a whole shoe along with a floor and contaminant to test slip-resistant properties (Chang et al., 2001a). These devices often measure available coefficient of friction (ACOF) between the shoe outsole and floor surface in the presence of surface contaminants (Blanchette & Powers, 2015b; Powers et al., 2007; Redfern & Bidanda, 1994). ACOF is a

significant predictor of slip risk and an increase in ACOF is associated with reduction in slipping risk (Burnfield & Powers, 2006; Siegmund et al., 2006). Mechanical friction measurement devices can be used by a safety practitioner to assess slip risk of a shoe or floor at the workplace as a substitute for human slipping experiments.

Mechanical friction measurement devices, both whole shoe testers and portable devices, are intended to simulate the relevant tribology phenomena occurring during a slip. A survey of these devices can be found in Chang et al. (2001a). Whole shoe testers are generally categorized as laboratory based devices since they are often not portable. Whole shoe testers typically have the capability to operate across a range of vertical forces, shoe-floor angles, sliding speeds and contact durations (Figure 2-8). On the other hand, portable devices are intended to be utilized for field measurements. Common portable devices include the variable incidence tribometer (Burnfield & Powers, 2006; Powers et al., 2007) and the portable inclinable articulated strut sliptester (Powers et al., 2007), which measure ACOF based on the tangent of the angle between the vertical and shear force that the shoe material slips out. Portable devices use a piece of shoe outsole as specimen. The choice of mechanical friction measurement devices may rely on several factors like biofidelity, portability, intended use, versatility, and cost.

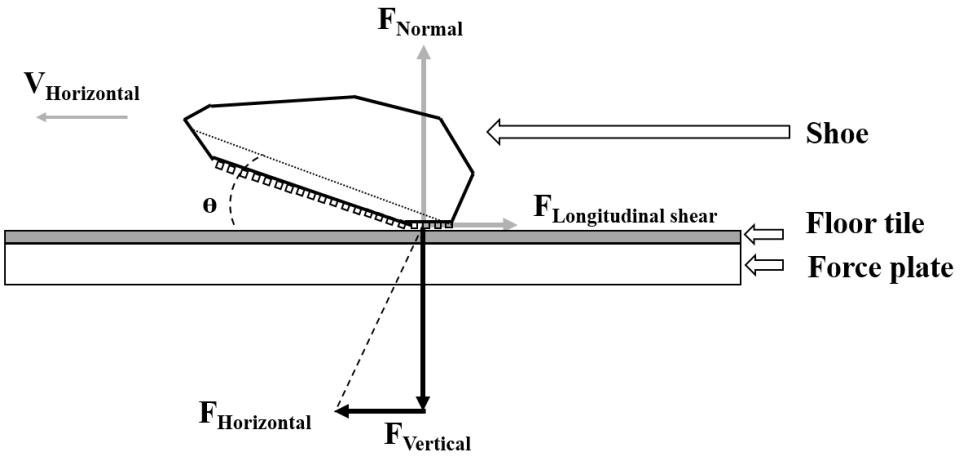

Figure 2-8. Biomechanical testing parameters during mechanical friction measurement. The normal force (F_{Normal}), sliding speed ($V_{Horizontal}$), and shoe-floor angle (ɵ) are the biomechanical parameters set as input for the whole shoe testers.

Whole shoe testers are generally a suitable candidate for measuring slip risk due to their closeness to actual heel slip and their adjustability of biomechanical parameters. The biomechanical parameters can be set to the values pertaining to actual footwear-floor condition during a slip in order to become relevant to human slips. This is important to acquire valid slip-resistant properties of shoe-floor-contaminant conditions since biomechanical parameters like vertical force (Beschorner et al., 2007; Blanchette & Powers, 2015b), shoe-floor angle (Beschorner et al., 2007; Blanchette & Powers, 2015b), sliding speed (Beschorner et al., 2007; Blanchette & Powers, 2015b; Redfern & Bidanda, 1994) and contact duration (Gronqvist et al., 2003) affect ACOF in complex ways. However, there exists a lack of consensus in what these conditions should be. Variation in these biomechanical parameters across literature is evident (Table 2-2). These differences in ACOF testing methods may lead to inaccurate inference about the traction performance of the shoe. Another concern with the choice of ACOF testing methods is that they are not often validated

in their ability to predict human slip risk. One study has investigated the effect of testing parameters to predict human slip risk (Blanchette & Powers, 2015b). However, Blanchette and Powers (2015b) study was limited to a single shoe-floor-contaminant condition and therefore, may lack generalizability. Thus, there is a need to identify a set of biomechanical testing parameters that best predicts human slip risk across various shoe-floor-contaminant conditions.

Table 2-2. Common vertical forces, shoe-floor angles and sliding speeds used by whole-shoe testers for ACOF measurements.

Study	Vertical force (N)	Shoe-floor angle (°)	Sliding speed (m/s)
(Grönqvist et al., 1989)	700	0, 5	0.4
(Wilson, 1990)	400	5	0.1
(Redfern & Bidanda, 1994)	40, 80	5, 15	0.01, 0.05, 0.15
(Hanson et al., 1999)	89	5	0.1
(Menz et al., 2001)	350	10	0.5
(Gronqvist et al., 2003)	210-630, 570-810, 540-700, 500	5	0.4
(Aschan et al., 2005)	170, 250, 500	5	0.2
(Beschorner et al., 2007)	180, 360, 540	10, 20	0.05, 0.2, 0.35, 0.5
(ASTM F2913-11, 2011)	400, 500	7	0.3
(Blanchette & Powers, 2015b)	400, 500, 600	1, 3, 5, 9	0.1, 0.3, 0.5

2.6 FOOTWEAR TRACTION

The role of footwear as a personal protective equipment has a significant role in reducing slip-initiated falls. As mentioned previously, the use of shoes that are labeled as slip-resistant is associated with a reduction of slipping accidents (Verma et al., 2011), due to a higher ACOF of slip-resistant shoes compared to non-slip resistant shoes (Beschorner et al., 2017). Generally, slip-resistant shoes have outsole tread (Jones et al., 2018), which possess drainage capability and reduce hydrodynamic fluid pressures (Beschorner et al., 2014). This reduction in fluid pressures will improve contact between the outsole tread and floor surface, thus enhancing ACOF. Although slip-resistant footwear has a higher ACOF compared to non-slip-resistant footwear, there exists significant variation in ACOF across slip-resistant footwear (Jones et al., 2018). Jones et al. (2018) demonstrated that some slip-resistant footwear may still pose a slip risk when exposed to a slippery

condition during level walking. Therefore, the interaction between shoe outsole tread design and ACOF should be further investigated to determine the shoe features that predict performance.

Shoe traction is affected by both the outsole geometry and material. Previous research has indicated that contact area is positively correlated with ACOF (Jones et al., 2018) whereas material hardness is negatively correlated with ACOF (Jones et al., 2018; Tsai & Powers, 2008). The higher contact area reduces the contact pressures (Moghaddam et al., 2018) and increases the total number of contacting asperities (Moore, 1975), and subsequently ACOF increases. The influence of contact area and material hardness on ACOF is strongest where hysteresis friction is dominant and adhesion friction is minimized (Jones et al., 2018). Other tread features have also been found to affect ACOF. For instance, heel shape (Moghaddam & Beschorner, 2017), tread depth (Li et al., 2006; Yamaguchi et al., 2017), orientation (Blanchette & Powers, 2015a; Li & Chen, 2005; Yamaguchi et al., 2017) and groove channel (Li & Chen, 2004) affect ACOF. Heel shape may contribute to the contact area since beveled edge heel shape tends to achieve larger contact area compared to flat-edge heel shape under the assumption that hysteresis friction is the significant contributor of ACOF (Moghaddam & Beschorner, 2017). Moreover, tread depth and groove channel may primarily contribute to the reduction of hydrodynamic pressures. An important finding about tread depth by Yamaguchi et al. (2017) was that a non-monotonic relationship exists between tread depth and ACOF. As tread depth initially increases, hydrodynamic pressures are decreased and ACOF is increased (Beschorner & Singh, 2012). But further increase in tread depth will result in a decrease of bending stiffness of the tread block, which reduces the contact area of the tread block and results in lower ACOF values (Yamaguchi et al., 2017). Consequently, there appears to be an optimal tread depth that reduces hydrodynamic pressures but does not bend enough to reduce contact area. Thus, the effect of outsole design on ACOF explained by the

lubrication mechanisms and friction of elastomers could establish the development of tread assessment methods.

2.7 STATISTICAL MODELS FOR PREDICTION OF FOOTWEAR TRACTION AND SLIP RISK

Statistical modeling for prediction of a slip incident has been widely used in the literature (Beschorner et al., 2016; Blanchette & Powers, 2015b; Burnfield & Powers, 2006; Hanson et al., 1999; Siegmund et al., 2006). Predictive modelling methods, specifically regression analyses (e.g., linear regression or logistic regression), are statistical techniques to develop an empirical relationship between the predictor variable(s) and response variable (Montgomery et al., 2006). These techniques are used mainly to make an inference about the relationship between the predictor and response variable and/or prediction of the response variable (James et al., 2013). Some regression models are considered parametric analysis since assumptions of normality and homoscedasticity are made. The advantages of linear models are that they are relatively simple and have interpretable inference (James et al., 2013). In slip-initiated fall research, statistical models are generally developed using coefficient of friction data as the predictor and slip outcome as the response variable. Slip prediction models are commonly based on a single predictor, i.e. the difference between ACOF and RCOF (ACOF-RCOF) (Eq. 2-15) (Hanson et al., 1999; Siegmund et al., 2006). This is based on the theory that if the RCOF (frictional demand to continue gait) is greater than the ACOF (available friction at the shoe-floor interface), then an individual is likely to experience a slip incident (Redfern et al., 2001). This slip prediction model is developed using a logistic regression method due to the dichotomous outcome of the liquid-contaminated/slip trials

(slip vs. no slip). Results from the previous studies indicated that ACOF-RCOF is a significant predictor of slipping risk (Hanson et al., 1999; Siegmund et al., 2006). Although, some studies have also shown that ACOF (Eq. 2-16) (Burnfield & Powers, 2006; Siegmund et al., 2006) or RCOF (Eq. 2-17) (Beschorner et al., 2016) alone can predict slip outcomes. However, generally slip prediction models tend to improve when ACOF-RCOF is used as the predictor compared to ACOF alone (Burnfield & Powers, 2006; Siegmund et al., 2006) since RCOF accounts for the individual differences during gait that contributes to increased risk of slipping.

$$\text{Slip\_Risk} = \frac{e^{\beta_0+\beta_1*(\text{ACOF-RCOF})}}{1+e^{\beta_0+\beta_1*(\text{ACOF-RCOF})}} \quad \text{Eq. 2-15}$$

$$\text{Slip\_Risk} = \frac{e^{\beta_0+\beta_1*(\text{ACOF})}}{1+e^{\beta_0+\beta_1*(\text{ACOF})}} \quad \text{Eq. 2-16}$$

$$\text{Slip\_Risk} = \frac{e^{\beta_0+\beta_1*(\text{RCOF})}}{1+e^{\beta_0+\beta_1*(\text{RCOF})}} \quad \text{Eq. 2-17}$$

Predictive modelling has been further utilized to relate the individual contribution of the shoe, floor and contaminant to friction and rate of slipping. For instance, Verma et al. (2011) used a multivariate regression model to relate the use of slip-resistant shoes and mean floor coefficient of friction to the rate of slipping in the service industry. Li and Chen (2004) used a regression model to determine the effect of tread groove width, shoe material, floor and contaminant on ACOF. Furthermore, Li and Chen (2005) extended the model to incorporate tread orientation as a predictor too. Predictive modelling has been further implemented to understand the tribology principles relevant to shoe-floor-contaminant combination. For example, Strobel et al. (2012) related the adhesion component of friction with shoe material, flooring, lubricant and their interactions. Thus, the usefulness of statistical modelling can further enhance our understanding of the complex

interaction between shoe-floor-contaminant combination and traction, and lay the foundation for development of potential assessment tools to prevent slip-related injuries.

2.8 SUMMARY

Slip-initiated falls are a significant problem in occupational environments. Reduction of slip-related injuries is achievable through ergonomic interventions like the use of slip-resistant shoes, high traction flooring, cleaning and drying of floor surfaces. The effectiveness of the shoe or floor interventions is assessed using mechanical friction measurement devices that ideally simulate the shoe-floor tribosystem during a human slipping event. Previous section on footwear traction measurement (Section 2.5) outlined the evident variation in the biomechanical parameters used to operate these devices in the literature. When tests are performed in a way that deviates from human slipping, these tests may lead to incorrect decision about the effectiveness of footwear interventions. This issue can be addressed through human-centered approaches. Human gait and slipping experiments could validate ACOF test conditions as well as provide a biomechanical insight to achieve biofidelity.

The magnitude of slip-initiated falls requires additional assessment tools as an alternative to mechanical friction measurement devices. These devices are useful to assess slip risk, but they may not be cost-effective and available for all safety practitioners. This creates a barrier for practitioners to eliminate slip hazards. This barrier can be removed by developing an alternative tread assessment method based on tribology principles and statistical modelling. Previous research has established the relationship between outsole tread design and ACOF using lubrication theory and friction of elastomers. These important findings from the previous research along with

statistical modelling can lay the foundation to develop and validate an inexpensive, accurate and quick tread assessment tool.

3.0 COEFFICIENT OF FRICTION TESTING PARAMETERS INFLUENCE THE PREDICTION OF HUMAN SLIPS

3.1 ABSTRACT

Measuring the available coefficient of friction (ACOF) of a shoe-floor interface is influenced by the choice of normal force, shoe-floor angle and sliding speed. The purpose of this study was to quantify the quality of slip prediction models based on ACOF values measured across different testing conditions. A dynamic ACOF measurement device that tests entire footwear specimens (Portable Slip Simulator) was used. The ACOF was measured for nine different footwear-contaminant combinations with two levels of normal force, sliding speed and shoe-floor angle. These footwear-contaminant combinations were also used in human gait studies to quantify the required coefficient of friction (RCOF) and slip outcomes. The results showed that test conditions significantly influenced ACOF. The condition that best predicted slip risk during the gait studies was 250 N normal force, 17° shoe-floor angle, 0.5 m/s sliding speed. These findings can inform footwear slip-resistance measurement methods to improve design and prevent slips.

3.2 INTRODUCTION

Falls on the same level due to slippery conditions are among the leading causes of fatal and non-fatal occupational injuries. Slips, trips and falls accounted for 27% of non-fatal (U.S. Department of Labor- Bureau of Labor Statistics, 2016b) and 16.5% of fatal occupational accidents in 2015 (U.S. Department of Labor- Bureau of Labor Statistics, 2016a). According to the 2017 Liberty Mutual Safety Index, falls on the same level were ranked second among the leading causes of disabling U.S. workplace injuries, cost businesses $10.62 billion in direct costs, and accounted for 17.7% of the overall national burden in 2014 (Liberty Mutual Research Institute for Safety, 2017). Slipperiness and slipping are among the primary factors responsible for falling events (Courtney et al., 2001).

A slip is likely to initiate when the friction required (as measured by the RCOF) to sustain gait is greater than the available friction at the contact between the footwear and floor (ACOF) (Burnfield & Powers, 2006; Hanson et al., 1999). ACOF is typically measured using a number of portable mechanical devices such as a drag slip-meter (Powers et al., 2007; Yamaguchi et al., 2015) and variable incidence tribometer (Burnfield & Powers, 2006; Powers et al., 2007); as well as whole-shoe tribometers like the Portable Slip Simulator (Aschan et al., 2005) and the SATRA STM 603 (Blanchette & Powers, 2015b). RCOF is measured on dry surfaces by using a force plate during human gait (Beschorner et al., 2016; Cham & Redfern, 2002a; Chang et al., 2011a; Hanson et al., 1999; Yamaguchi & Masani, 2016). Thus, a reduction in slipping events can typically be achieved by increasing the ACOF between a shoe and floor surface or reducing an individual's RCOF.

Human risk of slips and falls have been evaluated by comparing measured ACOF with human slips. A logistic regression approach developed by Hanson et. al. (Hanson et al., 1999) has

been broadly used in shoe-floor friction research to assess the empirical relationship between slip outcome and slip-testing measurements (Blanchette & Powers, 2015b; Burnfield & Powers, 2006; Siegmund et al., 2006; Tsai & Powers, 2008). According to the logistic regression model, the difference between the ACOF and RCOF predicts the probability of slipping (Burnfield & Powers, 2006; Hanson et al., 1999; Siegmund et al., 2006). Moreover, Burnfield and Powers (Burnfield & Powers, 2006) and Seigmund, et al. (Siegmund et al., 2006) developed a logistic regression with ACOF as the only predictor of slip risk. Another approach has been used to rank surfaces of slipperiness by determining differences in unexpected slip rates across surfaces using a $\chi 2$ test (Powers et al., 2007). Rank-based approaches have been used to test if a slip-testing device can correctly rank and differentiate the level of slipperiness across these categories (Powers et al., 2007). One advantage of the logistic regression approach is its ability to quantify the goodness of fit using receiver operating characteristic curves (Beschorner et al., 2016) whereas rank based methods tend to have binary outcomes (i.e., pass/fail) (Powers et al., 2007).

Mechanical friction-testing devices generally fall into two groups: (1) portable devices that use a sample of footwear outsole as the specimen and exert low normal forces relative to human body mass (Burnfield & Powers, 2006; Chang et al., 2001a; DiDomenico et al., 2007), and (2) whole-shoe testers that use an entire footwear as the specimen and exert a wide range of normal forces, shoe-floor angles and sliding speeds (Aschan et al., 2005; Blanchette & Powers, 2015b; Chang et al., 2001a; Redfern & Bidanda, 1994). Whole-shoe testers are often selected over portable devices when assessing footwear due to their ability to test an entire footwear outsole design and their ability to exert normal forces, shoe-floor angles and sliding speeds that approximate gait.

Measuring ACOF is dependent upon the normal force, shoe-floor angle, and the horizontal sliding speed. There is general agreement that the conditions of the test should be ‘biofidelic’ (i.e.

match the biomechanical conditions that are found during walking) (Redfern et al., 2001). Biomechanical studies have reported values of these key parameters during the initiation of a slip (Table 3-1). Normal force (normalized to body weight) has been reported to be 24.5±13.4 % (Iraqi & Beschorner, 2017) and 64±16 % (Strandberg & Lanshammar, 1981) at the onset of slipping. Shoe-floor angle has been reported at heel contact as 28.2±3.0° (Chambers et al., 2002) and 25.3±5.4° (McGorry et al., 2010), and at slip initiation as 14.7° (Albert et al., 2017), 5.5±5.9° (Strandberg & Lanshammar, 1981), 1.5±0.6° in the case of a slip recovery and 2.2±1.8° for a slip leading to a fall (Cham & Redfern, 2002b). The horizontal sliding speed of the shoe is reported as 0.08-0.32 m/s (Strandberg & Lanshammar, 1981) and 0.27 m/s (Albert et al., 2017). However, few studies have compared different test parameters for their ability to predict slips based on ACOF using whole-shoe testers. This gap is evident in the literature, where a wide range of normal forces (40-810 N), shoe-floor angles (0-20°) and sliding speeds (0.01-0.5 m/s) are used for measuring ACOF (Aschan et al., 2005; ASTM F2913-11, 2011; Beschorner et al., 2007; Blanchette & Powers, 2015b; Gronqvist et al., 2003; Grönqvist et al., 1989; Hanson et al., 1999; Menz et al., 2001; Redfern & Bidanda, 1994; Wilson, 1990). Since ACOF has a complex dependency on these testing parameters (Beschorner et al., 2007; Blanchette & Powers, 2015b), finding the best set of conditions is important. Some research has used whole-shoe testers that are operated under different combinations of normal force, horizontal speed and shoe-floor angle, to predict slip outcome (Blanchette & Powers, 2015b). However, the Blanchette and Powers' study was limited to a single footwear-floor-contaminant condition (2015b). Thus, more robust research is needed for identifying the levels of normal force, shoe-floor angle and horizontal sliding speed that best predicts human slip risk across different footwear-floor-contaminant conditions.

Table 3-1. Normal forces, shoe-floor angles and sliding speeds reported by biomechanical studies during slip initiation. (§ at forward slipping during slip recovery; * at forward slipping for slip leading to a fall). NA indicates that this variable was not reported for this study.

Study	Normal force (%BW)	Shoe-floor angle (°)	Sliding speed (m/s)
(Strandberg & Lanshammar, 1981)	64±16	5.5±5.9	0.08-0.32
(Cham & Redfern, 2002b)	NA	1.5±0.6§, 2.2±1.8*	NA
(Albert et al., 2017)	NA	14.7	0.27
(Iraqi & Beschorner, 2017)	24.5±13.4	NA	NA

Previous efforts to validate slip-testing devices based on human slipping studies have primarily focused on differentiating slip risk across floors (Powers et al., 2007; Siegmund et al., 2006), and are commonly limited to one type (Blanchette & Powers, 2015b; Burnfield & Powers, 2006; Powers et al., 2007; Siegmund et al., 2006) or two types (Tsai & Powers, 2008) of footwear. Gronqvist et. al. tested six pairs of boots and shoes (Gronqvist et al., 2003); however, they repeatedly slipped a small set of subjects (N=5). Multiple repeated slips within subjects may be inappropriate since subjects alter their gait when they anticipate a slipping incident (Cham & Redfern, 2002a). Studies that have included more than one design of footwear outsoles have shown differences in the ACOF across footwear indicating differences in slip rate would also be expected (Gronqvist et al., 2003; Jones et al., 2018; Tsai & Powers, 2008). Few efforts have been made to validate the ability of slip-testers to differentiate across footwear using human slipping data.

The primary purpose of this study was to investigate the impact of testing conditions on ACOF and quantify the prediction quality of ACOF values for predicting human slips across these testing conditions. We hypothesized that the biomechanical parameters will impact ACOF values and that ACOF as well as ACOF-RCOF values using different testing parameters would predict

human slips. The study used an experimental design, where the footwear conditions and testing parameters were controlled, and was cross-sectional, where the human gait and slipping data were used from a single testing session. The goal is to quantify the validity of slip-resistance measurements and guide further development of methods that accurately evaluate footwear traction.

3.3 MATERIALS AND METHODS

This study consisted of two components: ACOF measurements and gait experiments. ACOF measurements were conducted for nine footwear-floor-contaminant conditions using a whole-shoe tester. In the gait experiment, between eight and nineteen subjects walked across dry and liquid-contaminated flooring per footwear-floor-contaminant condition.

3.3.1 Subjects

Biomechanical data from four previously published human gait and slipping studies were pooled (Beschorner et al., 2016; Chambers & Cham, 2007; Jones et al., 2018; Moyer et al., 2006). This data was for shoes S1, S3-S5, B1-B3, which are furthered described in Section 2.2 and Table 2. Data for additional footwear-contaminant conditions (S2T and S2NT, which are described in Section 2.2 and Table 2) were added to the study to improve statistical power and generalizability. The inclusion criteria were that the study involved young adults (18-35 years); an experimental protocol where the exposure to a liquid-contaminant occurred on a force plate; and there had to be at least three gait trials on a dry force plate prior to liquid-contaminant exposure where their left

foot completely landed on the force plate (not on the edges). In total, there were data from 89 (35 female) subjects included in this study with a mean height of 174.4 ± 7.9 cm, body mass 71.8 ± 15.1 kg, age of 22.6 ± 3.7 years, and body mass index (BMI) of 23.5 ± 4.4. All studies used exclusion criteria of neurological, orthopaedic, cardiovascular, pulmonary abnormalities, as well as any problems hindering normal gait. Subjects provided informed consent prior to testing and the protocols were approved by the University of Pittsburgh Institutional Review Board.

3.3.2 Footwear, floor and contaminant conditions

Six shoe and three boot outsole designs were used (Figure 3-1). All walking trials were conducted on a vinyl floor with diluted glycerol or canola oil surface contaminants (Table 3-2). The footwear included a standard work shoe (S1), five work shoes labeled as slip-resistant (S2T, S2NT, S3, S4 and S5) (Table 3-2). One of the slip-resistant shoes (S2T) had the tread intact while the other had the tread removed (S2NT). The three boots had identical tread designs but differed in the material hardness (Soft: B1, Medium: B2; and Hard: B3, Table 3-2). Between eight and nineteen subjects were exposed to a liquid contaminant for each of these conditions (Table 3-4). Shore A hardness was used to characterize the shoe/boot materials (ASTM D2240-15, 2015).

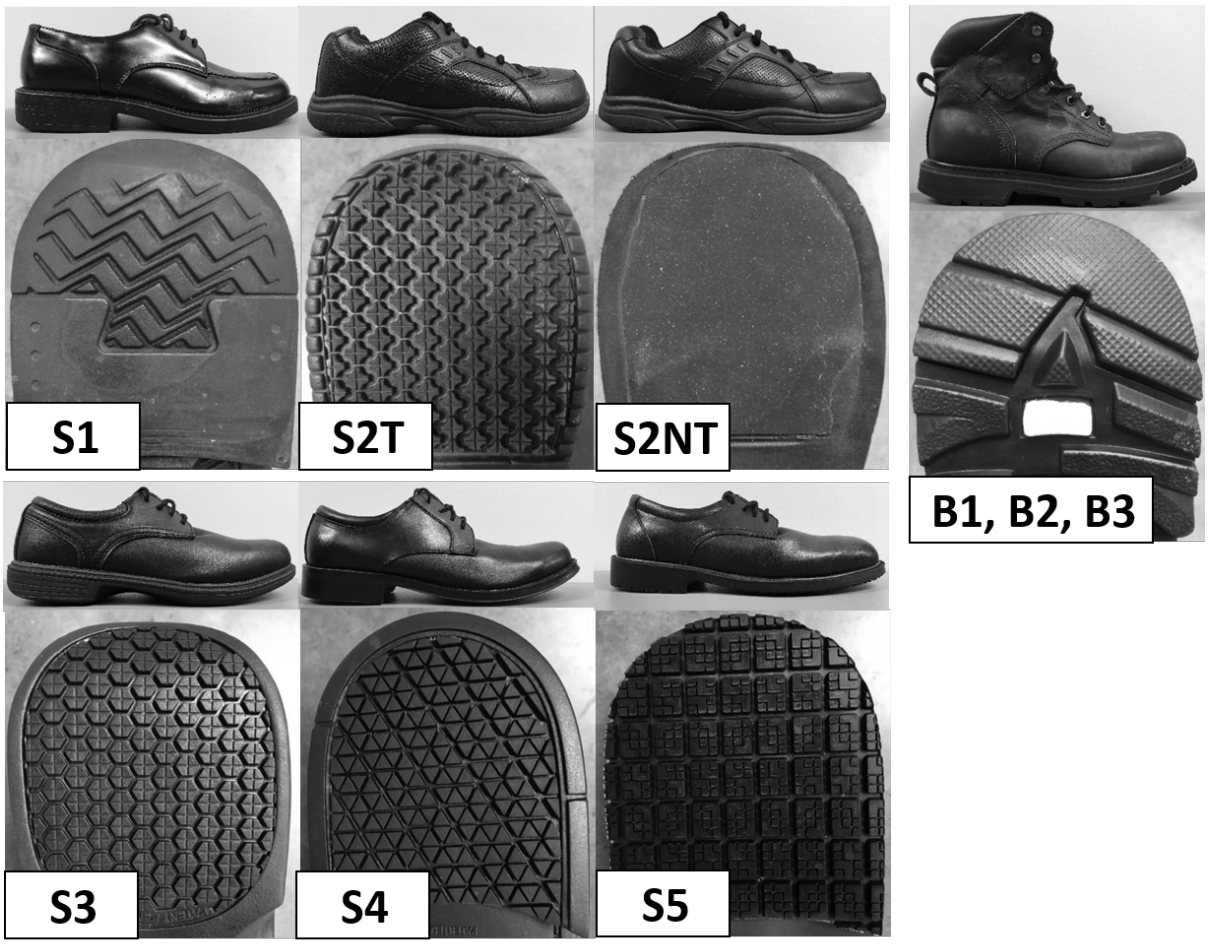

Figure 3-1. Shoes and boots (including the outsole of the heel section) used for ACOF measurements and human testing protocol.

Table 3-2. Footwear-floor-contaminant conditions included in this study.

Footwear	Shore A Hardness	Liquid contaminant	Floor
S1	61.0 (2.1)	75% glycerol-25% water	Vinyl
S2T	62.4 (3.2)	90% glycerol-10% water	Vinyl
S2NT	71.0 (1.9)	90% glycerol-10% water	Vinyl
S3	56.2 (2.9)	Canola oil	Vinyl
S4	60.6 (3.0)	Canola oil	Vinyl
S5	48.6 (1.5)	Canola oil	Vinyl
B1	54.0 (5.8)	50% glycerol-50% water	Vinyl
B2	70.4 (4.5)	50% glycerol-50% water	Vinyl
B3	79.2 (4.8)	50% glycerol-50% water	Vinyl

3.3.3 ACOF measurement

The ACOF measurements were carried out using the Portable Slip Simulator (Aschan et al., 2005). The Portable Slip Simulator is a whole-shoe tester that can approximate the under-shoe conditions (i.e., forces, sliding speeds and angles) of slipping, is well described in the literature and is not based on proprietary technology (Figure 3-2). This device has the capability to simulate the under-shoe conditions immediately after heel strike, the flexibility to control the normal force (0-600 N), shoe-floor angle (0-30°) and sliding speed (0-1 m/s), and is capable of capturing ACOF within the 600 ms of shoe contact that is recommended for friction measurement (Chang et al., 2001b). This device has three parallel electromagnetic motors (LinMot®, Elkhorn, WI, USA) oriented vertically to apply normal force and a horizontal motor to slide the shoe across the floor (Aschan et al., 2005). A shoemaker's last was mounted to the device to attach the shoe or boot. A 6DOF force plate (BERTEC Corporation, Columbus, OH, USA) was used to measure the ground reaction forces.

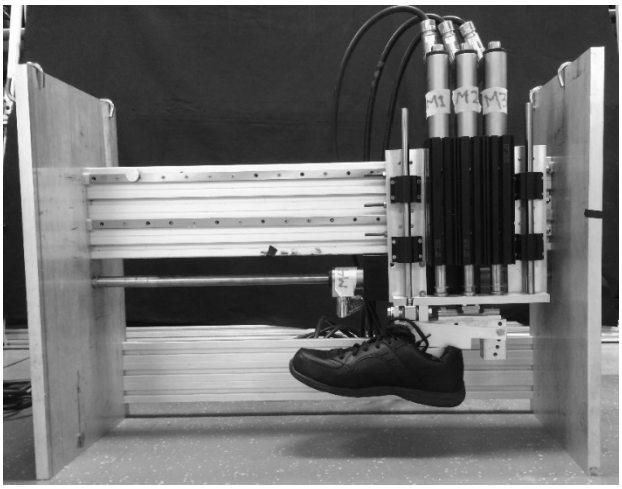

Figure 3-2. Portable Slip Simulator used for ACOF measurements.

The operating parameters were: normal forces of 250 N±10 N and 400 N±10 N, contact angles of 7±2° and 17±2°, and horizontal sliding speeds of 0.3 m/s and 0.5 m/s (Table 3-3). The average normal force of 250 N was selected based on one of the testing parameters used for Portable Slip Simulator by Aschan et. al. (Aschan et al., 2005) and because normal forces during slip initiation are typically less than 300 N (Iraqi & Beschorner, 2017). The 400 N normal force was selected based on the normal force recommended (400±20 N for US men's shoe size < 7.5) to be applied for a whole-shoe tester to evaluate the slip performance between shoe and flooring (ASTM F2913-11, 2011).

The 7° shoe-floor angle was chosen based upon the current ASTM standards (ASTM F2913-11, 2011) and, Strandberg and Lanshammar reported that actual human slips initiate when the shoe angle is at about 6° (Strandberg & Lanshammar, 1981). The steeper contact angle (17°) was added based on a recent analysis that showed the shoe-floor angle to be about 17° when the shoe begins to accelerate (i.e., slip start) during unexpected slipping trials (Albert et al., 2017).

The sliding speeds of 0.3 m/s and 0.5 m/s were selected based on ASTM standards (ASTM F2913-11, 2011) and the sliding speed (0.5 m/s) that best reduced bias of the SATRA STM 603 slip testing device (Blanchette & Powers, 2015b). Both speeds are within the range of sliding speeds (0-1 m/s) recommended for friction measurement between the shoe-floor interface (Chang et al., 2001b).

Table 3-3. Levels of testing parameters used in the study.

Testing parameters	Levels
Normal force (N)	250, 400
Shoe-floor angle (°)	7, 17
Sliding speed (m/s)	0.3, 0.5

During the testing, the normal force profile reached a steady state within ±10% of the desired normal force (Figure 3-3A). The footwear was in motion at heel contact and the sliding speed was constant during the entire duration of contact. The shoe-floor angle and horizontal sliding speed were tracked using motion capture camera systems (Vicon T40S, Oxford, UK) (Figure 3-3B). All the footwear tested were US men's shoe size 9. The fifteen repeated measurements were conducted across three separate days (five per day) for each testing condition.

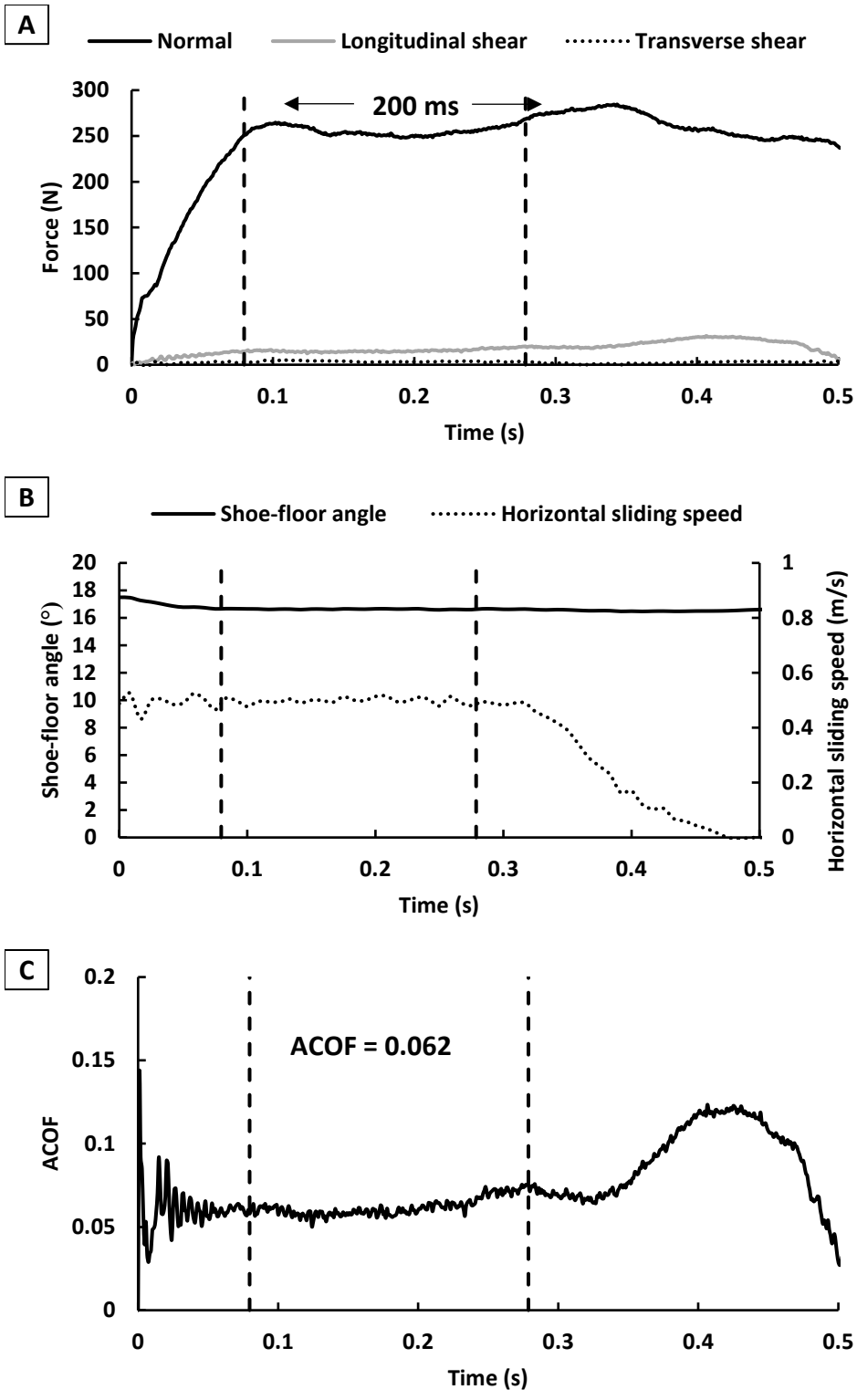

Figure 3-3. Example data collected from one trial with the Protable Slip Simulator at 250 N, 17º and 0.5 m/s : (A) Normal and shear force profiles; (B) shoe-floor angle and horizontal sliding speed; and (C) ACOF profile.

3.3.4 Human testing protocol

All of the human slip studies from which data were included in this analysis used the same slip protocol. Subjects donned a harness for safety purpose and were fitted with markers during data collection. Subjects were instructed to walk naturally with a self-selected comfortable pace. Subjects performed practice gait trials before data collection in order to become comfortable with the harness system and reflective markers. The lights were dimmed to conceal the slipperiness of the floor. The subject's starting position was adjusted so that the subject's left foot landed directly on a force plate. Prior to each trial, subjects listened to music, worked on a word puzzle and faced away from the walkway to distract them from the application of the contaminant.

Baseline walking trials on a dry surface were conducted on a level walkway equipped with force plates to measure ground reaction forces and a motion capture system to track subjects' movement. Subjects performed at least three gait trials prior to the unexpected liquid-contaminant exposure trials. For studies that included multiple shoes/boots (Beschorner et al., 2016; Jones et al., 2018) (including S2T and S2NT) each subject completed two unexpected liquid-contaminated trials wearing a different set of footwear for each trial. For studies that used only one footwear type (Chambers & Cham, 2007; Moyer et al., 2006), only the first unexpected trial was considered for each subject. Slips were induced by unexpectedly placing a glycerol solution or canola oil (Table 3-2: for different fluid contaminants) on the floor surface without the subject's knowledge. Subject's heel marker was tracked to identify a slip. The kinematics data were recorded at a sampling rate of 120 Hz. The forces were recorded at a sampling rate of 1080 Hz and synchronized with kinematics data.

3.3.5 Data and statistical analyses

ACOF values were quantified as the average ratio of resultant shear force to normal force over 200 ms after achieving the normal force threshold (250 N or 400 N) (Aschan et al., 2005) (Figure 3A and C) (Eq. 3-1).

$$ACOF = \frac{\sqrt{F^2_{\text{Longitudinal Shear}} + F^2_{\text{Transverse Shear}}}}{F_{\text{Normal}}} \quad \text{Eq. 3-1}$$

RCOF was calculated to assess individual friction demands, while slip distance was used to assess slip outcomes. A slip distance of greater or equal to 3 cm was considered as the criterion for occurrence of a slip event (Albert et al., 2017; Beschorner et al., 2016; Leamon & Li, 1990). For RCOF calculation, the average of the three baseline dry walking trials prior to an unexpected liquid-contaminated trial was used. The RCOF calculation was based on the following criteria by Chang, et al. (Chang et al., 2011a). First, the RCOF was considered for data with a normal force above a 100 N threshold. Second, the ground reaction force in the longitudinal direction had to be in the direction of gait at the instant of the RCOF. Once the first two criteria were attained, the third criterion was to exclude RCOF when the instantaneous RCOF was decreasing with time to bypass peak 1 (i.e. an artificially large COF instantly after heel contact), and peak 2 (i.e., a negative COF that corresponds to backward slip) (Chang et al., 2011a). Marker data were filtered using a phaseless 4th order low-pass Butterworth filter with a cutoff frequency of 24 Hz. Heel contact was defined as the instant when the vertical component of ground reaction forces exceeded baseline force levels by 25 N. Slip initiation was identified as the first local minimum in speed after heel

contact of a marker placed on the inferior-most point on the back of the heel (Lockhart et al., 2003; Strandberg & Lanshammar, 1981). Peak sliding speed was determined as the first local maximum occurring 50 ms after heel contact (Moyer et al., 2006). Slip distance was calculated between the time of slip initiation and the first local minimum after peak sliding speed. The slip distance was quantified based on the resultant slip distance including both the anterior/posterior and medial/lateral components. The second unexpected liquid-contaminated trial was excluded if the subjects either experienced a slip in the first unexpected liquid-contaminated trial or altered RCOF by more than 16% consistent with previous research (Albert et al., 2017). Subjects tend to change their RCOF by 16-32% when anticipating a slippery floor (Cham & Redfern, 2002a), which was the justification for this cutoff.

Logistic regression was used to model the effect of the ACOF (Eq. 3-2) and the difference between ACOF and RCOF (ACOF-RCOF) (Eq. 3-3) on slip risk. The dependent variable was the outcome of a slip event and the explanatory variables were either ACOF or ACOF-RCOF. A receiver operating characteristic (ROC) curve was generated for each logistic regression model with ACOF-RCOF as the predictor to quantify the optimal cutoffs for the sensitivity and specificity, and the area under the curve (AUC). A larger AUC typically indicates better sensitivity and specificity across the ROC. Odds ratio for each logistic regression model was calculated for a 0.01 increase in ACOF-RCOF from the regression coefficient $\beta 1$ as a measure of effect size. An ANOVA was performed to test the effect of the independent variables: footwear type (S1, S2T, S2NT, S3, S4, S5, B1, B2, B3), normal force (250 and 400 N), shoe-floor angle (7 and 17°), sliding speed (0.3 and 0.5 m/s) and first order interactions on the ACOF (dependent variable). For interaction effects involving footwear, post-hoc t-tests were used with Bonferroni correction ($\alpha=0.05/9$) to determine the shoes that were influenced by that testing parameter. A one-way

ANOVA method was performed to test the effect of footwear type (independent variable) on RCOF (dependent variable). A post hoc Tukey HSD test was performed if a significant difference was identified for footwear type. All statistical analyses were performed using commercial software (JMP® Pro 12.1.0, SAS Institute Inc., Cary, NC, USA) with a significance level of 5%.

$$\text{Slip\_Risk} = \frac{e^{\beta_0+\beta_1*\log_{10}(\text{ACOF})}}{1+e^{\beta_0+\beta_1*\log_{10}(\text{ACOF})}} \quad \text{Eq. 3-2}$$

$$\text{Slip\_Risk} = \frac{e^{\beta_0+\beta_1*(\text{ACOF-RCOF})}}{1+e^{\beta_0+\beta_1*(\text{ACOF-RCOF})}} \quad \text{Eq. 3-3}$$

3.4 RESULTS

Slips occurred in 45 (36.3%) of the 124 unexpected liquid-contaminated trials. Individual slip rate across footwear conditions indicated that S2NT had the highest slip rate (100.0%) whereas S2T (0.0%) and S5 (0.0%) had the lowest slip rate (Table 3-4). The mean RCOF values were not significantly different ($p = 0.127$) across the footwear (Table 3-4). The mean ACOF across all the nine footwear-floor-contaminant conditions (Figure 3-4) were significantly different ($p < 0.001$, $F_{8,33} = 548.8$, $\eta_{partial}^2 = 0.99$), and ranged from a minimum ACOF of 0.021 (0.004) for S2NT with 400 N, 7°, 0.3 m/s as the testing parameters (Figure 3-5A) to a maximum ACOF of 0.433 (0.039) for S5 with 250 N, 7°, 0.3 m/s as the testing parameters (Figure 3-5B). The shoe-floor angle ($p < 0.001$, $F_{1,33} = 115.2$, $\eta_{partial}^2 = 0.78$) and sliding speed ($p = 0.001$, $F_{1,33} = 12.4$, $\eta_{partial}^2 = 0.27$) had a significant effect on ACOF. The normal force ($p = 0.654$, $F_{1,33} = 0.2$, $\eta_{partial}^2 = 0.01$) did not have a significant effect on ACOF. Among the first order interactions, footwear type*shoe-floor angle ($p < 0.001$, $F_{8,33} = 34.7$, $\eta_{partial}^2 = 0.89$) and shoe-floor angle*normal force ($p = 0.024$, $F_{1,33} = 5.6$,

$\eta_{partial}^2$ = 0.15) had significant effects on ACOF. Other interactions were not significant. An increased shoe-floor angle reduced the ACOF values of S1, S3, S4 and S5 but had no effect on the other shoes. The post hoc Tukey test revealed significant differences across the nine types of footwear (Figure 3-4). Increased sliding speed was associated with a reduction in ACOF.

Table 3-4. The number of subjects unexpectedly slipped (n), individual slip rate (95% confidence interval: CI) and mean RCOF (standard deviation) for each footwear.

Footwear	n	Slip Rate % (CI)	RCOF
S1	19	42.1 (20.3-66.5)	0.195 (0.034)
S2T	8	0.0 (0.0-36.9)	0.192 (0.026)
S2NT	10	100.0 (69.2-100.0)	0.180 (0.019)
S3	15	66.7 (38.4-88.2)	0.213 (0.021)
S4	17	23.5 (6.8-49.9)	0.200 (0.030)
S5	15	0.0 (0.0-21.8)	0.198 (0.026)
B1	11	9.1 (0.2-41.3)	0.198 (0.029)
B2	14	42.9 (17.7-71.1)	0.211 (0.030)
B3	15	40.0 (16.3-67.7)	0.201 (0.023)

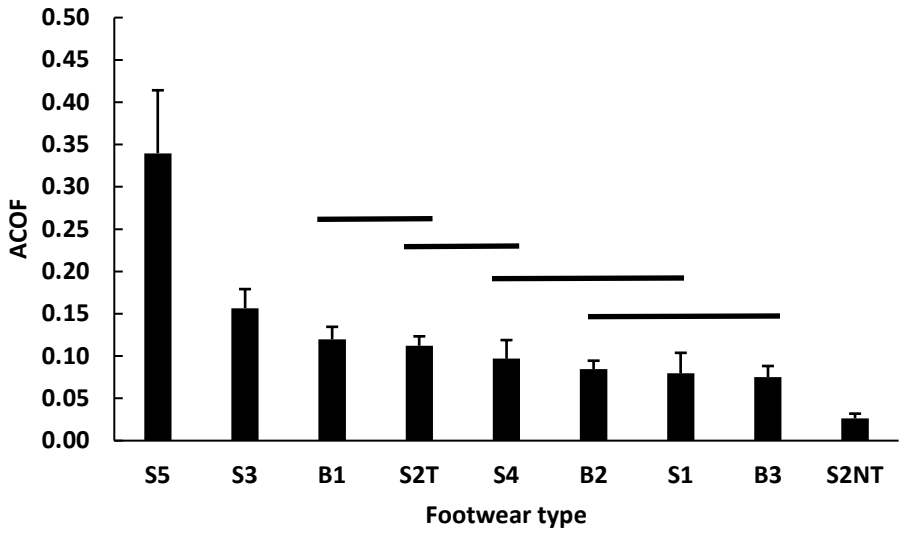

Figure 3-4. Mean (standard deviation) ACOF across footwear (footwear not connected by same line are significantly different).

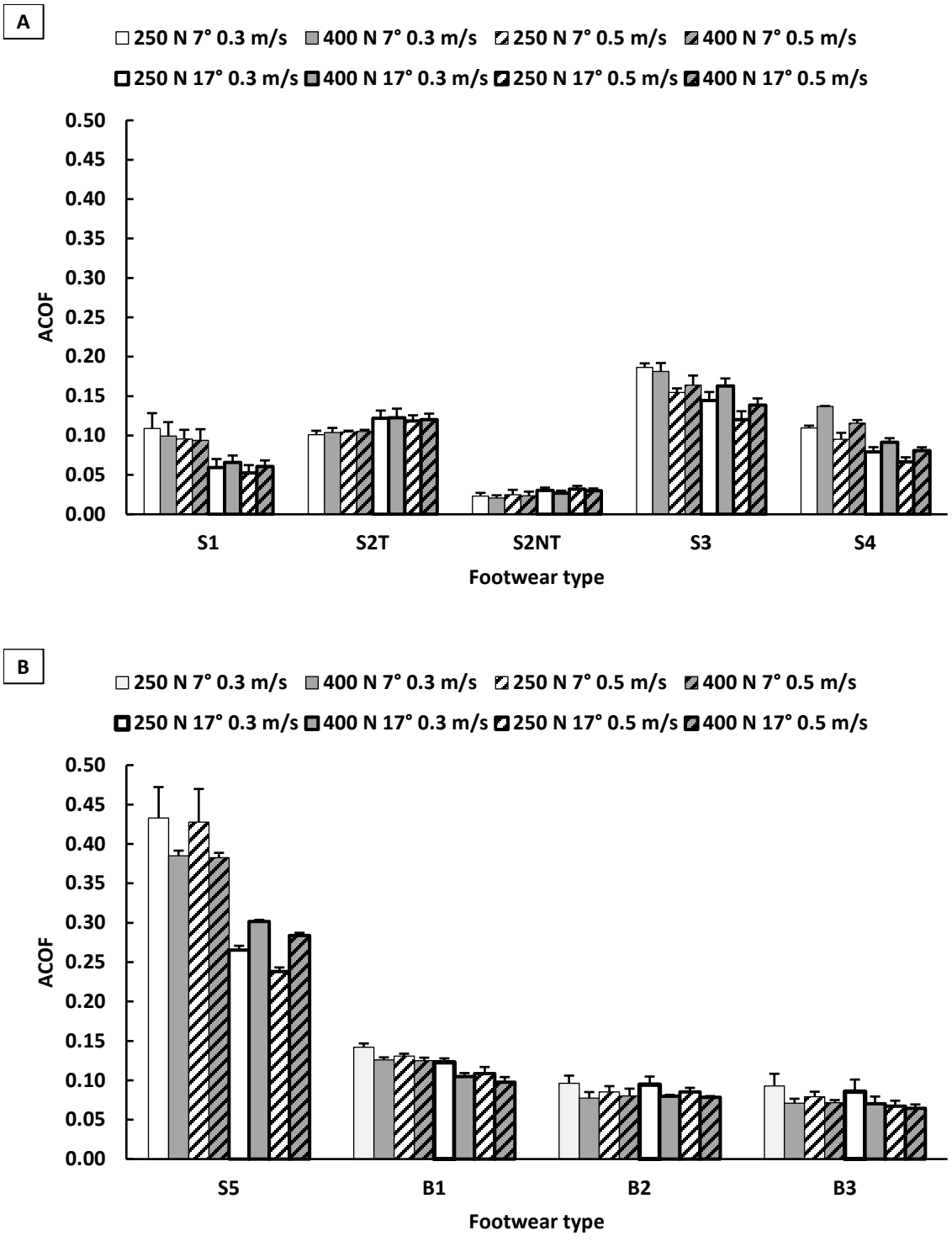

Figure 3-5. ACOF across all the sets of testing parameters for each footwear condition: (A) S1, S2T, S2NT, S3 and S4 (B) S5, B1, B2 and B3.

The logistic regression models indicated that both ACOF and ACOF-RCOF were significant predictors of slip risk for all sets of testing parameters (Table 3-5 and Table 3-6). ACOF-RCOF had higher Wald statistics (Wald = 14.54 to 20.40, $p < 0.001$) than ACOF alone (Wald = 13.23 to 15.23, $p < 0.001$). The set of testing parameters with the highest Wald statistic was 250 N, 17°, 0.5 m/s for both ACOF (Wald = 15.23, $p < 0.001$) (Figure 3-6A) and ACOF-RCOF (Wald = 20.40, $p < 0.001$) (Figure 3-6B). Furthermore, the second highest Wald statistic was for the test conditions of 250 N, 17°, 0.3 m/s for both ACOF (Wald = 15.18, $p < 0.001$) and ACOF-RCOF (Wald = 19.59, $p < 0.001$). The set of testing parameters with the lowest Wald statistics was 250 N, 7°, 0.3 m/s for both ACOF (Wald = 13.23, $p < 0.001$) and ACOF-RCOF (Wald = 14.54, $p < 0.001$). The ROC curves for the logistic regression models with ACOF-RCOF as the predictor showed that 250 N, 17°, 0.5 m/s had the maximum AUC of 0.815 (Table 3-6) (Figure 3-6C). The sensitivity and specificity at ACOF-RCOF at the optimal cutoff of -0.128 were 66.7% and 84.8%, respectively (Table 3-6). The ROC curves for the logistic regression models with ACOF-RCOF as the predictor indicated that 400 N, 7°, 0.3 m/s (Figure 3-7A) had the lowest AUC of 0.774 (Table 3-6 and Figure 3-7B).

Table 3-5. Testing parameter sets sorted based on the Wald statistic of the logistic regression models with ACOF as the predictor (including beta values).

Testing parameter set	Intercept ß0	ACOF ß1	Wald	p-value (Wald)
250 N, 17° , 0.5 m/s	-5.21	-4.22	15.23	<0.001
250 N, 17°, 0.3 m/s	-4.75	-4.01	15.18	<0.001
400 N, 7°, 0.3 m/s	-3.83	-3.33	14.72	<0.001
400 N, 7° , 0.5 m/s	-4.35	-3.80	14.63	<0.001
400 N, 17°, 0.5 m/s	-4.96	-4.07	14.42	<0.001
400 N, 17°, 0.3 m/s	-4.41	-3.68	14.19	<0.001
250 N, 7° , 0.5 m/s	-4.64	-4.08	13.70	<0.001
250 N, 7°, 0.3 m/s	-3.93	-3.56	13.23	<0.001

Table 3-6. Testing parameter sets sorted based on the Wald statistic, and sensitivity (specificity) and AUC (95% confidence interval: CI) from ROC curves of the logistic regression models with ACOF-RCOF as the predictor (including beta values). Sensitivity and specificity were taken from the point of the ROC curve where the line most deviated from a line with slope of 1. Odds ratio (95% confidence interval: CI) were calculated for 0.01 increase in ACOF-RCOF.

Testing parameter set	Intercept ß0	ACOF-RCOF ß1	Wald	p-value (Wald)	AUC (CI)	Sensitivity (Specificity)	Odds ratio (CI)
250 N, 17°, 0.5 m/s	-4.76	-35.46	20.40	<0.001	0.815 (0.726-0.880)	66.7 (84.8)	0.70 (0.60-0.82)
250 N, 17°, 0.3 m/s	-3.74	-30.12	19.59	<0.001	0.806 (0.713-0.875)	66.7 (86.1)	0.74 (0.65-0.85)
250 N, 7°, 0.5 m/s	-3.34	-28.43	18.40	<0.001	0.804 (0.707-0.874)	62.2 (92.4)	0.75 (0.66-0.86)
400 N, 17°, 0.5 m/s	-3.88	-29.29	18.05	<0.001	0.797 (0.700-0.868)	73.3 (77.2)	0.75 (0.65-0.85)
400 N, 7°, 0.5 m/s	-2.88	-24.44	17.48	<0.001	0.791 (0.693-0.864)	57.8 (92.4)	0.78 (0.70-0.88)
400 N, 17°, 0.3 m/s	-2.93	-22.78	16.31	<0.001	0.787 (0.685-0.863)	73.3 (79.8)	0.80 (0.71-0.89)
400 N, 7°, 0.3 m/s	-2.20	-18.88	15.86	<0.001	0.774 (0.674-0.850)	57.8 (88.6)	0.83 (0.75-0.91)
250 N, 7°, 0.3 m/s	-2.24	-20.43	14.54	<0.001	0.776 (0.670-0.855)	55.6 (96.2)	0.82 (0.73-0.91)

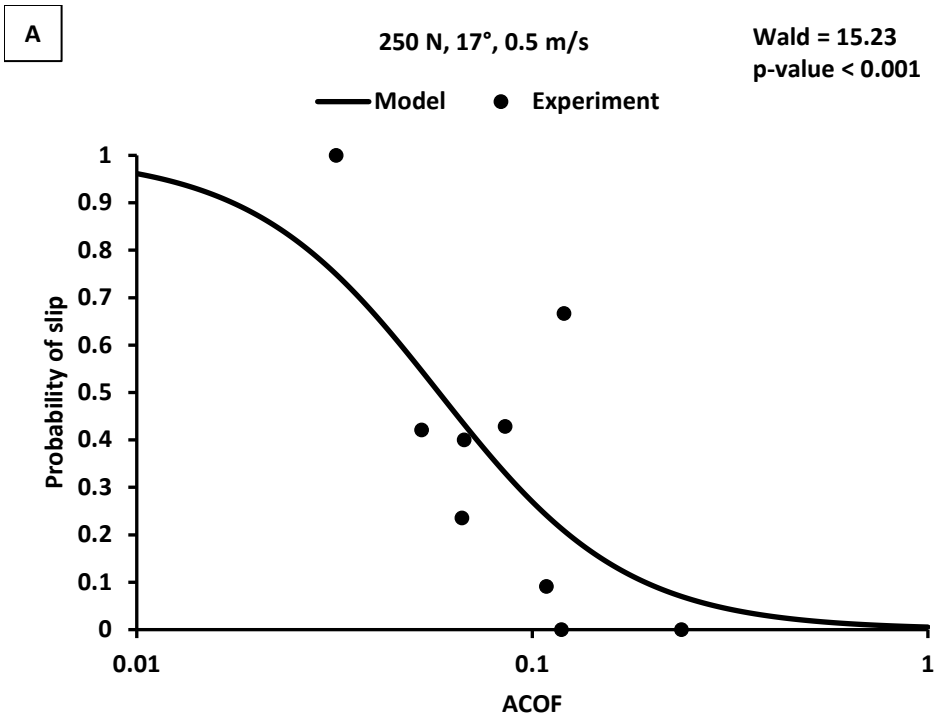
A
250 N, 17°, 0.5 m/s
Wald = 15.23
p-value < 0.001
Model
Experiment
Probability of slip
1
0.9
0.8
0.7
0.6
0.5
0.4
0.3
0.2
0.1
0
0.01
0.1
1
ACOF

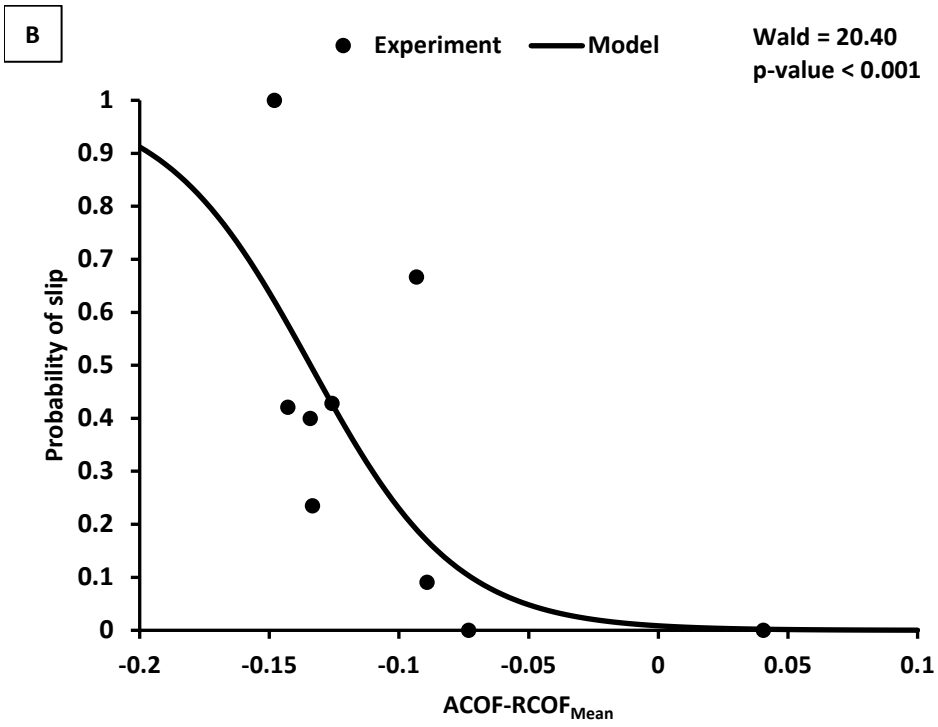
B
Experiment
Model
Wald = 20.40
p-value < 0.001
Probability of slip
1
0.9
0.8
0.7
0.6
0.5
0.4
0.3
0.2
0.1
0
-0.2
-0.15
-0.1
-0.05
0
0.05
0.1
ACOF-RCOF$_{Mean}$

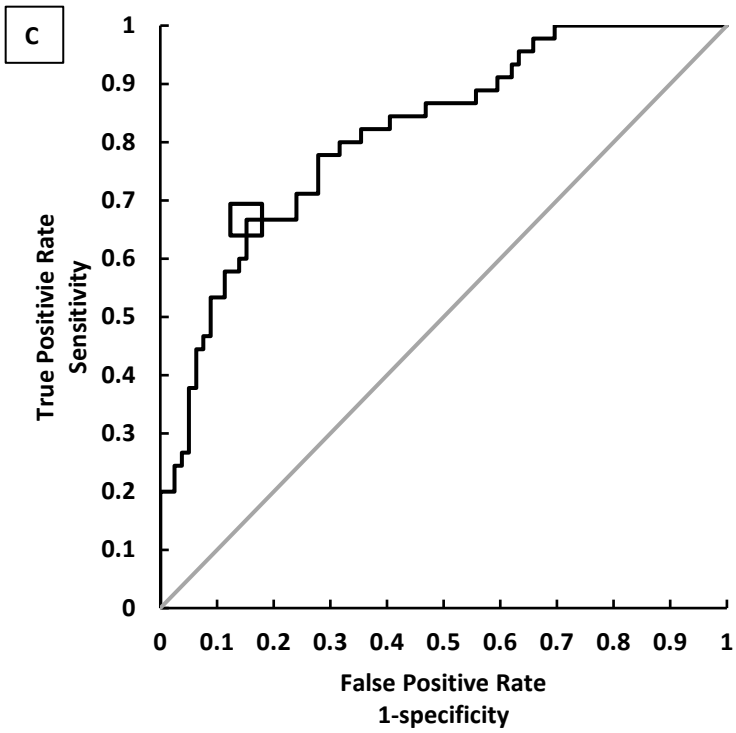

Figure 3-6. Logistic regression models with (A) ACOF and (B) ACOF-RCOF as the predictor and occurrence of a slip event as the outcome for 250 N, 17°, 0.5 m/s. (C) The ROC curve using ACOF-RCOF as the predictor for 250 N, 17°, 0.5 m/s. The black line represents the True Positive Rate-False Positive Rate curve and the gray line represents a slope of 1. The square symbol represents an optimal ACOF-RCOF cutoff of -0.128.

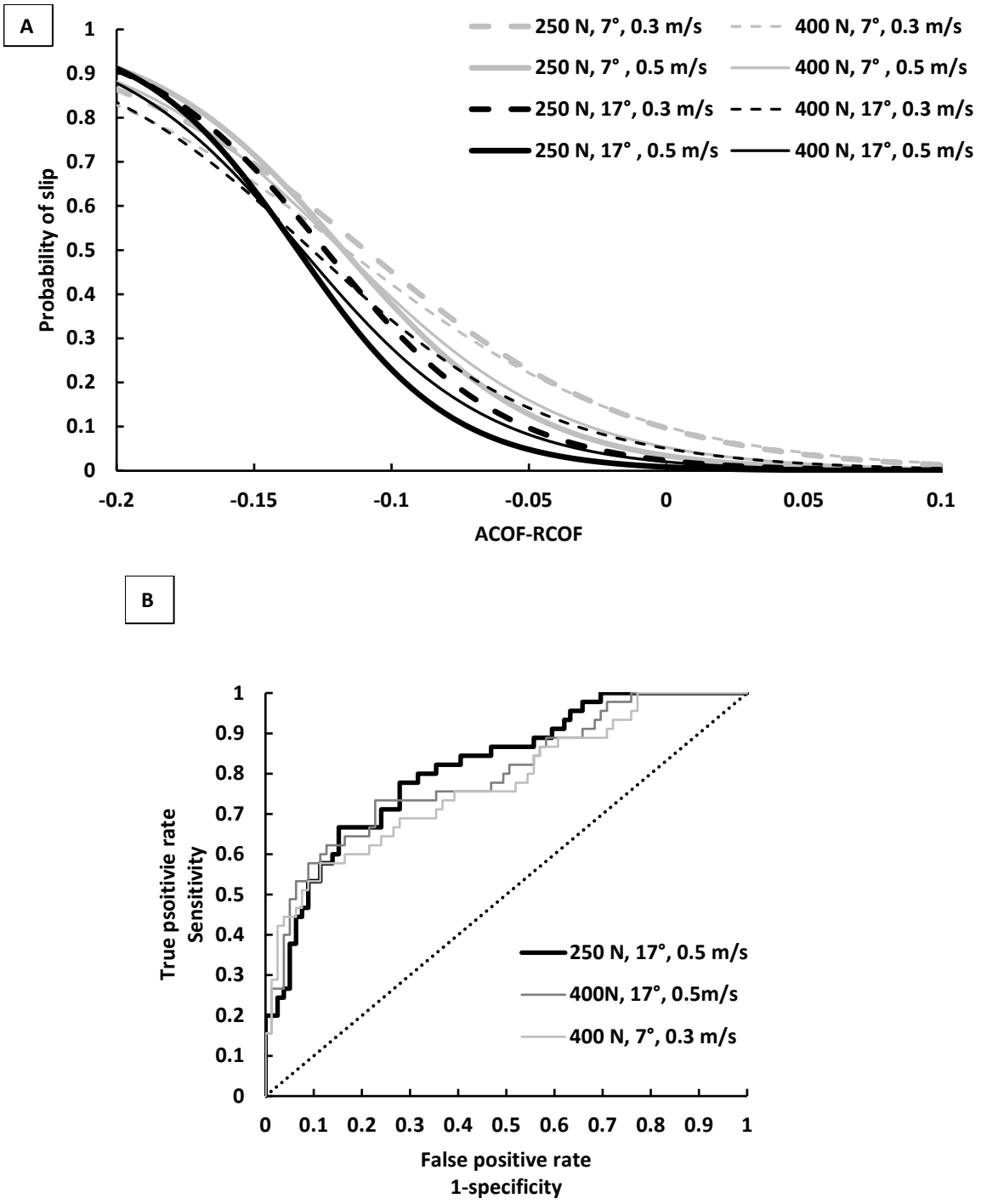

Figure 3-7. (A) Logistic regression model for the eight ACOF testing parameter sets. (B) The ROC curve using ACOF-RCOF as the predictor for the highest (250 N, 17°, 0.5 m/s, AUC: 0.815), fourth highest (400 N, 17°, 0.5 m/s, AUC: 0.797) and lowest AUC (400 N, 7°, 0.3 m/s, AUC: 0.774). The dashed line represents a slope of 1.

3.5 DISCUSSION

All of the testing parameter sets predicted slipping but the best test set for predicting slips was 250 N, 17°, 0.5 m/s. The next most predictive test set was 250 N, 17°, 0.3 m/s, which demonstrates the ability of using a normal force of 250 N and a shoe-floor angle of 17° to predict slips with this slip-tester. Based on an ACOF-RCOF cutoff of -0.128 for the 250 N, 17°, 0.5 m/s test set, the sensitivity and specificity were 66.7% and 84.8%, respectively.

The normal force (250 N) and shoe-floor angle (17°) from the best set (250 N, 17°, 0.5 m/s) were consistent with the state of heel at slip initiation reported by recent biomechanics studies. Specifically, the vertical component of ground reaction forces has been shown to be less than 300 N (Iraqi & Beschorner, 2017) and the shoe-floor angle has been reported as 14.7° (Albert et al., 2017) at the moment of slip initiation. Furthermore, the results were consistent with the previous research that ACOF (Burnfield & Powers, 2006; Siegmund et al., 2006) and ACOF-RCOF (Burnfield & Powers, 2006; Siegmund et al., 2006; Tsai & Powers, 2008) are significant predictors of slip risk for same level walking. Using the difference between ACOF and RCOF improved the slip prediction models, which is consistent with the previous findings (Burnfield & Powers, 2006; Siegmund et al., 2006).

The effect of testing parameters on ACOF was consistent with previous research that biomechanical factors affect ACOF (Beschorner et al., 2007; Blanchette & Powers, 2015b; Redfern & Bidanda, 1994). The effect of shoe-floor angle ($p < 0.001$), sliding speed ($p = 0.001$) and shoe-floor angle*normal force ($p = 0.024$) on ACOF were in agreement with findings of Beschorner et al. (Beschorner et al., 2007). Beschorner et al. found that normal force had significant effect on ACOF. However, these effects were inconsistent and varied with shoe-floor angle and sliding speed. The lack of effect of normal force on ACOF was consistent with Redfern

and Bidanda who reported that normal force levels (40-80 N) had small effects on ACOF (Redfern & Bidanda, 1994). Therefore, this research is consistent with other research demonstrating that shoe-floor angle and sliding speed have the greatest impact on ACOF.

Accurately evaluating the slip-resistance properties of footwear can guide footwear development. Footwear manufacturers use ACOF experiments to test and improve their footwear's slip-resistance. Using a test that poorly predicts slip outcome may guide footwear designers toward suboptimal outsole designs. For example, the heel shape (e.g., bevel angle) may lead to different ACOF values at different shoe angles since it will influence contact area (Moghaddam & Beschorner, 2017). Therefore, using the conditions that best predict slips is likely to lead to improve footwear designs.

Results of this study suggest that certain test sets yield ACOF values that predict slips with better certainty than other tests sets. For instance, the test sets with the highest AUC (i.e., 250 N, 17°, 0.5 m/s) and lowest AUC (400 N, 7°, 0.3 m/s) predicted a similar slip rate at an ACOF-RCOF value of -0.2, i.e. 91.2% and 82.9%, respectively. However, at an ACOF-RCOF value of -0.08, the slip rate is over 20% higher for 400 N, 7°, 0.3 m/s (33.4%) than for 250 N, 17°, 0.5 m/s (12.8%). Moreover, 250 N, 17°, 0.5 m/s showed a sensitivity of 86.7% at a 50% specificity level whereas 400 N, 7°, 0.3 m/s showed a sensitivity of 75.6% at a 50% specificity level (Figure 7B). Thus, altering the test conditions can improve slip prediction certainty.

The slipping rate across the footwear-floor-contaminant conditions were supported by the ACOF values measured using the Portable Slip Simulator, suggesting that a lower ACOF at the footwear-floor interface will be associated with a higher slipping risk. However, the results from one of the shoes, S3, appeared to deviate from the trends observed for the other shoes (i.e., a relatively high ACOF as well as high slip rate). Certain factors may explain the surprisingly high

slip rate for this shoe. First, while the RCOF values were not significantly different across footwear, S3 had the highest mean RCOF compared to the other footwear. RCOF is a sensitive predictor of slipping on moderately slippery surfaces (Beschorner et al., 2016). Second, subtle differences in biomechanical/gait parameters might exist due to the individual differences and footwear design, which may not be fully explained by RCOF. Third, random statistical variations might have overestimated the slip rate for S3. Thus, further biomechanical analysis during gait and slipping might be needed to better understand the complex interactions between slip outcome, an individual gait patterns, and footwear design.

Certain limitations of the study should be acknowledged. First, while the number of outsole-contaminated conditions were larger than any previous study to-date, they were still limited to nine conditions. More data from other conditions and parameters would improve our understanding of the best set or parameters under various conditions. Second, ACOF measurements were carried out only for footwear US men's shoe size 9 and the effect of footwear size was not included in the study. Third, the normal force and shoe-floor angle were fixed within each ACOF trial. Biomechanical studies have shown that these variables change over time and mimicking these changes may improve prediction of slips. Lastly, this research may not apply to alternative footwear which are known to have different slipping biomechanics (Chander et al., 2015a, 2015b).

This study showed that the choice of testing parameters (normal force, shoe angle, and sliding speed) is important to obtaining measures that predict slips across different types of footwear and contaminants. Using a normal force of 250 N and a shoe-floor angle of 17° resulted in a predictive model that was sensitive and specific. The other testing conditions generated models that were predictive of slip too, but were less sensitive. The testing conditions have complex

interactions with the footwear conditions. Specifically, an interaction effect between shoe-floor angle and shoe type on ACOF values indicates that this variable may be especially influential in determining a shoe's performance. Using a set of testing parameters that predicts slips will likely lead to a better capability to create new footwear designs with better slip-resistance, resulting in a reduction in slip and fall injuries and deaths.

4.0 KINEMATICS AND KINETICS OF THE SHOE DURING HUMAN SLIPS

4.1 ABSTRACT

This paper quantified the heel kinematics and kinetics during human slips with the goal of guiding available coefficient of friction (ACOF) testing methods for footwear and flooring. These values were then compared to the testing parameters recommended for measuring shoe-floor ACOF. Kinematic and kinetic data of thirty-nine subjects who experienced a slip incident were pooled from four similar human slipping studies for this secondary analysis. Vertical ground reaction force (VGRF), center of pressure (COP), shoe-floor angle, side-slip angle, sliding speed and contact time were quantified at slip start (SS) and at the time of peak sliding speed (PSS). Statistical comparisons were used to test if any discrepancies exist between the state of slipping foot and current ACOF testing parameters. The main findings were that the VGRF (26.7 %BW, 179.4 N), shoe-floor angle (22.1º) and contact time (0.02 s) at SS were significantly different from the recommended ACOF testing parameters. Instead, the testing parameters are mostly consistent with the state of the shoe at PSS. We argue that changing the footwear testing parameters to conditions at SS is more appropriate for relating ACOF to conditions of actual slips, including lower vertical forces, larger shoe-floor angles and shorter contact duration.

4.2 INTRODUCTION

Slips and falls are among the leading causes of occupational injuries. Slips, trips and falls (STF) lead to over 9 million treated cases in hospital emergency departments (Centers for Disease Control and Prevention, 2017) and more than one-fourth of the non-fatal occupational injuries in 2015 (U.S. Department of Labor- Bureau of Labor Statistics, 2016b). A survey among young adults indicated that about half of the falling accidents are caused by slips (Heijnen & Rietdyk, 2016). STF prevention programs often recommend use of slip-resistant footwear to reduce slip risk (Bell et al., 2008).

Mechanical slip-testing devices that measure available coefficient of friction (ACOF) are frequently utilized to assess the slip-resistant performance of footwear and flooring. These devices sometimes attempt to simulate the dynamics of the foot slip in order to achieve "biofidelity" (i.e., similarity between test conditions and shoe dynamics during slipping) since the kinematics and kinetics applied to footwear affect ACOF measurements (Chang et al., 2016). For instance, ACOF measurements are affected by shoe-floor angle (Beschorner et al., 2007; Blanchette & Powers, 2015b), vertical force (Beschorner et al., 2007; Blanchette & Powers, 2015b), horizontal sliding speed (Beschorner et al., 2007; Blanchette & Powers, 2015b; Redfern & Bidanda, 1994) and contact duration (Gronqvist et al., 2003). Prior research has suggested that using test conditions that are more biofidelic improves the ability of ACOF measurements to predict slips (Iraqi et al., 2018). Furthermore, other biomechanical parameters that have not been formally incorporated in ACOF testing may need to be considered to improve biofidelity. For example, the side-slip angle (i.e., direction of heel velocity relative to the footwear orientation in the transverse plane) (Albert et al., 2017) has generally been limited to sliding the footwear specimen along the axis of the shoe (toe-to-heel) during ACOF measurements. This testing parameter may be important since the

orientation of tread design affects ACOF (Blanchette & Powers, 2015a; Li & Chen, 2005; Yamaguchi et al., 2017). Another parameter that has not been considered is the location of the center of pressure (COP) for ground reaction forces, which may affect the portion of the tread in contact during ACOF testing. Thus, additional studies that report biomechanics of slipping would contribute knowledge towards developing ACOF measurement methods with improved biofidelity.

Biomechanical studies have reported certain kinematic and kinetic variables during slipping. These variables have been parameterized at times including heel strike (HS) (Chambers et al., 2002; McGorry et al., 2010), slip start (SS) (Albert et al., 2017; Strandberg & Lanshammar, 1981), and peak sliding speed (PSS) (Albert et al., 2017; Lockhart et al., 2003; Moyer et al., 2006; Strandberg & Lanshammar, 1981). These times represent the initial condition of the step, beginning of slip, and most severe portion of the slip, respectively. Table 4-1 summarizes key biomechanical variables at the times of HS, SS, and PSS reported in previous studies. The reported values are variable within each time and across times. These biomechanical studies serve as an important resource regarding the slipping biomechanics, which can be used to guide ACOF measurement techniques.

Table 4-1. Vertical force, shoe-floor angle, sliding speed, contact time, and side-slip angle reported by biomechanical studies at HS, SS and PSS. Values are reported as mean ± standard deviations.

Study	Time points	Vertical force (%BW)	Shoe-floor angle (°)	Sliding speed (m/s)	Contact time from HS (ms)	Side-slip angle (+Medial)	Floor with liquid contaminant
(Strandberg & Lanshammar, 1981)	HS	NA	21.3±5.5	0.67±0.76 ʊ	NA	NA	NA-soap
	SS	64±16	5.5±5.9	0.15±0.12 ʊ	48 ± 21	NA	
(Cham & Redfern, 2002b)	HS	NA	16.8±1.5§, 20.5± 0.9*	1.01±0.20§, 0.62±0.41*	NA	NA	Vinyl with motor oil (10W-40)
	SS	NA	1.5±0.6§, 2.2±1.8*	NA	78.9±9.5§ 65.7±3.5*	NA	
	PSS	NA	NA	0.31±0.06§, 0.78±0.16*	121.4±12.4§, 171.4±28.7*	NA	
(Chambers et al., 2002)	HS	NA	28.2±3.0	NA	NA	NA	Vinyl with glycerol
	PSS	NA	NA	1.79±0.37	NA	NA	
(McGorry et al., 2010)	HS	NA	25.3±5.4	1.10±0.74	NA	NA	Delrin dry, Teflon dry, Teflon with aerosol furniture polish
(Albert et al., 2017)	SS	NA	14.7±6.9	0.27±0.18	NA	66°±54.1	Vinyl with 90% glycerol-10% water solution
	PSS	NA	9.5±7.0	1.72±0.71	NA	3.2±15.9	

ʊ the average sliding speed have been calculated based on the individual results reported from each subject in the study
§ at forward slipping during slip recovery
***** at forward slipping for slip leading to a fall
NA indicates that this variable was not reported for this study

Gaps in the literature exist regarding the biomechanical state of the foot during slipping. One limitation is that some studies only considered one type of footwear (Albert et al., 2017; Cham & Redfern, 2002b), which might not be generalizable. Other studies have been limited to few participants repeatedly exposed to slippery conditions (Strandberg & Lanshammar, 1981). Data from repeated slips may not represent the dynamics during unexpected human slips since participants alter their gait when anticipating a slippery condition (Cham & Redfern, 2002a). The limitations in the previous biomechanical studies impede the development of test methods that are biofidelic. Thus, additional research on this topic is needed.

The aim of the current study was to quantify biomechanical variables during unexpected human slips to guide biofidelic measurements of ACOF. Additionally, this study will determine if these variables deviate from the ACOF testing parameters recommended by a footwear traction testing standard (ASTM F2913-11, 2011) (Table 4-2) for variables specified in this testing standard.

Table 4-2. ACOF testing parameters recommended by footwear traction testing standards (ASTM F2913-11, 2011; EN ISO 13287, 2012)

ACOF testing parameters	Levels
Vertical force (N)	400, 500
Shoe-floor angle (°)	7
Side-slip angle (°)	0
Sliding speed (m/s)	0.3
Contact time (s)§	0.10-0.30
Contact time (s)*	0.30-0.60
Contaminants§δ	water, detergent aqueous solution, oil
Contaminants*	glycerol aqueous solution, detergent aqueous solution, ethanol aqueous solution

§ ASTM F2913-11
* EN ISO 13287
δ The ACOF testing methods specified by ASTM F2913 are reportedly applicable to a wide variety of surface contaminants including but not limited to liquid water, ice, grease and oil.

4.3 METHODS

4.3.1 Subjects

Kinetic and kinematic data for 39 subjects (18 female; mean age: 22.3±3.3years ; mean height: 173.1±8.3cm; mean body mass: 68.3±10.0kg; mean BMI: 22.8±3.2) were extracted from four different human slipping studies performed in the same laboratory (Beschorner et al., 2016; Chambers & Cham, 2007; Iraqi et al., 2018; Jones et al., 2018; Moyer et al., 2006). The exclusion criteria for subject recruitment were any conditions that potentially impede regular gait such as orthopaedic, cardiovascular, neurological and pulmonary abnormalities. The human slipping protocols were authorized by the University of Pittsburgh Institutional Review Board and subjects

were provided with informed consent. The inclusion criteria into this post-hoc analysis were: 1. young adults (18-35 years), 2. slips that were preceded by at least three gait trials where their left foot landed clearly on the dry force plate preceding the exposure to liquid-contaminant, and 3. a slip distance of greater than 3cm (Albert et al., 2017; Beschorner et al., 2016; Leamon & Li, 1990). In addition, subjects or liquid-contaminated trials were further excluded during data processing based on the following criteria: 4. subjects' left foot did not land completely on the liquid-contaminated force plate, 5. if the subject experienced a heel slip in the first liquid-contaminated exposure, then their second exposure was discarded, 6. if the subject's required coefficient of friction (RCOF) changed more than 16% after exposure to the first liquid-contaminated trial, their second exposure was discarded, and 7. the subject reported that they noticed the liquid contaminant before stepping on it (Iraqi & Beschorner, 2017; Iraqi et al., 2018; Jones et al., 2018). The rationale for criteria 5-7 were that these subjects might be anticipating a slip and could have different gait patterns. These criteria were established a priori (i.e., prior to performing statistical analyses).

4.3.2 HUMAN SLIPPING PROTOCOL

Subjects wore a whole-body marker set and donned a safety harness. Subjects were instructed to ambulate across a level vinyl composite tile walkway in a lab space equipped with a motion capture camera system (Vicon, Oxford, UK) and force plates (Bertec 4060A, Columbus, OH). Subjects performed three to five gait trials on the dry walkway where their left foot fully landed on the force plate. Then, the subjects were unexpectedly exposed to a liquid contaminant that was placed on the force plate. Subjects were distracted before each walking trial by facing away from the walkway, listening to music using earphones, and working on a word puzzle. The lights were dimmed to obscure the application of liquid contaminants. After their first unexpected liquid-

contaminated exposure, the subjects were assigned to a different pair of footwear, performed 15-20 gait trials on the dry walkway and were exposed to the second unexpected liquid-contaminated trial. Kinematic and kinetic data were sampled at 120Hz and 1080Hz, respectively.

Three types of shoes and two types of boots were included in this analysis. The shoe types included a work shoe (S1), a work shoe labeled as slip-resistant with completely worn tread (S2), and another work shoe labeled as slip-resistant (S3). The two boots had the same collar height and tread design but different outsole material hardness (B1 and B2). The liquid contaminants included diluted glycerol and canola oil (Table 4-3).

Table 4-3. Footwear-floor-contaminant conditions and number of slips (n) for each condition.

Study	Footwear	n	Liquid contaminant	Floor	Footwear style	Tread design	ACOF§ (Iraqi et al., 2018)
(Chambers & Cham, 2007; Moyer et al., 2006)	S1	7	75% glycerol-25% water	Vinyl		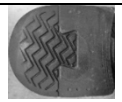	0.052 (0.010)
(Iraqi et al., 2018)	S2	10	90% glycerol-10% water	Vinyl		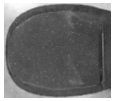	0.032 (0.004)
(Jones et al., 2018)	S3	10	Canola oil	Vinyl			0.120 (0.011)
(Beschorner et al., 2016)	B1	6	50% glycerol-50% water	Vinyl			0.085 (0.005)
(Beschorner et al., 2016)	B2	6	50% glycerol-50% water	Vinyl		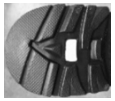	0.067 (0.007)

§ The testing parameters for ACOF measurements were 250 N normal force, 17° shoe-floor angle and 0.5 m/s sliding speed.

4.3.3 Data and statistical analysis

Kinematic and kinetic variables were quantified from the left foot (i.e., slipping foot) and included the vertical component of ground reaction forces (VGRF), COP, shoe-floor angle, side-slip angle, sliding speed and contact time. The COP data were quantified relative to the local coordinate system (LCS) of the heel. A LCS was created for the heel originating at the inferior portion of the calcaneus (inferior heel) and based on markers placed on the medial (medial heel) and lateral (lateral heel) side of the shoe about one third of the footwear length anterior from the heel (Figure 4-1A and B). The y-axis connected the inferior heel marker to the mid-point of medial and lateral heel markers. The z-axis pointed superiorly and was perpendicular to the plane formed by the three markers. The side-slip angle was defined as the angle between the heel's y-axis and the velocity vector in the transverse plane of the heel LCS (Figure 4-1) (Albert et al., 2017). The sliding speed was tracked using the position of the inferior heel marker in the plane parallel to the floor. The shoe-floor angle was calculated using the inferior heel marker and medial toe marker (Albert et al., 2017; Cham & Redfern, 2002b). The shoe-floor angle for static trials was quantified and subtracted from the shoe-floor angles in the gait trials. Position data were filtered using a 4th order low-pass Butterworth filter with a cutoff frequency of 24Hz (Iraqi et al., 2018).

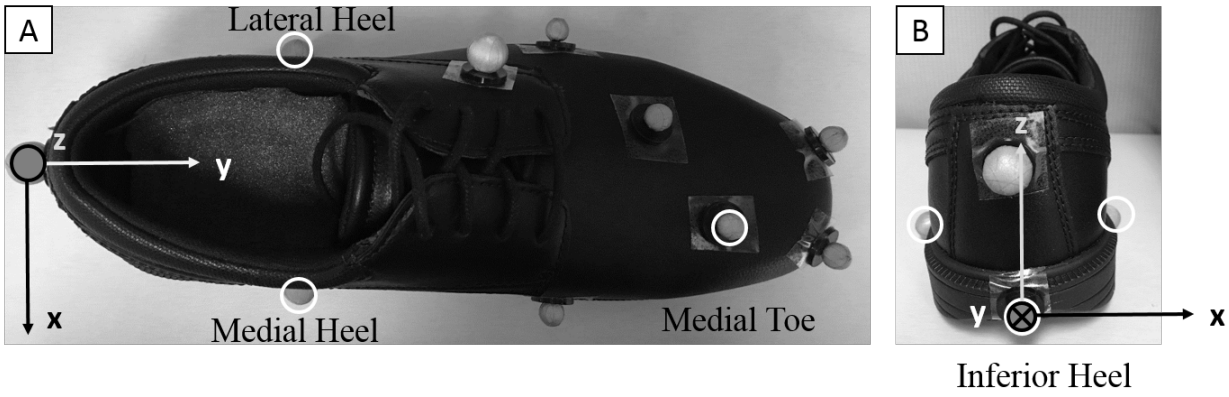

Figure 4-1. Reflective markers placed on the footwear from (A) top view and (B) posterior view.

Two time points were used to parameterize the kinematic and kinetic variables: (1) SS; and (2) PSS (Figure 4-2A-C). The start of slipping (SS) was defined as the first local minimum in the sliding speed (Figure 4-2A) of the inferior heel marker after HS (Figure 4-1B) (Albert et al., 2017; Lockhart et al., 2003; Strandberg & Lanshammar, 1981). HS was defined as the instant when VGRF first exceeded 25 N (Figure 4-2A). The PSS was defined as the first local maximum in heel speed 50 ms after HS (Moyer et al., 2006) (Figure 4-2A). SS was chosen since this represents the moment when ACOF is insufficient to prevent the foot from accelerating. PSS was selected as the moment of greatest slip severity.

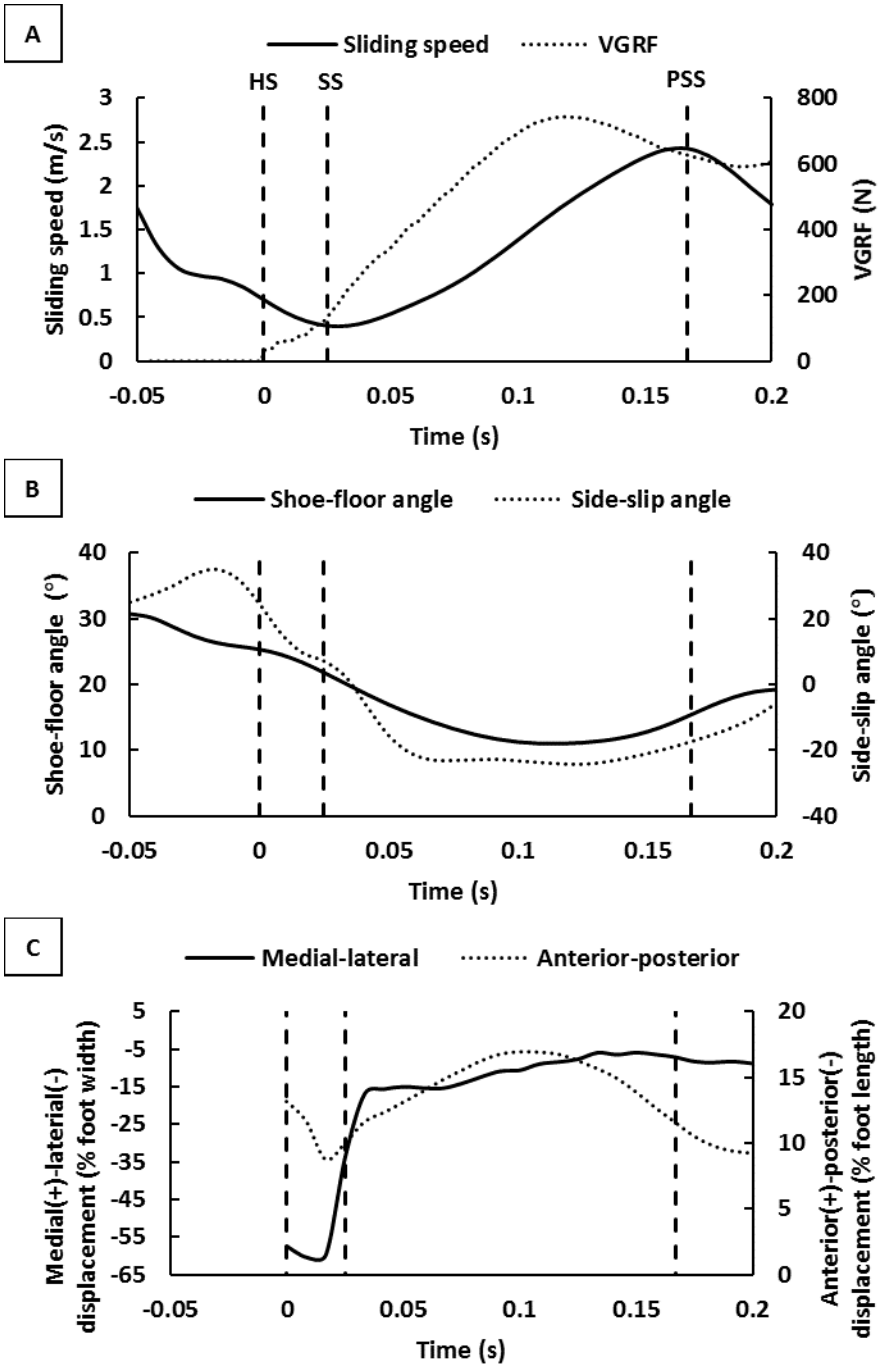

Figure 4-2. Typical heel dynamics at heel strike (HS), slip start (SS) and peak sliding speed (PSS) from an unexpected liquid-contaminated exposure: (A) sliding speed and VGRF, (B) shoe-floor angle and side-slip angle, and (C) COP. HS occurs at time = 0. SS was defined as the first local minimum after HS in the sliding speed. PSS was defined as the first local maximum in the sliding speed.

The slip distance and RCOF values were quantified to determine the occurrence of a slip in each liquid-contaminated exposure and to assess potential anticipation of a slippery condition, respectively. The resultant slip distances were calculated between the SS and the first local minimum after PSS (Iraqi et al., 2018). The RCOF values were calculated from the three preceding gait trials (on the dry walkway) based on a method by Chang et. al. (Chang et al., 2011b).

Statistical analyses were performed to test different statistical model assumptions, to test whether kinematic and kinetic differences exist across the footwear conditions, and to test if any discrepancies exist between the state of slipping foot and ACOF testing parameters (ASTM F2913-11, 2011). A Shapiro-Wilk test was used to test if each kinematic and kinetic variables (response variables) at SS and PSS met the required assumptions for ANOVA of normally distributed residuals. A Levene test was used to test the ANOVA assumption for homoscedasticity across the footwear type. Transformation of the response variables were often successful in achieving homoscedasticity and normally-distributed residuals. In these circumstances, the reciprocal transformation was performed for reporting the mean and confidence intervals. If the ANOVA assumptions were met, a one-way ANOVA was performed to test differences across the footwear type on the response variable at SS and PSS. A Tukey HSD multiple comparison procedure was performed as a post-hoc analysis if a significant effect was found for footwear type. Simultaneous confidence intervals (CI) were calculated using Bonferroni method to test if the ACOF testing parameters (Table 4-2) used in standard measurement of ACOF by whole-shoe testers (ASTM F2913-11, 2011) were within the 95% CI of the corresponding kinematic and kinetic variables across each footwear type at SS and PSS. If the ANOVA assumptions were not met, non-parametric analyses were performed to test for differences across footwear type (Kruskal-Wallis test); post-hoc analyses when a significant footwear type effect was observed (Steel-Dwass test);

and whether the standard measurement value was within the 95% CI (Wilcoxon Signed-Rank test). All statistical analyses were performed using commercial software (JMP® Pro 13.1.0, SAS Institute Inc., Cary, NC, USA) with a significance level of 0.05.

4.4 RESULTS

Transformations were used to correct for skew and homoscedasticity (positive skew: square root of VGRF and contact time, logarithm of sliding speed; and negative skew: square of contact angle). When transformations were unsuccessful, non-parametric methods were used on data that were not normally distributed including $COP_{Anterior\text{-}Posterior}$ ($W= 0.80$, p-value < 0.001) at SS, shoe-floor angle ($W=0.92$, p-value $= 0.007$) at PSS, and $COP_{Medial\text{-}Lateral}$ ($W = 0.91$, p-value $= 0.004$) at PSS. Non-parametric methods were also used for contact time at PSS since it had an unequal variance ($F_{4,34} = 4.74$, p-value $= 0.004$).

Table 4-4. Statistical results for the effect of footwear type on the kinematic and kinetic variables. Significant F, χ^2 and p-values ($p<0.05$) have been made bold. Horizontal lines separate the kinematic variables, kinetic variables and contact time.

Biomechanical variables	Time point	$F_{4,34}$ (p-value)	χ^2_4 (p-value)
Shoe-floor angle	SS	0.57 (0.688)	
	PSS		6.59 (0.159)
Side-slip angle	SS	1.96 (0.123)	
	PSS	**3.38 (0.020)**	
Sliding speed	SS	**4.89 (0.003)**	
	PSS	1.60 (0.198)	
VGRF	SS	2.40 (0.070)	
	PSS	1.78 (0.156)	
$COP_{Medial-Lateral}$	SS	**2.89 (0.037)**	
	PSS		8.56 (0.073)
$COP_{Anterior-Posterior}$	SS		**10.42 (0.034)**
	PSS	2.64 (0.051)	
Contact time	SS	0.99 (0.428)	
	PSS		**12.88 (0.012)**

4.4.1 Kinematic variables

The shoe-floor angle across all the subjects were 22.1º (mean) at SS and 11.3º (median) at PSS. The 7° shoe-floor angle suggested by ASTM F2913 was lower than the 95% CI of the mean shoe-floor angle for all of the footwear types at SS (Figure 4-3A). At PSS, the 7° shoe-floor angle was not significantly different from the median shoe-floor angle for each footwear (Figure 4-3B). The central tendency of the side-slip angle across all the subjects was primarily in the medial direction at SS (mean = 15.6°) and then changed to the lateral direction at PSS (mean = -6.3°). The 0° side-slip angle incorporated in the ASTM F2913 was within the 95% CI of the mean side-slip angle of all the footwear types at SS and PSS (Figure 4-3C). The average sliding speed across all the subjects was 0.10 m/s at SS and 1.87 m/s at PSS. The 0.3m/s sliding speed suggested by ASTM

F2913 was within the CI of the mean sliding speed of S1 and S2, but was higher than the CI of the mean sliding speed of S3, B1 and B2 at SS (Figure 4-3D). The 0.3 m/s was significantly lower than PSS across all the footwear types (Figure 4-3D).

Among the kinematic variables, the sliding speed at SS and side-slip angle at PSS were significantly different across footwear conditions (Table 4-4). The post-hoc analysis at SS indicated that the sliding speed for B2 was significantly lower than S1 and S2. The post-hoc analysis at PSS indicated that the side-slip angle for S2 was pointing in medial direction whereas S3 was in lateral direction.

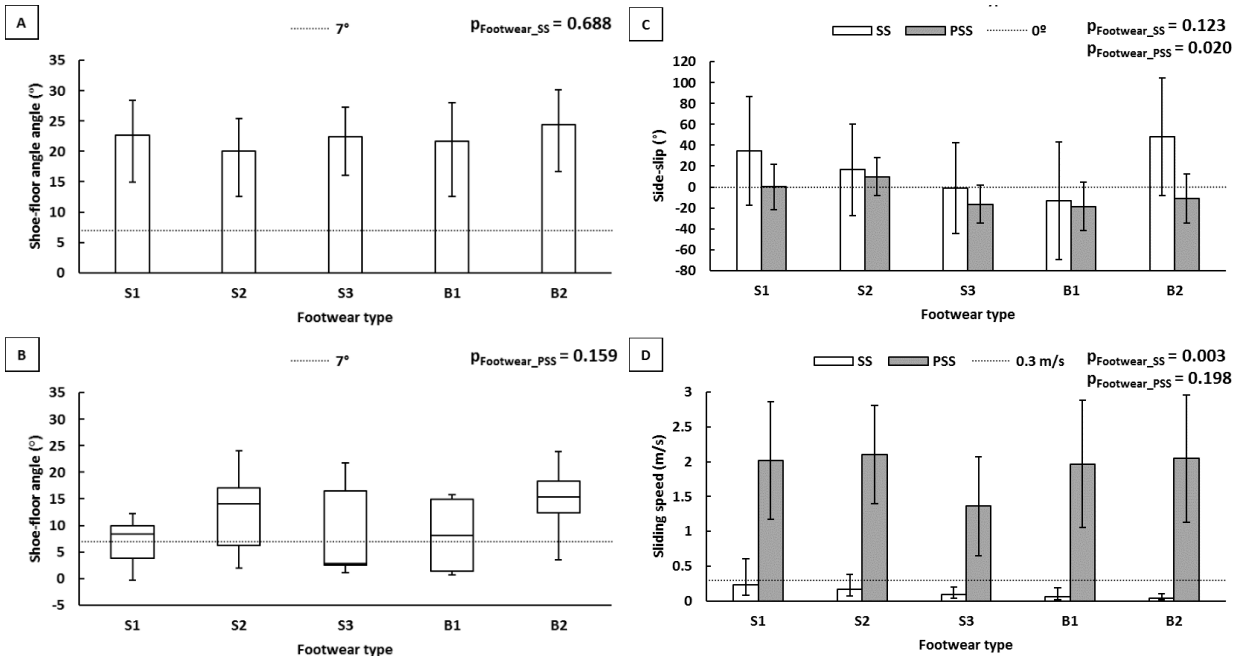

Figure 4-3. Kinematic variables across different footwear conditions: (A) Shoe-floor angle (°) at SS (The error bars represent 95% CI). (B) Summary statistics (minimum, 1st quartile, median, 3rd quartile and maximum) of shoe-floor angle () at PSS. (C) side-slip angle (°) at SS and PSS (Positive angles represent a medial angle and negative angles represent a lateral angle) (The error bars represent 95% CI), and (D) Sliding speed (m/s) at SS and PSS (The error bars represent 95% CI).

4.4.2 Kinetic variables

The average VGRF across all the subjects was 26.7 %BW (179 N) at SS and 74.0 %BW (497 N) at PSS. At SS, the 400 N and 500 N normal force suggested by ASTM were significantly higher than S2, S3, B1 and B2 (Figure 4-4). However, 400 N and 500 N were within the CI of S1 at SS. The 400 N and 500 N were within the CI of the mean VGRF for all the footwear at PSS, except for S3 where the 400 N was below the CI (Figure 4-4B). The average $COP_{Medial-Lateral}$ across all the subjects was primarily in the lateral direction at SS (mean = -30.2% foot width) and PSS (median=-11.6% foot length). The $COP_{Anterior-Posterior}$ across all the subjects was 9.6% foot length at SS (median) and 16.2% foot length at PSS (mean).

The $COP_{Medial-Lateral}$ and $COP_{Anterior-Posterior}$ were significantly different across footwear conditions at SS (Table 4-4) (Figure 4-5). The post-hoc analysis at SS indicated that B2 had significantly more lateral COP than S2. At SS, S3 was more anterior than B1.

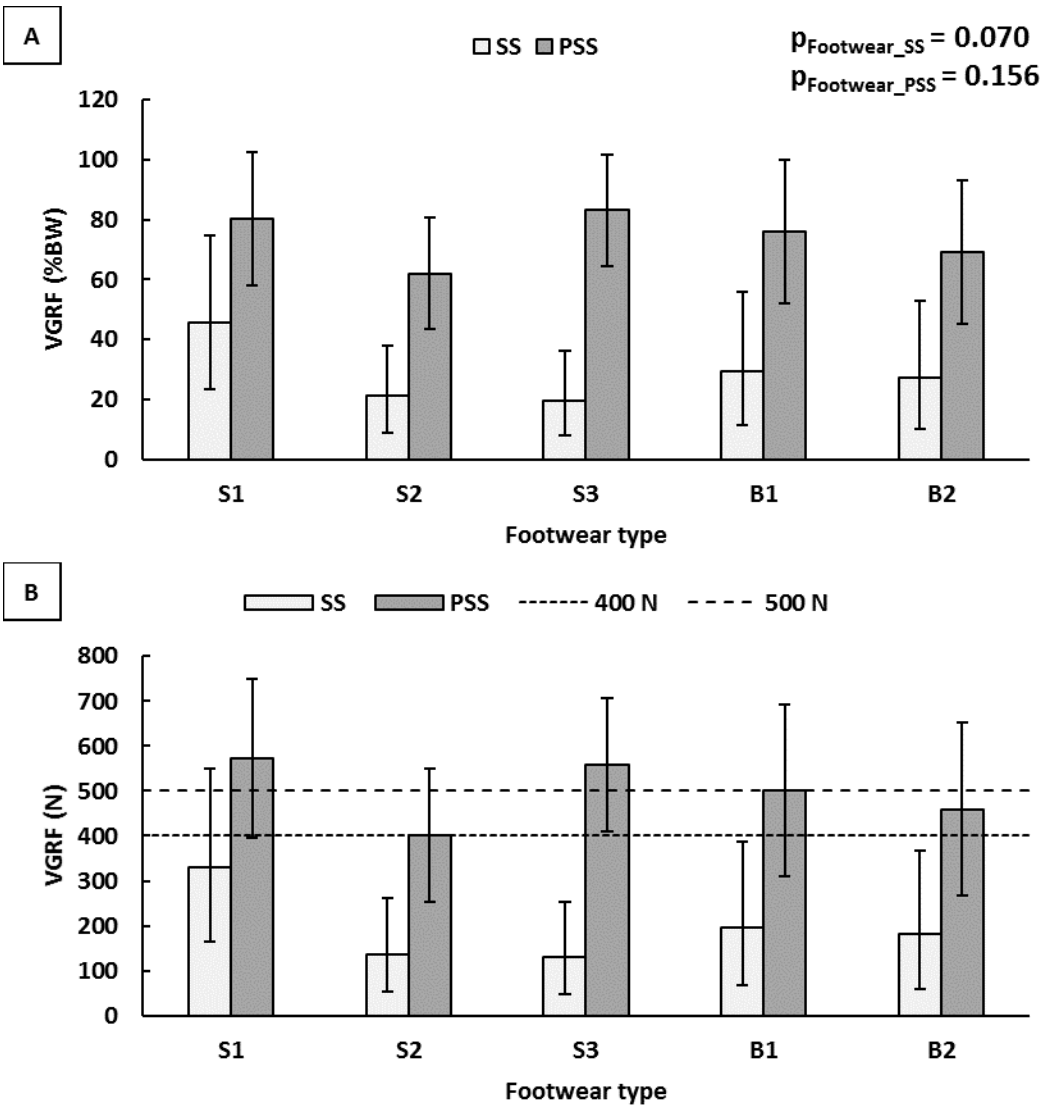

Figure 4-4. VGRF across different footwear (A) normalized to bodyweight and (B) raw force value at SS and PSS. (The error bars represent 95% CI). Horizontal dashed lines represent the force values included in the ASTM F2913 standard.

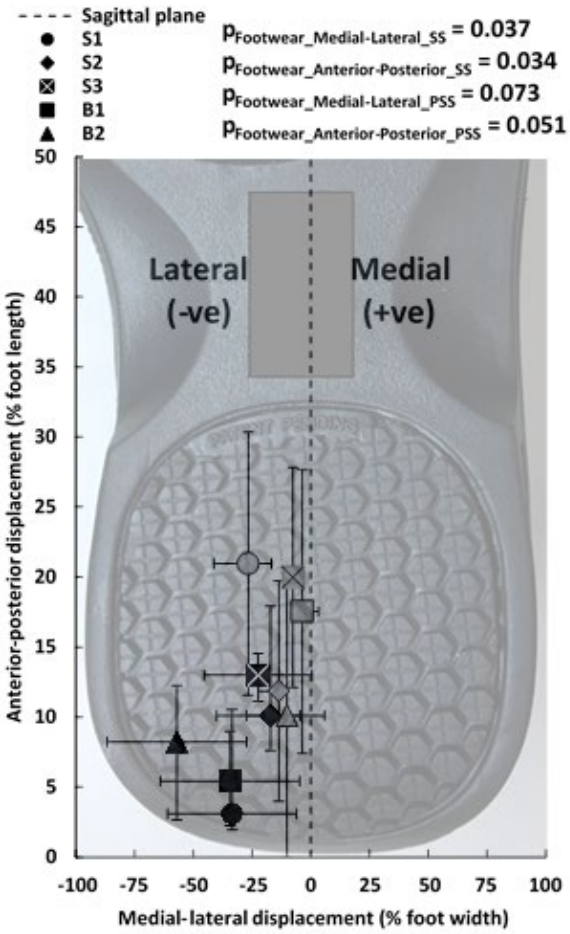

Figure 4-5. COP (% foot length and width) across different footwear at SS (black) and PSS (gray). The error bars represent 95% CI for $COP_{Medial\text{-}Lateral}$ at SS and $COP_{Anterior\text{-}Posterior}$ at PSS. The error bars represent IQR for $COP_{Anterior\text{-}Posterior}$ at SS and $COP_{Medial\text{-}Lateral}$ at PSS.

4.4.3 Contact time

The contact time across all the subjects at SS and PSS were 0.02 s (mean) and 0.15 s (median), respectively. The contact time was significantly different between footwear types at PSS (Table 4-4) (Figure 4-6B). The post-hoc analysis at PSS indicated that the contact time for S3 was significantly shorter than B2. The measurement period of 0.10-0.30 s suggested by ASTM F2913

was significantly higher than the contact time for all the footwear type at SS (Figure 4-6A). The CI for contact time was within the range of 0.10-0.30 s for all footwear at PSS.

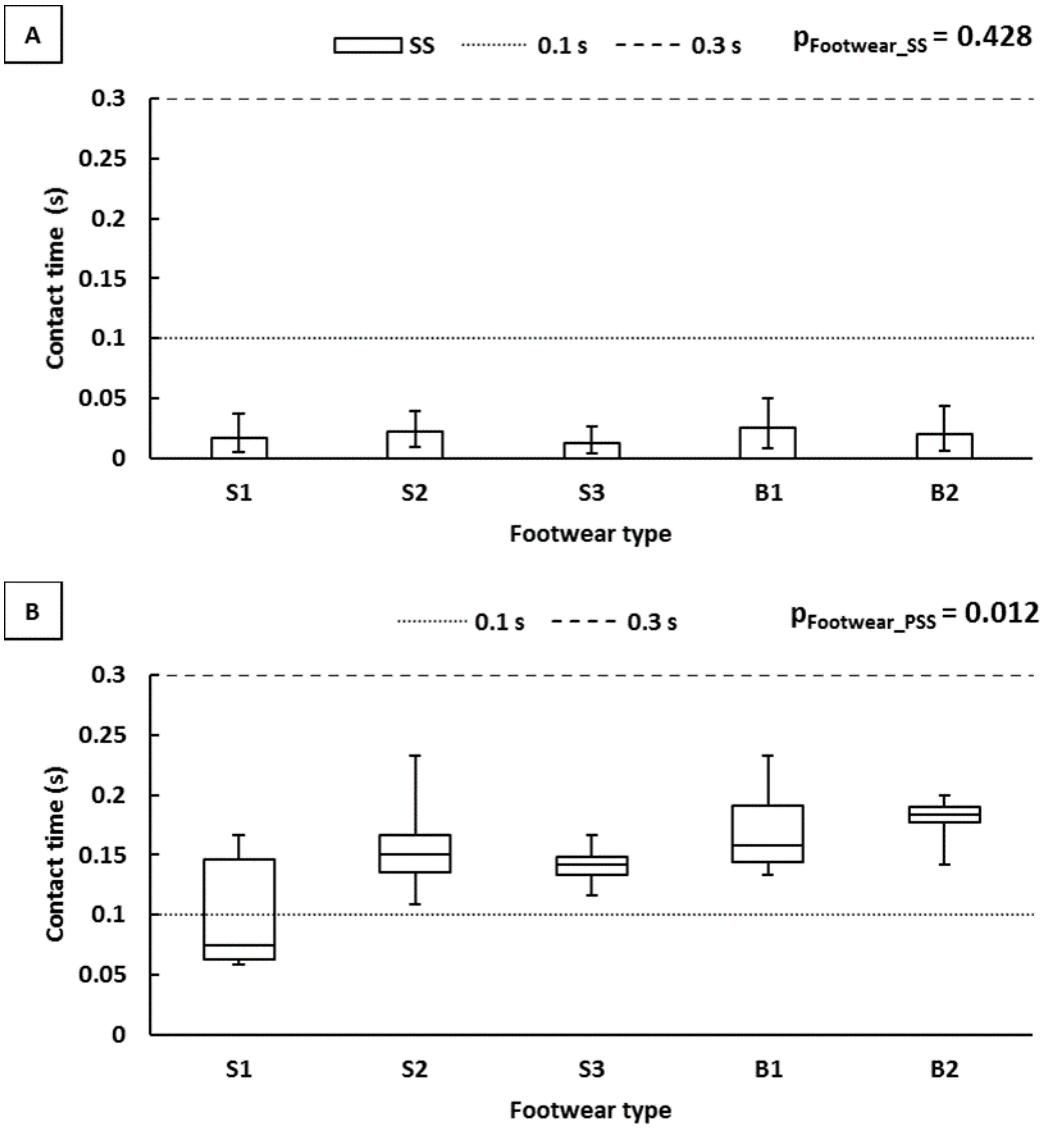

Figure 4-6. (A) Contact time (s) across different footwear at SS. (The error bars represent 95% CI). (B) Box plot including summary statistics (minimum, 1st quartile, median, 3rd quartile and maximum) of contact time (s) across different footwear at PSS.

4.5 DISCUSSION

The main finding of this study was that significant discrepancies exist between the footwear traction testing parameters and the heel dynamics during the onset of slipping. The central tendency of the VGRF, shoe-floor angle and contact time at SS were significantly different from the ACOF testing parameters suggested by ASTM F2913-11 (ASTM F2913-11, 2011). In particular, the average VGRF at SS was less than the typical normal forces (400 N to 500 N) applied during ACOF testing. In addition, the average shoe-floor angle at SS exceeded the contact angle (7º) used for the ACOF testing methods. The general consensus is that ACOF testing conditions should match the biomechanics of human gait during slipping accidents (Chang et al., 2016; Redfern et al., 2001). Thus, current footwear traction testing methods may become more biofidelic by including lower vertical forces (< 400N), larger shoe-floor angles (> 7º) and shorter contact duration (< 0.10s) to be more consistent with heel dynamics at SS. The biomechanical variables at SS may be more informative with respect to friction that prevents slips, whereas increased friction at PSS might be important to lessen the severity of slip. A few of the biomechanical variables were consistent across footwear conditions while others were more footwear-dependent like the sliding speed at SS and side-slip angle at PSS. Thus, data across multiple designs of footwear should be considered when making determinations of what constitutes biofidelic for these specific variables.

Differences were observed in biomechanical parameters at SS between the current study and previous biomechanics of slipping studies. The average VGRF (26.7%BW) was substantially less than the vertical force of 64% BW (Strandberg & Lanshammar, 1981) and the median shoe-floor angle (22.1°) was significantly higher than the contact angle of 5.5° (Strandberg & Lanshammar, 1981), 1.5° (slip recovery) (Cham & Redfern, 2002b) and 2.2° (slip leading to a fall)

(Cham & Redfern, 2002b). In addition, the contact time (0.02 s) quantified in this study was shorter than the time of slip start of 0.05 s (Strandberg & Lanshammar, 1981), 0.08 s (slip recovery) (Cham & Redfern, 2002b) and 0.07 s (slip leading to a fall) (Cham & Redfern, 2002b). One explanation for these discrepancies is that one of the studies repeatedly slipped subjects (Strandberg & Lanshammar, 1981). Thus, the kinematic and kinetic parameters reported may have been influenced by anticipation of a slippery condition (Cham & Redfern, 2002a; Chambers et al., 2002). The differences between this study and Cham and Redfern's (2002b) study might be due to the higher severity of slips (as measured by PSS) in the current study (1.87m/s) compared to 0.31 m/s (slip recovery) and 0.78 m/s (slip leading to a fall) reported by Cham and Redfern's (2002b). Another reason for the differences between the current study and the previous studies may be due to different shoe-floor-contaminant combinations (Table 4-1), which may lead to different levels of slippery conditions. The shoe-floor angle (22.1°) was closer to the value reported by Albert et al. (2017) (14.7°). We should note that Albert et al. (2017) used the same testing condition as S2 but with a different set of subjects. The average sliding speed (0.10 m/s) at SS was within the range of sliding speeds observed in other studies, i.e., 0.08-0.32 m/s (Strandberg & Lanshammar, 1981) and 0.27 m/s (Albert et al., 2017). Moreover, the side-slip angle was primarily pointing to the medial direction during SS, which was consistent with Albert et al. (2017).

The kinematic and kinetic parameters quantified in this study provide insight on the state of the heel during SS. The dynamics of the heel has significant implication on slip-resistance measurements since biomechanical factors affect ACOF (Beschorner et al., 2007). First, the results suggest that lower VGRF (< 400N) and higher shoe-floor angles (> 7º) should be included in the ACOF testing parameters to achieve higher relevance to the onset of slipping. Inappropriate vertical force and contact angle during ACOF measurements may yield incorrect conclusion about

the slip-performance of the footwear since ACOF is sensitive to the biomechanical parameters (Beschorner et al., 2007; Blanchette & Powers, 2015b). For instance, a contact angle of 7° may result in a higher ACOF value compared to 22.1° due to a higher contact area (Moghaddam & Beschorner, 2017), which may provide an incorrect inference about the slip-performance of the footwear. Second, the non-zero value of sliding speed during slip start suggests that ACOF performed by dynamic test methods might be more relevant to the dynamics of heel slip compared to static test methods. The static friction is generally higher than the dynamic friction (Gronqvist et al., 2003), which may overestimate the slip-performance of the footwear. Third, the lateral COP location at slip start may suggest that during ACOF testing a slight inversion angle of the footwear to achieve a lateral COP may need to be considered. This indicates that tread on the lateral portion of the footwear may be more critical than tread on the medial side.

The limitations of this study should be acknowledged. First, the effect of footwear size was not considered in the analyses. Second, the footwear styles were limited to the oxford and boot, therefore the results may not be generalizable to alternative footwear, which have different biomechanical properties during slipping (Chander et al., 2016). Third, this study only included young adults and may not be generalizable to older adults since kinematic and kinetic differences may exists between these age groups during slipping accidents (Moyer et al., 2006).

In summary, the current study suggests that the footwear traction testing methods may not resemble the vertical force, shoe-floor angle, sliding speed and contact duration at SS or the sliding speed at PSS. These variables may need to be adjusted to account for the biomechanics of the foot during slip start and to improve the accuracy of the footwear traction testing methods.

5.0 PREDICTION OF THE FOOTWEAR TRACTION BASED ON OUTSOLE DESIGN FEATURES

5.1 ABSTRACT

The evaluation and proper selection of slip-resistant footwear is inhibited by expensive shoe traction testing methods. This is a major obstacle for occupational health and safety practitioners to design out the slipping hazard and to implement the Prevention through Design (PtD) process. This study aimed to develop a statistical model that predicts ACOF based on simple and inexpensive measurement of footwear outsole design features. The model is only applicable to boundary lubrication (shoes with tread on liquid contaminated walking surfaces). To create this model, geometric and material hardness parameters of sixty-three footwear designs labeled as slip-resistant were measured. A robotic friction measurement device was used to simulate a foot slip after heel strike and a force plate was used to quantify ACOF. A backward elimination, forward selection and hybrid regression method were used to develop the model based on the outsole design features to predict ACOF. A k-fold cross-validation method was performed to test the prediction ability of the regression model. Results indicated that 88% of the variability in ACOF was explained by the contact area, heel shape, hardness, shape factor, and floor type. Moreover, considerable variation in the slip-resistant performance of the shoes was observed within brands likely due to different heel geometries. The results from this study may provide a valid, cost-

effective and simple assessment tool for occupational health and safety practitioners to select footwear with improved traction to protect workers and promote occupational safety.

5.2 INTRODUCTION

One barrier that impedes the selection of appropriate slip-resistant footwear by employers and consumers is the expense and expertise required for current shoe traction testing technology. Currently, experimental methods that are used to assess ACOF are expensive (friction testing of a single shoe-floor-contaminant combination is approximately $250), which limits access to these methods. Given the compelling evidence that ACOF is affected by footwear tread design features, a valid assessment tool to predict ACOF values based on the outsole design features could be useful for assessing the slipping risk associated with the shoe design. This may provide safety practitioners with the opportunity to select higher performance slip-resistant shoes through these assessments and reduce worker's slip propensity. However, a lack of observational tools and infrequent use of solely hardware-based methods are evident from previous research. A recent survey study has revealed that only 14.8% of the safety practitioners utilized slipmeters to evaluate slip risk (Lowe et al., 2018). Lowe et al. (2018)'s study was a follow-up to the survey conducted by Dempsey et al. (2005), which indicated that 21.4% of practitioners used slipmeters. Use of tribometers to *assess footwear* is probably even lower than the use of tribometers in general given that whole shoe tribometers are more expensive and less portable than floor tribometers. An observational assessment tool may increase the use of ergonomic tools by practitioners to address slip-related injuries.

One challenge in developing an observational assessment tool to evaluate shoe traction is the different tribology mechanisms that dictate the relationship between shoe-floor-contaminant combination and ACOF. For instance, Li and Chen (2004) showed that an increase in ACOF can be achieved by implementation of tread groove design in footwear pads compared to pads with no groove in water, detergent aqueous solution and vegetable oil. However, an increase in the groove width from 0.3 cm to 1.2 cm increased ACOF for water and detergent aqueous solution, but had no significant effect for vegetable oil. Redfern and Bidanda (1994) demonstrated that concrete had higher ACOF for PVC (polyvinyl chloride) soles (with no tread) for water, low and high viscosity motor oil compared to steel surface, but did not have the same effect for rubber soles (with tread). These complexities may be due to tribosystems that are operating across different tribology mechanisms (see Section 2.3.2 and 2.3.3). An approach to overcome this challenge is to limit the scope of the model to only a single tribology mechanism. In this study, we aim to focus only on hysteresis friction operating in boundary lubrication.

A precondition to develop a tread assessment tool is to identify the outsole features that contribute to the different types of lubrication mechanism at the shoe-floor interface. The presence of outsole tread with drainage capability reduces hydrodynamic fluid pressures (Beschorner et al., 2014; Singh & Beschorner, 2014) and ensures boundary lubrication. As discussed previously (Section 2.3.2, Lubrication mechanism of shoe-floor interface), boundary lubrication has higher ACOF than hydrodynamic lubrication since the shoe and floor asperities are in contact in boundary lubrication. This distinction of lubrication mechanism at shoe-floor interfaces is important since the governing equations of one lubrication regime may not be applicable to the other regime. Thus, the assumptions for a boundary lubrication tool may be the presence of tread.

In the boundary lubrication regime, certain tread features are correlated with the ACOF. Often, hysteresis is the dominant friction mechanism in the presence of high viscous lubricants (e.g., canola oil) operating in boundary lubrication since the presence of these contaminants reduces adhesion friction. Previous research has indicated that material hardness and contact area are correlated with hysteresis friction. Material hardness negatively impacts ACOF (Cowap et al., 2015; Jones et al., 2018; Strobel et al., 2012; Tsai & Powers, 2008) since softer material are subjected to higher deformations which increase contact area and reduce contact pressures (Moghaddam et al., 2018). Thus, hardness contributes to hysteresis component of friction (Cowap et al., 2015; Strobel et al., 2012). Contact area of outsole tread has shown to positively impact ACOF (Jones et al., 2018; Moghaddam et al., 2018) due to a reduction in contact pressures (Moghaddam et al., 2018). Other outsole features that have been shown to affect hysteresis friction are heel shape (in the sagittal plane) (Moghaddam & Beschorner, 2017) and heel width (in the frontal plane) (Jones et al., 2018). This is primarily explained by the changes in contact area. Beveled edge shoes tend to secure higher contact area than flat-edge shoes (Moghaddam & Beschorner, 2017). Higher heel width may also reduce contact pressures by increasing the contact area, which may subsequently increase hysteresis friction. Therefore, these outsole tread design features may form a basis for a tread assessment tool.

The objective of the current study was to develop a statistical model to predict footwear traction based on observable outsole design features. The rationale of this study was that developing assessment tools based on cost-effective and easily evaluated measures of outsole tread will enable more occupational health and safety practitioners to assess footwear and improve workers' safety.

5.3 MATERIALS AND METHODS

This study consists of three main components: shoe outsole tread measurements, ACOF measurements, and statistical model building. Geometric and material measurements were made from the outsole tread of sixty-three footwear designs. ACOF measurements were conducted using a robotic whole shoe tester for these shoes against two types of flooring. A multiple linear regression model was developed based on cross-validation for the statistical model building.

5.3.1 Materials

Sixty-three footwear that were marketed as slip-resistant from six brands (Shoe for Crews, Tredsafe, SR Max, SafeTstep, Dr. Scholl's, and Timberland PRO®) with low-collar height and laces were selected (Table 5-1). No alternative footwear was included such as overshoes, slip-on, and clog shoe since wearing alternative footwear tends to lead to different slipping biomechanics (Chander et al., 2016) and may be inappropriate for the specified ACOF test methods (Section 5.3.2). Slip-resistant footwear included casual, work, athletic and dress style that were marketed as men's, women's, and unisex shoes. Shoe selection was aimed to achieve variation in outsole geometry and material hardness between and within shoe brands. Twenty of the selected footwear (four per each brand, except Timberland PRO®) were modified to systematically control outsole geometry. Three pairs of shoes were custom made to have identical outsole tread geometry but with different levels of material hardness (F1, F2, F3). All sixty-three footwear were US size 9 men's shoe or the equivalent size for women's shoes.

Table 5-1. Lists of slip-resistant shoes included in the study from different brands (Rows that are bold represent modified shoes) (continued)

Shoe Code	Brand	Model	Style/item #	Style	Gender
A1	Shoes for Crews	Cambridge	6006	Dress	M
A2		Condor	24734	Athletic	M
A3		Delray - Canvas	38852	Casual	M
A4		Creed	21771	Athletic	M
A5		Senator	1201	Dress	M
A6		Avery	34545	Athletic	F
A7		Old School Low-Rider IV - Leather	39362	Casual	F
A8		Heather	9048	Athletic	F
A2HS		**Condor**	**24734**	**Athletic**	**M**
A1HW		**Cambridge**	**6006**	**Dress**	**M**
A1CA		**Cambridge**	**6006**	**Dress**	**M**
A1SF		**Cambridge**	**6006**	**Dress**	**M**
B1	Tredsafe	Axel	555307251	Athletic	M
B2		Executive II	553701356	Work	M
B3		Mario	553996011	Athletic	M
B4		Engage	565589700	Casual	U
B5		Kitch Canvas	553926483	Work	U
B6		Rig	553802532	Casual	U
B7		Nitro	556595638	Athletic	M
B8		Bailey	553987412	Athletic	W
B1HS		**Axel**	**555307251**	**Athletic**	**M**
B1HW		**Axel**	**555307251**	**Athletic**	**M**
B1CA		**Axel**	**555307251**	**Athletic**	**M**
B1SF		**Axel**	**555307251**	**Athletic**	**M**
C1	SR Max	Arlington	SRM350	Dress Oxford	F
C2		Tampa	SRM125	Athletic Oxford	F
C3		Abilene	SRM400	Casual Oxford	F
C4		Portland	SRM621	Skate	F
C5		Maxton	SRM620	Athletic	F
C6		Fairfax	SRM1580	Low Athletic	M
C7		Rialto	SRM6000	Athletic Sneaker	M
C8		Atlanta	SRM3700	Oxford	M
C2HS		**Tampa**	**SRM125**	**Athletic Oxford**	**F**
C1HW		**Arlington**	**SRM350**	**Dress Oxford**	**F**
C1CA		**Arlington**	**SRM350**	**Dress Oxford**	**F**

Table 5-1. (continued)

C1SF		Arlington	SRM350	Dress Oxford	F
D1	safeTstep	Deidre	162446	Oxfords	F
D2		Camina	159959	Runner	F
D3		Andre	173851	Court	F
D4		Kandice	163896	Canvas Oxfords	F
D5		Blast	159961	Runner	F
D6		Zeus	158795	Athletic	M
D7		Monroe	160023	Oxfords	M
D8		Halfpipe	166413	Canvas Oxfords	M
D1HS		**Deidre**	**162446**	**Oxford**	**F**
D1HW		**Deidre**	**162446**	**Oxford**	**F**
D1CA		**Deidre**	**162446**	**Oxford**	**F**
D1SF		**Deidre**	**162446**	**Oxford**	**F**
E1	Dr. Scholl's	Proudest	88626	Oxford	M
E2		Intrepid	88622	Sneaker	M
E3		Aiden	25311	Work Sneaker	M
E4		Roberts	14064	Oxford	M
E5		Hiro	25318	Oxford	M
E6		Kimberly II	88755	Sneaker	F
E7		Brave	88751	Sneaker	F
E8		Inhale	22876	Sneaker	F
E2HS		**Intrepid**	**88622**	**Sneaker**	**M**
E1HW		**Proudest**	**88626**	**Oxford**	**M**
E1CA		**Proudest**	**88626**	**Oxford**	**M**
E1SF		**Proudest**	**88626**	**Oxford**	**M**
F1	Timberland PRO	PRO-232	54.2±2.3Ψ	Work	M
F2		PRO-232	60.4±1.5Ψ	Work	M
F3		PRO-232	63.2±2.4Ψ	Work	M

Ψ shore A hardness
HS modified to control heel shape
HW modified to control heel width
CA modified to control contact area
SF modified to control shape factor

Footwear outsole features such as material hardness (Jones et al., 2018; Tsai & Powers, 2008), contact area (Jones et al., 2018; Moghaddam et al., 2018), heel width (Jones et al., 2018) and heel shape (Moghaddam & Beschorner, 2017) were selected for measurements based on their association with hysteresis friction from previous research. Additionally, shape factor (i.e., the loaded area of a rubber block divided by its area of lateral surface free to bulge) was considered since shape factor has been found to affect the deformability of the rubber block in other tribology applications (elastomeric bearings and tire tread) subjected to vertical loading (Imbimbo & De Luca, 1998; Sridharan & Sivaramakrishnan, 2012). We hypothesized that the shape factor of the individual tread will affect the ACOF.

The Shore A material hardness of five different treads was measured using a durometer (ASTM D2240-15, 2015). A mass of 1 kg was affixed and centered on the axis of the indentor as recommended by the ASTM D2240-15 (2015) to improve repeatability of handheld measurements and additionally shoes were secured using a bench vise during measurements. The contact area of the heel was measured using an ink pad, a white blank sheet of paper and a scanner (Jones et al., 2018; Tencer et al., 2004). Ink was applied to the outsole and the outsole was firmly pressed over a white blank sheet of paper. At least three imprints per shoe were created to ensure that pressure was applied across the entire heel section of the outsole and the heel imprint that had the maximum inked area was selected. The heel imprint was scanned and a MATLAB script (MATLAB, MathWorks®, Natick, MA) was developed to calculate the contact area (black region, Figure 5-1). The posterior-most point of the tread to 5 cm anterior of that point was used for calculation of the contact area (Figure 5-1) (Jones et al., 2018). The heel width and dimensions of the tread blocks were measured using a ruler and digital calipers, respectively. The heel width was measured 1.5 cm anterior of the posterior-most point of the tread (Figure 5-1) (Jones et al., 2018). Shoe beveling

features were observed by placing the shoe on a level surface. The heel part of the outsole was categorized as flat-edge or beveled edge if the outsole (heel region) was parallel to the leveled surface or formed a convex shape with respect to the leveled surface, respectively. The shape factor (S) was calculated based on the tread geometry at five different locations (Eq. 5-1) (Imbimbo & De Luca, 1998). The loaded area was defined as the top surface area of a tread (assuming no sipes, which are cuts or grooves on the tread surface) that was subjected to the normal load and the surface area free to bulge was considered as the lateral surface area (assuming no sipes) of a tread.

$$S = \frac{\text{Loaded area}}{\text{Surface area free to bulge}} \qquad \text{Eq. 5-1}$$

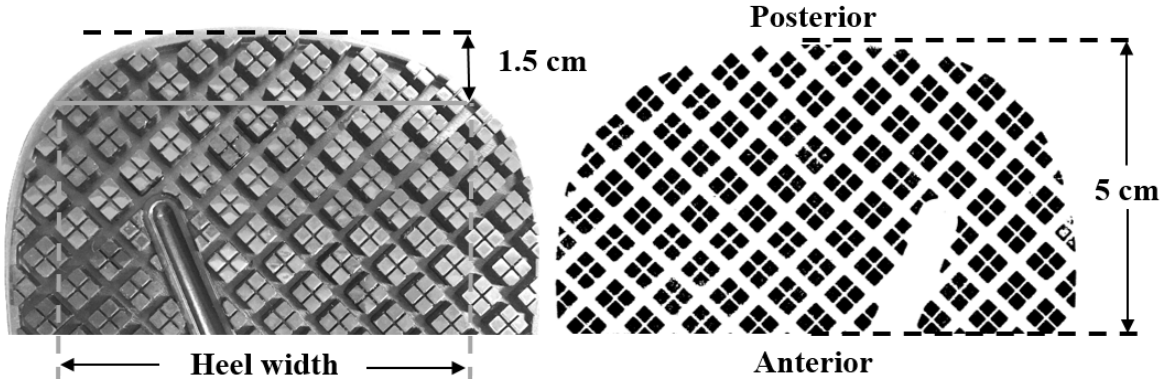

Figure 5-1. Contact area and heel width measurement

Four footwear from each brand (except Timberland PRO®) were altered to systematically vary contact area (A1CA-E1CA), heel width (A1HW-E1HW), shape factor (A1SF-E1SF) and heel shape (A2HS, B1HS, C2HS, D1HS, E2HS) within brands (Figure 5-2). (1) One flat-edge footwear per brand had tread removed at the midline (A1CA-E1CA). (2) One flat-edge footwear per brand

had individual tread removed at the outer edge (A1HW-E1HW). (3) One beveled edge footwear had individual tread removed (A2HS, C2HS, D2HS, E2HS) to approximate the heel width and contact area of the corresponding flat-edge footwear (A1, C1, D1, E1) if the beveled edge had higher contact area than the flat-edge shoe. Otherwise the flat-edge shoe had tread removed (B1HS, D1HS) to closely match the heel width and contact area of the corresponding beveled edge footwear (B2, D2). (4) One flat-edge footwear per brand had tread depth shortened (about 1 mm) by abrasion on a belt sander with 36 grit belt (A1SF-E1SF). Modification 1 and 2 allowed for contact area and heel width to be systematically modified while keeping the heel shape, shape factor and material hardness consistent across shoes. Modification 3 allowed to discern the effect of heel shape while keeping the shape factor, material hardness, contact area and heel width consistent across shoes. Modification 4 modified the shape factor by decreasing the tread depth. Roughness measurements were taken after abrasion to monitor the surface roughness of the abraded shoes with respect to the brand new shoes. Five roughness measurements on five different treads were recorded for each shoe in the direction of the shoe motion using a stylus profilometer (Surtronic S128, Taylor-Hobson®, AMETEK®, Leicester, United Kingdom). The scan length and cutoff frequency during roughness measurements of the tread surface were 0.16 cm and of 0.08 cm, respectively. The abrasion caused significant changes to the shoe tread surfaces (A1SF-E1SF). The average peak to valley height (R_z) for new shoes and abraded shoes (A1SF-E1SF) were 13.2±5.7 μm and 47.1±14.5 μm, respectively. The abraded shoes (A1SF-E1SF) were excluded *a priori* in the statistical analysis since the model does not account for dramatic changes to surface roughness.

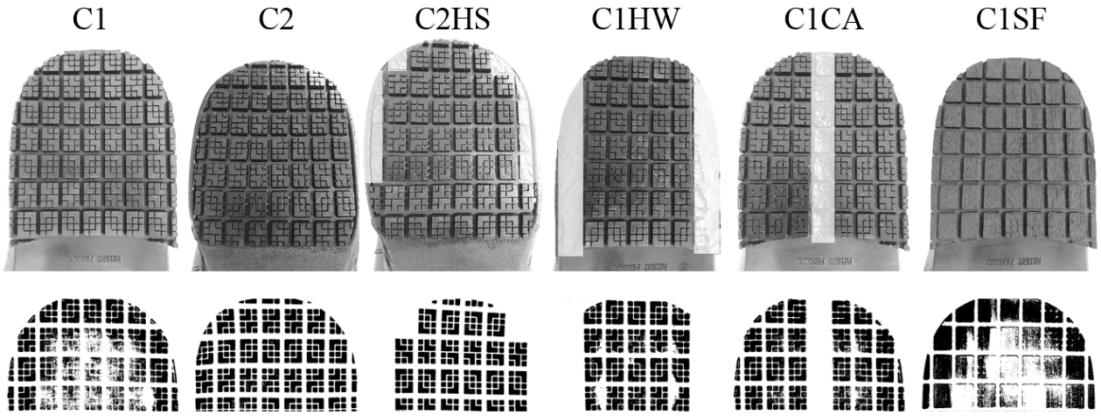

Figure 5-2. A representative of shoe samples being modified and their corresponding contact area (Grey area on the shoe outsole represents regions where individual treads were removed).

Canola oil was used as the liquid contaminant to simulate slippery conditions. A high and low traction tile were used for flooring condition: (1) ceramic tile (model: ADJF250802, make: ASTM), and (2) high pressure laminate tile (model: 00503 Stone Grafix, make: Formica®), respectively. Five roughness measurements were recorded for each tile in the direction of the shoe motion and 1 cm apart using the stylus profilometer. The scan length and cutoff frequency during roughness measurements were 0.8 cm and of 0.08 cm, respectively. The average peak to valley height (R_z) for ceramic and laminate tile were 22.2±1.4 μm and 17.0±0.9 μm, respectively. A total of 126 footwear-floor-contaminant combinations (63 footwear * 1 liquid contaminant * 2 floor surfaces) were tested.

5.3.2 ACOF measurements

A robotic friction measurement device, i.e. Portable Slip Simulator (Aschan et al., 2005; Iraqi et al., 2018), as described in Chapter 3.0 was used to measure the ACOF between the footwear outsole and floor surface in the presence of liquid contaminant. A 6 degree-of-freedom force plate (BERTEC Corporation, Columbus, OH, USA) with a floor tile mounted on top was used to record ground reaction forces with a sampling frequency of 500 Hz.

The ACOF testing parameters were an average normal force of 250 ± 10 N, shoe-floor angle of 17 ± 1º and sliding speed of 0.5 m/s. The 250 N, 17º, 0.5 m/s was selected based on the set of testing parameters that best predicted slip outcomes in a previous study (Iraqi et al., 2018). The shoe-floor angle was measured when the shoe was fully loaded and forefoot was rotated 17° to be elevated. The shoe angle was with respect to the shoe's orientation when the shoe was unloaded and placed on the floor (Jones et al., 2018). Five repeated trials were carried out for each shoe-floor combination.

5.3.3 Data and statistical analysis

The ACOF data analysis were the same as section 3.3.3 and 3.3.5. The ACOF was quantified as the ratio of resultant shear force to normal force (Eq. 5-2) (Iraqi et al., 2018; Siegmund et al., 2006). The ACOF was averaged over the first 200 ms after the desired 250 N was achieved. Data was collected such that the average normal force during the 200 ms was within ±10 N of 250 N and the range of normal force levels during the 200 ms was within 10% of 250 N (Iraqi et al., 2018).

$$ACOF = \frac{\sqrt{F^2_{\text{Longitudinal Shear}} + F^2_{\text{Transverse Shear}}}}{F_{\text{Normal}}} \quad \text{Eq. 5-2}$$

A multiple linear regression model was developed to predict ACOF based on the tread design features in the presence of canola oil while controlling for the floor type. The independent variables were as follows: material hardness, contact area, heel width, shape factor, heel shape, floor type, and first order interactions between the other independent variables. The heel shape and floor type were modeled as categorical variables.

The model's overall significance was tested using ANOVA method for multiple linear regression. Tests on individual regression coefficients (relative to zero) were performed using t-tests. A backward elimination method was used to screen the candidate regressors and eliminate regressors that have negligible effects. Additionally, forward selection and hybrid method were performed to determine if the model building approach influenced the parameters resulting in the model. A k-fold cross-validation method (k = 5) was used to select the optimal model, i.e. to only select the predictors in the reduced model that minimizes the cross-validation error. The 5-fold cross-validation method was repeated five times for each model size since cross-validation error changes due to different split of data in the cross-validation folds. The model was selected based on the one-standard-error-rule (i.e., cross-validation error is within one standard error of the lowest point on the curve) (James et al., 2013). This method assessed how well the trained models predicted an independent data set and is a stable method to determine the model's predictive capabilities. The advantage of the k-fold cross-validation is that each subset of data will be used for both training (i.e., estimation) and testing (i.e., validation) data set (James et al., 2013). Residual analysis was performed to ensure normality and homoscedasticity assumptions of the regression

model were met. A Shapiro-Wilk test was used to test if the ACOF residuals from the model were following a normal distribution. The statistical analyses were performed using commercial software (JMP® Pro 14.0.0, SAS Institute Inc., Cary, NC, USA) with a significance level of 5%.

5.4 RESULTS

The shoes were evenly distributed between beveled edge (50%, 29 shoes) and flat-edge (50%, 29 shoes) heel shapes. The shore A hardness and shape factor values ranged from 44.2 to 65.6 and from 0.19 to 0.91, respectively. The contact area ranged from 6.36 to 16.08 cm^2 for all shoes and had also the same range without the modified shoes. The heel width was between 3.8 cm and 7.4 cm (5.0 to 7.4 cm without the modified shoes). The ACOF values for the 43 shoes (excluding the modified shoe outsoles) with ceramic and laminate tile ranged from 0.283 (D7) to 0.710 (C7) and 0.127 (D7) to 0.413 (C8), respectively (Figure 5-3A-F).The ACOF for the 15 modified shoes ranged from 0.358 (E1CA) to 0.677 (C1HW) for ceramic tile and 0.197 (D1CA) to 0.385 (C2HS) for laminate tile, which were within the ACOF range of unmodified shoes on the corresponding floorings. For unmodified shoes, brand D had the highest ACOF range (0.320) on ceramic and brand C had the highest ACOF range (0.194) on laminate tile. All shoes had higher ACOF on ceramic tile compared to laminate tile.

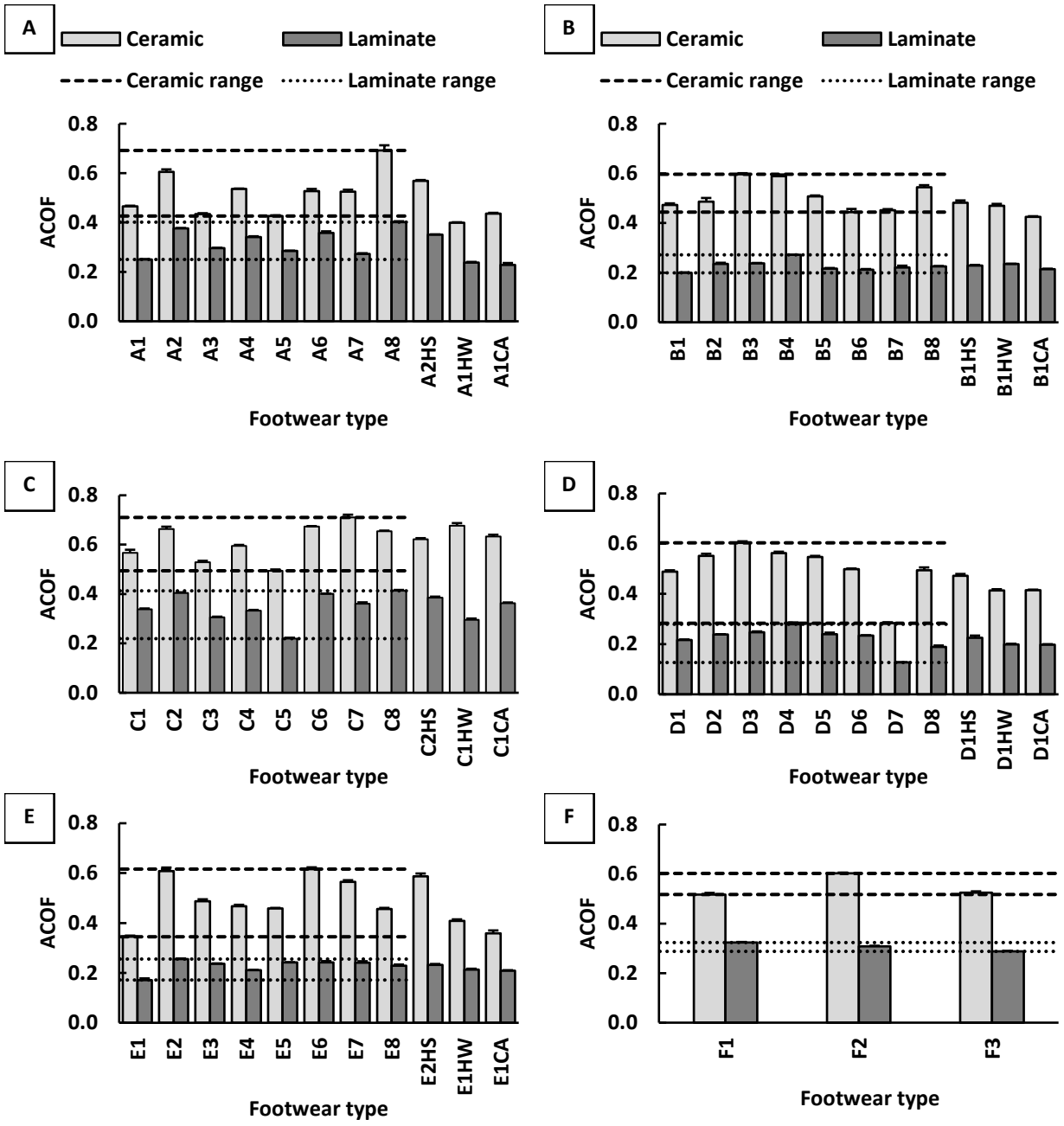

Figure 5-3. ACOF for ceramic (light grey) and laminate tile (dark grey) with canola oil across each shoe brand: (A) Shoes for Crews, (B) Tredsafe, (C) SR Max, (D) safeTstep, (e) Dr. Scholl's, and (F) Timberland PRO. The dashed lines and round dots on each plot show the range of ACOF within brands (for unmodified shoes) on both ceramic and laminate tile, respectively.

The ACOF was related to the predictors for the full model (including all predictors and first order interaction terms) based on the significance of the regression ($F_{21,94} = 37.3$, $p < 0.001$). The t-test performed on the individual regression coefficients indicated that the heel shape (beveled: $t_{95} = 3.43$, $p = 0.001$), contact area ($t_{95} = 3.80$, $p < 0.001$), hardness ($t_{95} = -2.25$, $p = 0.027$), floor type (ceramic: $t_{95} = 25.12$, $p < 0.001$), and the interaction between the heel shape and shape factor ($t_{95} = -2.25$, $p = 0.027$) were statistically significant. The heel width ($t_{95} = -0.61$, $p = 0.544$) and shape factor ($t_{95} = 1.29$, $p = 0.201$) were insignificant in the full model. This model explained 89.3% ($R^2 = 0.893$, $R^2_{adj} = 0.869$, RMSE = 0.054) of the variation in ACOF based on the full set of predictor variables.

The backward elimination method resulted in a reduced model ($F_{6,109} = 135.7$, $p < 0.001$) and included the heel shape ($t_{110} = 3.86$, $p < 0.001$), contact area ($t_{110} = 4.97$, $p < 0.001$), hardness ($t_{110} = -2.90$, $p = 0.005$), shape factor ($t_{110} = 2.67$, $p = 0.009$), floor type ($t_{110} = 25.77$, $p < 0.001$), and the interaction between the heel shape and shape factor ($t_{110} = -2.39$, $p = 0.019$) (Table 5-2). The heel width and other first order interactions were removed in the reduced model by the backward elimination method. The forward selection method resulted in a reduced model ($F_{4,111} = 188.0$, $p < 0.001$) that included four of the six factors that were part of the model identified through the backward elimination method. The model resulting from the forward selection method included the heel shape ($t_{112} = 3.46$, $p < 0.001$), contact area ($t_{112} = 5.31$, $p < 0.001$), hardness ($t_{112} = -2.63$, $p = 0.010$), and floor type ($t_{112} = 24.91$, $p < 0.001$) (Table 5-2). The heel width, shape factor and all first order interactions were not added to the model via the forward selection method. The hybrid method resulted in the same model as the backward elimination method. A lower standard error was achieved with 6 predictors (i.e. backward elimination model) than what was achieved with 4 predictors (i.e., forward selection model) (Figure 5-4). Therefore, the model with

6 predictors was considered the optimal model. The predictor variables in the optimal/backward elimination model explained 88.2% (R^2 = 0.882, R^2_{adj} = 0.875, RMSE = 0.053) of the variation in ACOF (Figure 5-5). The forward selection model explained 87.1% (R^2 = 0.871, R^2_{adj} = 0.867, RMSE = 0.055) of the variation in ACOF. The normal quantile plot for the optimal model showed an approximate straight line indicating no extreme violations of the normality assumption (Figure 5-6A). Additionally, the Shapiro-Wilk test indicated that the ACOF residuals follow a normal distribution (W = 0.983, p = 0.142). The plot of the residual vs. predicted ACOF did not exhibit any extreme unusual patterns that suggest violations of homoscedasticity assumption (Figure 5-6B).

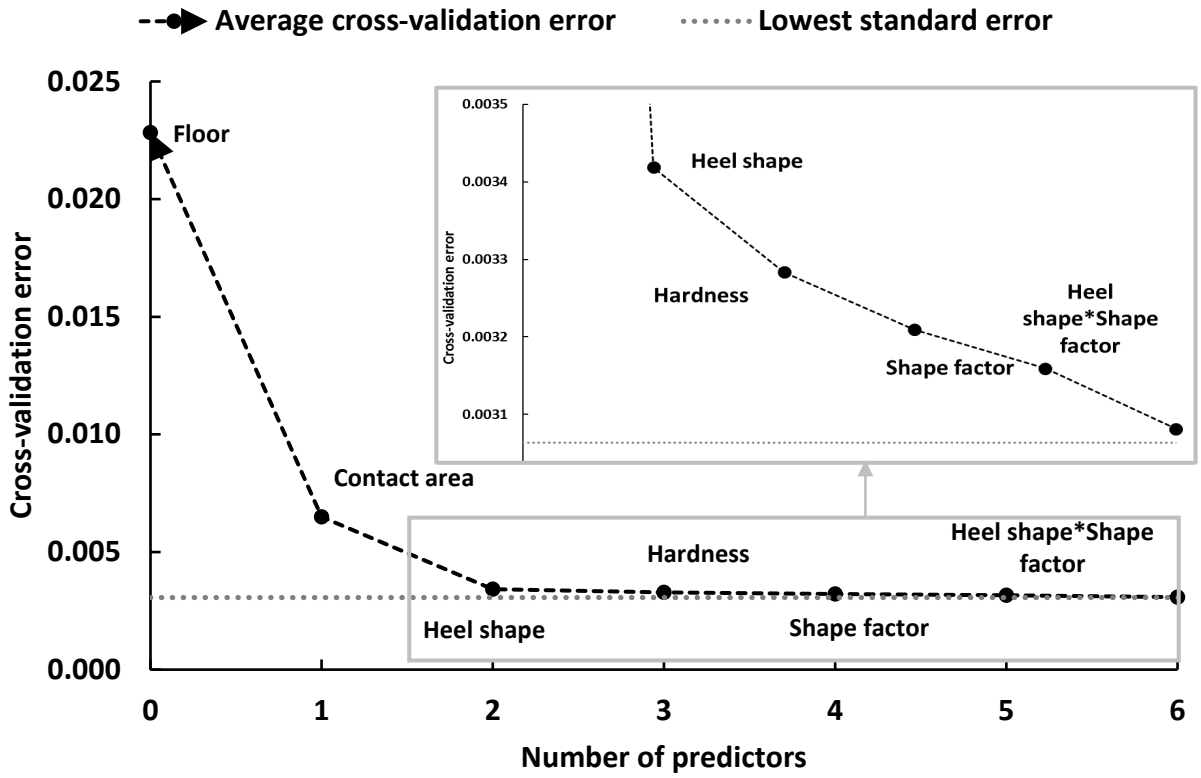

Figure 5-4. Cross-validation error for different number of significant predictors in the reduced models.

Table 5-2. Summary of parameter estimates (95% confidence interval: CI and standard error: Std error) for the backward elimination (column 2-4) and forward selection (column 5-7) model. NA represents variables that were removed.

Terms	β (CI)	Std error	t-test (p-value)	β (CI)	Std error	t-test (p-value)
Intercept	0.348 (0.181 to 0.514)	0.084	4.14 (<.001)	0.369 (0.205 to 0.533)	0.083	4.46 (<.001)
Heel shape[beveled]	0.022 (0.011 to 0.033)	0.006	3.86 (<.001)	0.020 (0.009 to 0.032)	0.006	3.46 (0.001)
Floor[ceramic]	0.127 (0.117 to 0.137)	0.005	25.77 (<.001)	0.127 (0.117 to 0.137)	0.005	24.91 (<.001)
Contact area (cm^2)	0.014 (0.008 to 0.020)	0.003	4.97 (<.001)	0.015 (0.010 to 0.021)	0.003	5.31 (<.001)
Heel width (cm)	NA	NA	NA	NA	NA	NA
Shape factor	0.083 (0.021 to 0.144)	0.031	2.67 (0.009)	NA	NA	NA
Hardness	-0.003 (-0.005 to -0.001)	0.001	-2.9 (0.005)	-0.003 (-0.005 to -0.001)	0.001	-2.63 (0.010)
Heel shape[beveled] *Shape factor	-0.076 (-0.139 to -0.013)	0.032	-2.39 (0.019)	NA	NA	NA
Other first order interactions	NA	NA	NA	NA	NA	NA

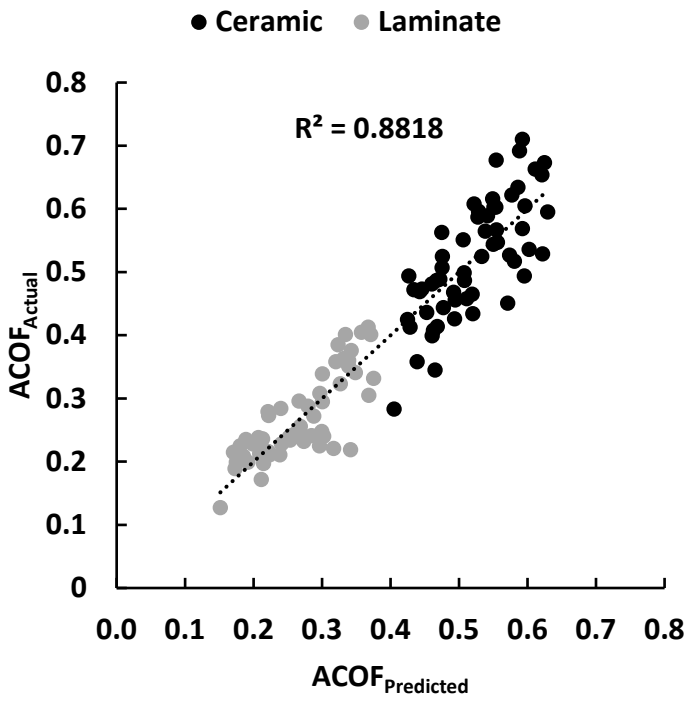

Figure 5-5. Actual vs. predicted ACOF (response variable) from the optimal model (6 predictors).

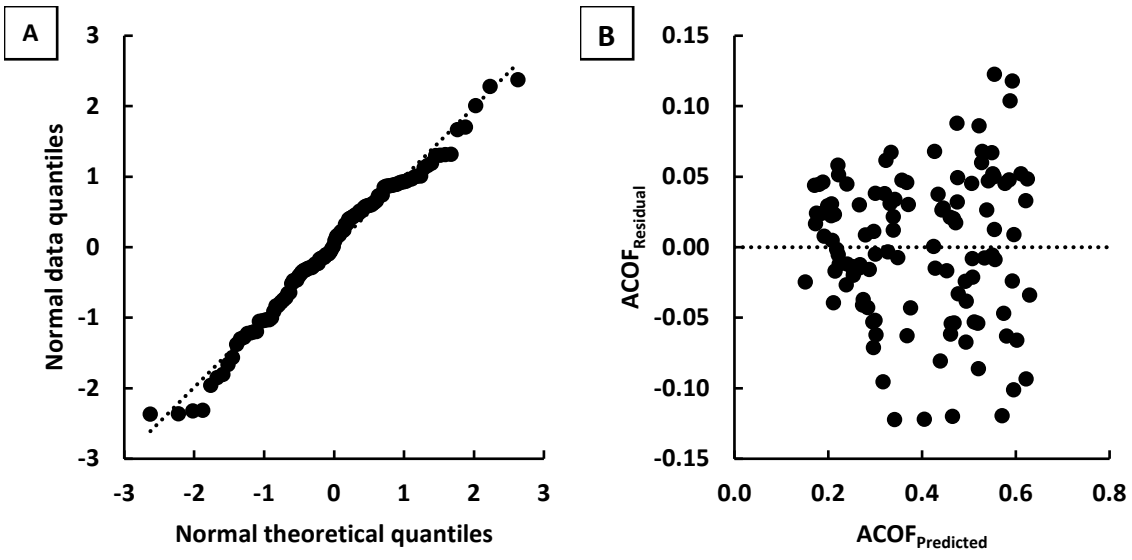

Figure 5-6. Residual analysis performed on the optimal model: (A) normal quantile plot to assess the assumption of normality; and (B) Plot of residual vs. predicted ACOF to assess assumption of homoscedasticity.

According to the regression coefficients from the optimal model (Table 5-2), a unit increase in the contact area (cm^2) and shape factor increased the ACOF by 0.014 ($\beta_{Contact\ area}$) and 0.083 ($\beta_{Shape\ factor}$), respectively. For instance, an increase in the contact area from the first quartile (9.6) to the third quartile (13.4) added 0.053 (interquartile range * $\beta_{Contact\ area}$ = 3.8 * 0.014) to the ACOF. A unit increase in the shape from the first quartile (0.46) to the third quartile (0.68) increased ACOF by 0.018 (interquartile range * $\beta_{Shape\ factor}$ = 0.22 * 0.083). A unit increase in the Shore A hardness decreased the ACOF by 0.003 ($\beta_{Hardness}$). A unit increase in the Shore A hardness from the first quartile (49.8) to the third quartile (60.8) reduced ACOF by 0.033 (interquartile range * $\beta_{Hardness}$ = 11.0 * -0.003). The change from flat-edge to beveled edge heel shape increased ACOF by 0.022 ($\beta_{Heel\ shape[beveled]}$). The change of floor type from ceramic to laminate tile added 0.127 ($\beta_{Floor[ceramic]}$) to the ACOF.

5.5 DISCUSSION

The main finding of this study was that simple and relatively inexpensive measurements of footwear outsole tread design could be utilized to predict the variation in oily traction performance across shoes labeled as slip-resistant. This finding indicated that geometric (heel shape, contact area and shape factor) and material hardness properties of the outsole tread while controlling for floor type, explained 88.2% of the variation in ACOF in the presence of canola oil. Change in heel shape from flat to beveled edge and increase in contact area were favorable in the traction performance within each brand. Moreover, the prediction of ACOF was based on mostly main effects and only a single interaction term (heel shape*shape factor, p-value = 0.019). These findings have two-fold benefits. First, assessing slip-resistant shoes will be possible for safety

practitioners without actually performing experimental shoe traction testing. Second, footwear manufacturers can improve shoe traction by prioritizing heel shape (flat to beveled edge) and contact area. Thus, a potential assessment tool for selection of slip-resistant shoes can be developed by predictive modelling and safety practitioner can select slip-resistant shoes that can yield higher ACOF values to ensure worker's safety.

The relationship between shoe outsole tread, floor type, and ACOF in the current study are generally in agreement with previous research. The contact area was positively associated with ACOF, consistent with previous findings (Jones et al., 2018; Moghaddam et al., 2018). As the contact area increases, contact pressures reduce and consequently cause an increase in hysteresis friction (Moghaddam et al., 2018). The higher ACOF values associated with beveled edge heel shape compared to flat edge were also consistent with findings of Moghaddam and Beschorner (2017). Beveled edge increased the area of contact by conforming the tread to the floor when the shoe is at an angle during the early stages of stance. This has a positive impact on ACOF. The effect of material hardness on ACOF has been also supported by previous research (Cowap et al., 2015; Jones et al., 2018; Strobel et al., 2012; Tsai & Powers, 2008) since hardness contributes to hysteresis friction in the presence of high viscous lubricants (Cowap et al., 2015; Strobel et al., 2012). The softer elastomer (low hardness level) may be subjected to higher deformation and potentially more conforming to the surface asperities of the floor compared to the harder material (high hardness level), which increases ACOF (Strobel et al., 2012). The shape factor also positively affected ACOF which might be explained by the findings of Yamaguchi et al. (2017) that the bending stiffness of a rubber block is positively correlated with ACOF. The deflection of the rubber block due to bending reduces the contact area at the tread-floor interface, which reduces ACOF (Yamaguchi et al., 2017). Hence, higher shaper factor increases bending stiffness and

reduces lateral bending of the treads, and possibly increase ACOF. However, this should be further investigated by imaging techniques (Yamaguchi et al., 2017) to verify if the shape factor affects contact area due to lateral bending. Furthermore, the floor surface with a higher roughness was associated with a higher ACOF, which has been demonstrated in previous research (Chang et al., 2001c; Cowap et al., 2015; Moghaddam et al., 2015).

The statistical model developed in the current study to predict footwear traction based on the simple and inexpensive measurement of outsole tread may be a useful assessment tool. The contact area and heel shape had the strongest association with ACOF in canola oil among all the shoe parameters. Contact area was measured with an ink pad, paper and scanner. Heel shape was visually observed without use of any equipment. A safety manager could utilize these parameters to screen out slip-resistant shoes that pose a high or moderate slip risk. For instance, the shoes that have a portion of their tread missing in the shoe imprint (low contact area) and have flat edged heel shape (Figure 5-7) would probably not be a suitable candidate to design out slip hazard. Even without calculating the contact area using software, some shoes show evidence of poor outsole backing design that could lead to low contact area and most likely low ACOF (Figure 5-7, left). Thus, the observational methods described in this study may help to select shoes with higher slip-resistant properties and reduce the slipping hazard. Particularly, some slip-resistant shoes posed a moderate slip risk. About 70% of unmodified shoes tested on laminate tile had ACOF below 0.30. An ACOF level above 0.30 (Grönqvist et al., 1989) or 0.29 (ANSI/NFSI B101.7, 2018) has been suggested for safe level walking. Furthermore, the range of ACOF values (0.127-0.413) for laminate tile had overlap with RCOF range (0.155-0.272) for level walking (Beschorner et al., 2016; Perkins & Wilson, 1983; Redfern & DiPasquale, 1997). Thus, this study operated in conditions where certain shoes could lead to slips and certain shoes would likely prevent slips.

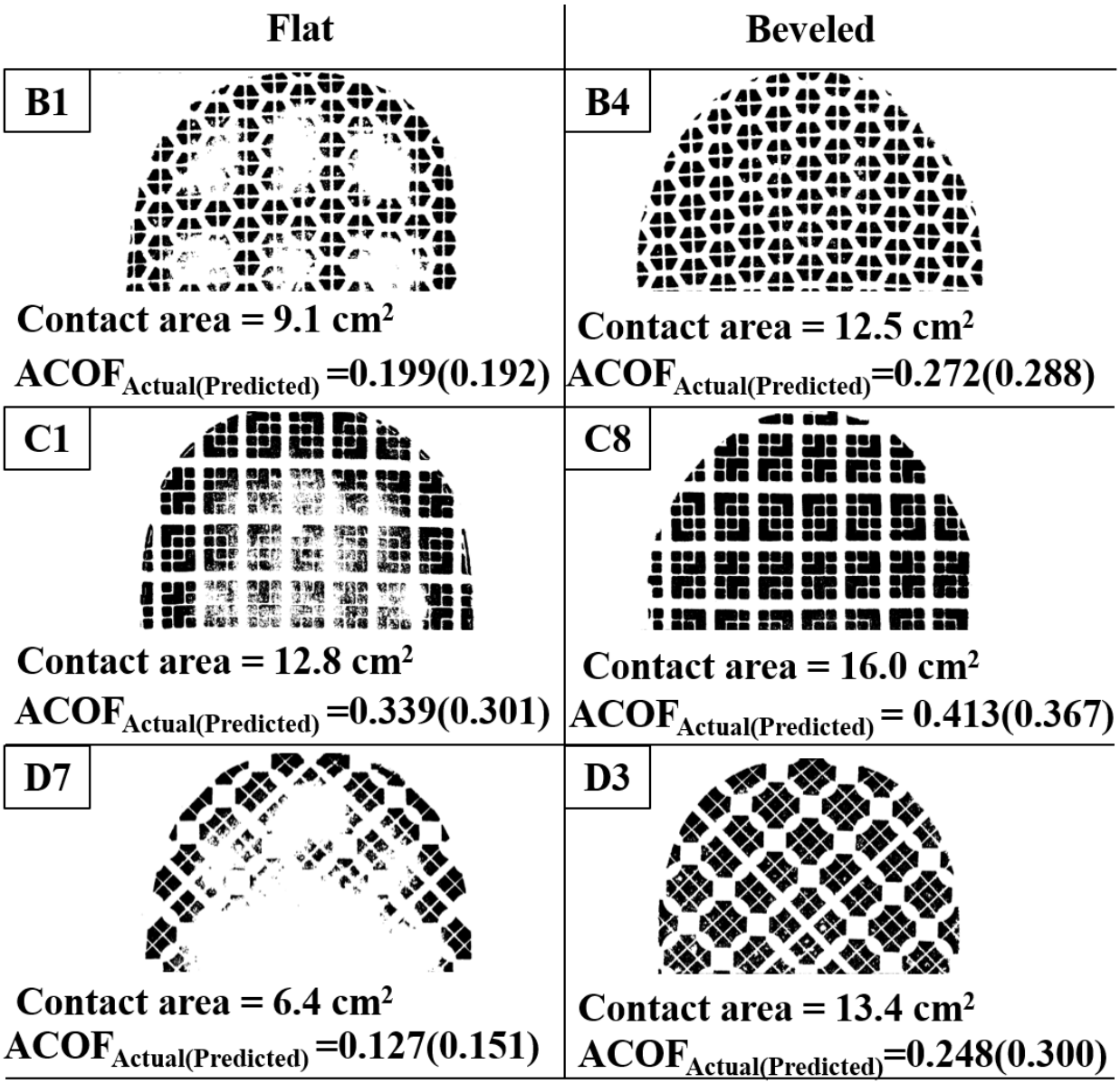

Figure 5-7. A comparison of ACOF across heel designs within brands (B, C, D) on laminate tile. The ACOF is relatively higher for the designs in column one (B4, C8, D3) compared to their corresponding shoe brand (B1, C1, D7) in column two primarily due to higher contact area and beveled edge heel shape.

Certain limitations of the current study should be acknowledged. Only two different floorings were included in the study. It is worth noting that interaction effects including flooring were small and

insignificant. Furthermore, other research has demonstrated that shoe performance across vinyl composite, quarry and ceramic floor surfaces are generalizable in the presence of canola oil (Chanda et al., 2018). Moreover, the liquid contaminant used was canola oil and further investigations may be required to generalize its applicability to other liquid contaminants such as water and detergent aqueous solution. Another limitation is that this model cannot be used to predict ACOF beyond the range of predictors that were used to develop the model (Shore A hardness: 44.2-65.6; shape factor: 0.19-0.91, heel shape: flat or beveled edge, contact area: 6.36-16.08 cm^2). This study only included shoes with tread that were presumed to operate in boundary conditions and may not be applicable to non-slip resistant or worn shoes that may operate in other lubrications regimes like hydrodynamic lubrication (Beschorner et al., 2014; Singh & Beschorner, 2014). Lastly, the ACOF testing parameters used in the study only approximate the slipping dynamics during level walking with regular pace and the model may not be applicable to foot slips on ladder rung, stair and during fast walking or running conditions.

In summary, the current study suggested that slip-resistant shoes with a beveled heel shape, higher contact area, lower material hardness and higher shaper factor generate higher traction in the presence of canola oil. Furthermore, a predictive model was generated that predicted ACOF based on these parameters. Safety practitioners can adopt this predictive model to select higher traction performance shoes. This assessment tool can aid practitioners to reduce slip-related injuries.

6.0 DISCUSSION AND CONCLUSIONS

This dissertation aimed to improve the quality of the current state of footwear traction test methods and to develop an alternative tread assessment tool. The important findings of this dissertation are:

1. The variation in the normal force (250 N and 400 N), shoe-floor angle (7° and 17°), and sliding speed (0.3 m/s and 5 m/s) to operate the Portable Slip Simulator significantly influenced ACOF. All eight biomechanical sets were predictive of slip risk across 124 unexpected liquid-contaminated trials, but with different levels of certainty. The set of biomechanical parameters that had the highest predictive ability in identifying human slip risk included a 250 N normal force, 17° shoe-floor angle and 0.5 m/s sliding speed. The second highest predictive set was 250 N, 17°, 0.3 m/s. Thus, the combination of 250 N normal force and 17° shoe-floor angle may improve the prediction quality of whole shoe testers that operate similar to the Portable Slip Simulator in simulating shoe dynamics during slips.
2. The biomechanical analysis of five footwear types during human slipping experiments revealed that the normal force (26.7 %BW, 179.4 N), shoe-floor angle (22.1°) and contact time (0.02 s) at slip initiation were significantly different from the recommended ACOF testing parameters by footwear traction testing standards. Instead, the testing parameters mostly resemble the shoe dynamics during the most severe part of a slip. The footwear traction testing methods may become more

biofidelic by including lower vertical forces (< 400 N), larger shoe-floor angles (> 7º) and shorter contact duration (< 0.10 s) to be more consistent with shoe dynamics at slip initiation. These changes in the footwear traction testing methods may further increase the prediction quality of slip risk.

3. An empirical model was developed to predict shoe traction based on outsole design features and floor type in boundary lubrication. The outsole geometry (contact area, heel shape and shape factor) and material hardness while controlling for floor type explained 88% of variation in ACOF for canola oil, where hysteresis friction presumably was the dominant contributor of ACOF. The model determined that slip-resistant shoes with high contact area, beveled edge heel shape, low material hardness and higher shape factor yield higher ACOF in boundary lubrication. Furthermore, high variation in ACOF was observed within brands. The input shoe parameters/predictors were based on relatively simple and inexpensive measurements. This empirical model may aid safety practitioners by providing an observational assessment tool to measure footwear traction.

The findings from this research demonstrated the validity of footwear traction test methods and ways to improve these methods through human-centered approaches. Future footwear traction testing methods or standards could build on the findings of this dissertation. Furthermore, an alternative method to footwear traction test methods was developed to aid use of ergonomic tools to address slip-initiated falls. The tread assessment tool is an initial step towards development of an observational assessment tool to evaluate shoe traction in slips and falls research. This work will contribute towards reduction of slip-related injuries.

The following subsections of this chapter will elaborate future directions to further improve the footwear traction test methods and to increase the applicability of the tread assessment tool to additional shoe-floor tribosystems.

6.1 FUTURE DIRECTIONS

6.1.1 Improvement of footwear traction measurements

Recommendations regarding the biomechanical parameters like normal force and shoe-floor angle were made for ACOF measurements to improve the prediction of slip risk in this dissertation through human-centered approaches, but challenges to predict slip outcome with high degree of certainty still exists. Additional research is required to tackle these challenges. Additional biomechanical parameters might be required to control during footwear traction measurements to improve biofidelity. A few candidate biomechanical parameters based on the secondary findings and limitations of this dissertation are as follows:

1. The shoe-floor angle is only considered in the sagittal plane during ACOF testing. However, the lateral center of pressure (COP) location at slip initiation (Chapter 4.0) may suggest that the contact angle in the frontal plane may need to be considered too. This could be achieved by a slight inversion angle of the footwear during ACOF testing to correspond to a lateral COP during human slipping.
2. The variability in side-slip angle within shoe design (Chapter 4.0) may suggest that gait variations exist due to foot orientation. Hence, the sliding of footwear specimen during ACOF measurements might also include slight deviation from the axis of the

shoe (toe-to-heel) to account for gait variations. This may have an important implication since tread orientation may affect ACOF for certain tread designs (Blanchette & Powers, 2015a; Yamaguchi et al., 2017).

3. The biomechanical parameters used during footwear traction measurements are approximately constant over time (Chapter 3.0). However, the biomechanical parameters change during the motion of the shoe for human slips (Chapter 4.0). For instance, the higher heel deceleration (negative acceleration) at heel strike reduces the occurrence of severe slips (Beschorner & Cham, 2008). Thus, future design of whole shoe testers might need to account for changes in biomechanical parameters over entire measurement period.
4. Generally, footwear traction measurements are conducted on a single shoe size across different footwear. However, different shoe size may have different contact pressures under same loading conditions, which may affect ACOF. Thus, ACOF testing may need to consider a range of shoe sizes per design.

6.1.2 Improvement of the tread assessment model

The empirical model for shoe traction assessment developed in this dissertation is in a primary stage and several improvements are needed to develop a comprehensive tread assessment tool. These improvements include increasing the applicability of the model to other liquid contamination, model validation and accessibility.

1. The current model is only applicable to boundary lubrication, specifically where hysteresis friction is dominant relative to adhesion friction. As previously mentioned in Chapter 2.0, the hysteresis friction is dominant in the presence of high viscous

liquid contaminants such as canola oil and motor oil. As the viscosity of the liquid contaminants decreases in the case of water and detergent aqueous solution, the contribution of adhesion friction to overall friction increases. Thus, the model may not account for shoe outsole design features that are associated with adhesion friction. Prediction of adhesion friction may increase the application of the model to a variety of industries where slippery conditions might be caused in the absence of oil.

2. Cross-validation method was used to select the optimal model. However, the validity of the model needs to be tested also on an independent set of slip-resistant shoes that are not utilized during model building. Moreover, the model needs to be validated using a human-centered approach to test if the model can reduce human slip hazard.
3. The tread assessment method needs to be accessible. Even though most equipment utilized for measurement of outsole geometry and material hardness are accessible, there might be issues with software accessibility. In this dissertation, a software (MATLAB) that required license was used to calculate contact area. This software accessibility issue might be addressed by use of open source software as an alternative option. Use of software and mobile apps have shown to effective for NIOSH lifting equation (Lowe et al., 2018). For instance, a mobile image scanning application could be used to scan shoe outsole imprints rather than use of a stand-alone image scanner device. These steps may facilitate the use of this model by safety practitioners and users.
4. The tread assessment method should account for the usability of the model for the safety practitioners. The tread measurements were simple from our research group's point of view, but the model has yet to be utilized or tested by the intended users

(Shorrock & Williams, 2016). Safety practitioners may have various levels of expertise or competence, which may lead to variability in their efficiency and effectiveness when using the proposed observational method. Future research that assesses safety practitioners' ability to utilize the method and considering their feedback may help to improve the usability of these methods.

6.2 CONCLUSIONS

This dissertation contributed towards enhancing the quality and accessibility of footwear traction test methods. This research was imperative to the long-term purpose of preventing slip-initiated falls due to liquid contamination. A combination of 250 N normal force and 17º shoe-floor angle as the biomechanical input variables to a dynamic whole shoe tester was found to increase the prediction quality of slip risk through a human validation study. Furthermore, a biomechanical analysis of slip events outlined the significant differences between shoe dynamics at slip initiation and current footwear traction testing standards. This revealed that lower normal force (< 400 N), larger shoe-floor angle (> 7º) and shorter contact duration (< 0.10 s) may improve the biofidelity of the test methods. These findings may be useful to ergonomists, footwear designers, and researchers for testing the slip-performance of footwear interventions. Additionally, a tread assessment tool was developed to identify higher traction performance shoes based on outsole design. This accessible tool may aid safety practitioners to design out slip hazard at workplace. Thus, it is expected that this dissertation will contribute to ergonomic interventions for preventing slip-initiated falls.

BIBLIOGRAPHY

Albert, D., Moyer, B., & Beschorner, K. E. (2017). Three-Dimensional Shoe Kinematics During Unexpected Slips: Implications for Shoe–Floor Friction Testing. *IISE Transactions on Occupational Ergonomics and Human Factors, 5*(1), 1-11.

Anderson, D. E., Franck, C. T., & Madigan, M. L. (2014). Age differences in the required coefficient of friction during level walking do not exist when experimentally-controlling speed and step length. *Journal of applied biomechanics, 30*(4), 542-546.

ANSI/NFSI B101.7. (2018). Standard Test Method for Lab Measurement of Footwear Heel Outsole Material Coefficient of Friction on Liquid-Contaminated Floor Surfaces: NFSI Standards Committee B101 Safety Requirements for Slip, Trip and Fall Prevention.

Aschan, C., Hirvonen, M., Mannelin, T., & Rajamäki, E. (2005). Development and validation of a novel portable slip simulator. *Applied ergonomics, 36*(5), 585-593.

ASTM D2240-15. (2015). Standard Test Method for Rubber Property - Durometer Hardness: ASTM International, West Conshohocken, PA.

ASTM F2913-11. (2011). Standard Test Method for Measuring the Coefficient of Friction for Evaluation of Slip Performance of Footwear and Test Surfaces/Flooring Using a Whole Shoe Tester. Annual Book of ASTM Standards: ASTM International, West Conshohocken, PA.

Bell, J. L., Collins, J. W., Wolf, L., Grönqvist, R., Chiou, S., Chang, W.-R., Sorock, G. S., Courtney, T. K., Lombardi, D. A., & Evanoff, B. (2008). Evaluation of a comprehensive slip, trip and fall prevention programme for hospital employees∗∗. *Ergonomics, 51*(12), 1906-1925.

Beschorner, K., & Cham, R. (2008). Impact of joint torques on heel acceleration at heel contact, a contributor to slips and falls. *Ergonomics, 51*(12), 1799-1813. doi:10.1080/00140130802136479

Beschorner, K. E., Albert, D. L., Chambers, A. J., & Redfern, M. S. (2014). Fluid pressures at the shoe–floor–contaminant interface during slips: Effects of tread & implications on slip severity. *Journal of biomechanics, 47*(2), 458-463.

Beschorner, K. E., Albert, D. L., & Redfern, M. S. (2016). Required coefficient of friction during level walking is predictive of slipping. *Gait & posture, 48*, 256-260. doi:http://dx.doi.org/10.1016/j.gaitpost.2016.06.003

Beschorner, K. E., Jones, T. G., & Iraqi, A. (2017). The Combined Benefits of Slip-Resistant Shoes and High Traction Flooring on Coefficient of Friction Exceeds Their Individual Contributions. *Proceedings of the Human Factors and Ergonomics Society Annual Meeting, 61*(1), 931-935. doi:10.1177/1541931213601715

Beschorner, K. E., Redfern, M. S., Porter, W. L., & Debski, R. E. (2007). Effects of slip testing parameters on measured coefficient of friction. *Applied ergonomics, 38*(6), 773-780.

Beschorner, K. E., & Singh, G. (2012). A Novel Method for Evaluating the Effectiveness of Shoe-Tread Designs Relevant to Slip and Fall Accidents. *Proceedings of the Human Factors and Ergonomics Society Annual Meeting, 56*(1), 2388-2392. doi:10.1177/1071181312561560

Blanchette, M. G., & Powers, C. M. (2015a). The influence of footwear tread groove parameters on available friction. *Applied ergonomics, 50*, 237-241.

Blanchette, M. G., & Powers, C. M. (2015b). Slip prediction accuracy and bias of the SATRA STM 603 whole shoe tester. *Journal of Testing and Evaluation, 43*(3), 491-498.

Burnfield, J. M., & Powers, C. M. (2006). Prediction of slips: an evaluation of utilized coefficient of friction and available slip resistance. *Ergonomics, 49*(10), 982-995.

Centers for Disease Control and Prevention. (2017, May 2, 2017). Causes of nonfatal injuries treated in hospital emergency departments. Retrieved from https://www.cdc.gov/injury/wisqars/leadingcauses.html

Cham, R., & Redfern, M. S. (2002a). Changes in gait when anticipating slippery floors. *Gait & posture, 15*(2), 159-171.

Cham, R., & Redfern, M. S. (2002b). Heel contact dynamics during slip events on level and inclined surfaces. *Safety Science, 40*(7), 559-576.

Chambers, A. J., & Cham, R. (2007). Slip-related muscle activation patterns in the stance leg during walking. *Gait & posture, 25*(4), 565-572.

Chambers, A. J., Margerum, S., Redfern, M. S., & Cham, R. (2002). Kinematics of the foot during slips. *Occupational Ergonomics, 3*(4), 225-234.

Chanda, A., Jones, T. G., Beschorner, K. E. J. I. T. o. O. E., & Factors, H. (2018). Generalizability of Footwear Traction Performance across Flooring and Contaminant Conditions. (just-accepted), 1-23.

Chander, H., Garner, J. C., & Wade, C. (2015a). Ground Reaction Forces in Alternative Footwear during Slip Events. *International Journal of Kinesiology & Sports Science, 3*(2), 1.

Chander, H., Garner, J. C., & Wade, C. (2015b). Heel contact dynamics in alternative footwear during slip events. *International Journal of Industrial Ergonomics, 48*, 158-166.

Chander, H., Wade, C., Garner, J. C., & Knight, A. C. (2016). Slip initiation in alternative and slip-resistant footwear. *International journal of occupational safety and ergonomics*, 1-12.

Chang, W.-R., Chang, C.-C., & Matz, S. (2011a). The effect of transverse shear force on the required coefficient of friction for level walking. *Human Factors, 53*(5), 461-473. doi:10.1177/0018720811414885

Chang, W.-R., Chang, C.-C., & Matz, S. (2011b). The effect of transverse shear force on the required coefficient of friction for level walking. *Human Factors: The Journal of the Human Factors and Ergonomics Society, 53*(5), 461-473.

Chang, W.-R., Grönqvist, R., Leclercq, S., Brungraber, R. J., Mattke, U., Strandberg, L., Thorpe, S. C., Myung, R., Makkonen, L., & Courtney, T. K. (2001a). The role of friction in the measurement of slipperiness, Part 2: Survey of friction measurement devices. *Ergonomics, 44*(13), 1233-1261.

Chang, W.-R., Grönqvist, R., Leclercq, S., Myung, R., Makkonen, L., Strandberg, L., Brungraber, R. J., Mattke, U., & Thorpe, S. C. (2001b). The role of friction in the measurement of slipperiness, Part 1: friction mechanisms and definition of test conditions. *Ergonomics, 44*(13), 1217-1232.

Chang, W.-R., Kim, I.-J., Manning, D. P., & Bunterngchit, Y. (2001c). The role of surface roughness in the measurement of slipperiness. *Ergonomics, 44*(13), 1200-1216. doi:10.1080/00140130110085565

Chang, W.-R., Leclercq, S., Lockhart, T. E., & Haslam, R. (2016). State of science: occupational slips, trips and falls on the same level. *Ergonomics, 59*(7), 861-883.

Courtney, T. K., Sorock, G. S., Manning, D. P., Collins, J. W., & Holbein-Jenny, M. A. (2001). Occupational slip, trip, and fall-related injuries-can the contribution of slipperiness be isolated? *Ergonomics, 44*(13), 1118-1137. doi:10.1080/00140130110085538

Cowap, M. J. H., Moghaddam, S. R. M., Menezes, P. L., & Beschorner, K. E. (2015). Contributions of adhesion and hysteresis to coefficient of friction between shoe and floor surfaces: effects of floor roughness and sliding speed. *Tribology - Materials, Surfaces & Interfaces, 9*(2), 77-84. doi:10.1179/1751584X15Y.0000000005

Dempsey, P. G. (2002). Usability of the revised NIOSH lifting equation. *Ergonomics, 45*(12), 817-828.

Dempsey, P. G., McGorry, R. W., & Maynard, W. S. (2005). A survey of tools and methods used by certified professional ergonomists. *Applied ergonomics, 36*(4), 489-503.

DiDomenico, A., McGorry, R. W., & Chang, C.-C. (2007). Association of subjective ratings of slipperiness to heel displacement following contact with the floor. *Applied ergonomics, 38*(5), 533-539.

EN ISO 13287. (2012). Tester Personal Protective Equipment - Footwear - Test Method for Slip Resistance: International Organization for Standardization, Geneva, Switzerland.

Espy, D. D., Yang, F., Bhatt, T., & Pai, Y.-C. (2010). Independent influence of gait speed and step length on stability and fall risk. *Gait & posture, 32*(3), 378-382.

Gronqvist, R., Matz, S., & Hirvonen, M. (2003). Assessment of shoe-floor slipperiness with respect to contact-time-related variation in friction during heel strike. *Occupational Ergonomics, 3*(4), 197-208.

Grönqvist, R., Roine, J., Järvinen, E., & Korhonen, E. (1989). An apparatus and a method for determining the slip resistance of shoes and floors by simulation of human foot motions. *Ergonomics, 32*(8), 979-995.

Hamrock, B. J. (1994). *Fundamentals of fluid film lubrication*. New York: McGraw-Hill.

Hanson, J. P., Redfern, M. S., & Mazumdar, M. (1999). Predicting slips and falls considering required and available friction. *Ergonomics, 42*(12), 1619-1633.

Heijnen, M. J. H., & Rietdyk, S. (2016). Falls in young adults: Perceived causes and environmental factors assessed with a daily online survey. *Human Movement Science, 46*(Supplement C), 86-95. doi:https://doi.org/10.1016/j.humov.2015.12.007

Imbimbo, M., & De Luca, A. (1998). FE stress analysis of rubber bearings under axial loads. *Computers & structures, 68*(1), 31-39.

Iraqi, A., & Beschorner, K. E. (2017). *Vertical ground reaction forces during unexpected human slips.* Paper presented at the Proceedings of the Human Factors and Ergonomics Society Annual Meeting.

Iraqi, A., Cham, R., Redfern, M. S., & Beschorner, K. E. (2018). Coefficient of friction testing parameters influence the prediction of human slips. *Applied ergonomics, 70*, 118-126. doi:https://doi.org/10.1016/j.apergo.2018.02.017

James, G., Witten, D., Hastie, T., Tibshirani, R., & SpringerLink. (2013). *An Introduction to Statistical Learning: with Applications in R* (Vol. 103). New York, NY: Springer New York.

Jones, T., Iraqi, A., & Beschorner, K. (2018). Performance testing of work shoes labeled as slip resistant. *Applied ergonomics, 68*, 304-312. doi:https://doi.org/10.1016/j.apergo.2017.12.008

Khonsari, M. M., & Booser, E. R. (2017). *Applied Tribology : Bearing Design and Lubrication*. New York, UNKNOWN: John Wiley & Sons, Incorporated.

Leamon, T., & Li, K. (1990). *Microslip length and the perception of slipping.* Paper presented at the 23rd International Congress on Occupational Health, Montreal, Canada.

Leclercq, S., Tisserand, M., & Saulnier, H. (1995). Tribological concepts involved in slipping accident analysis. *Ergonomics, 38*(2), 197-208.

Li, K. W., & Chen, C. J. (2004). The effect of shoe soling tread groove width on the coefficient of friction with different sole materials, floors, and contaminants. *Applied ergonomics, 35*(6), 499-507.

Li, K. W., & Chen, C. J. (2005). Effects of tread groove orientation and width of the footwear pads on measured friction coefficients. *Safety Science, 43*(7), 391-405.

Li, K. W., Wu, H. H., & Lin, Y.-C. (2006). The effect of shoe sole tread groove depth on the friction coefficient with different tread groove widths, floors and contaminants. *Applied ergonomics, 37*(6), 743-748. doi:http://dx.doi.org/10.1016/j.apergo.2005.11.007

Liberty Mutual Research Institute for Safety. (2017). 2017 Liberty Mutual Workplace Safety Index. Hopkinton, MA.

Lockhart, T. E., Woldstad, J. C., & Smith, J. L. (2003). Effects of age-related gait changes on the biomechanics of slips and falls. *Ergonomics, 46*(12), 1136-1160.

Lowe, B., Dempsey, P., & Jones, E. (2018). Assessment Methods Used by Certified Ergonomics Professionals. *Proceedings of the Human Factors and Ergonomics Society Annual Meeting, 62*(1), 838-842. doi:10.1177/1541931218621191

Marras, W. S., & Karwowski, W. (2006). *The occupational ergonomics handbook* (2nd ed.). Boca Raton, FL: CRC/Taylor & Francis.

Marras, W. S., Lavender, S. A., Leurgans, S. E., Rajulu, S. L., Allread, S. W. G., Fathallah, F. A., & Ferguson, S. A. (1993). The Role of Dynamic Three-Dimensional Trunk Motion in Occupationally-Related. *Spine, 18*(5), 617-628.

Marucci-Wellman, H. R., Courtney, T. K., Corns, H. L., Sorock, G. S., Webster, B. S., Wasiak, R., Noy, Y. I., Matz, S., & Leamon, T. B. (2015). The direct cost burden of 13 years of disabling workplace injuries in the US (1998–2010): Findings from the Liberty Mutual Workplace Safety Index. *Journal of Safety Research, 55*, 53-62.

McAtamney, L., & Corlett, E. N. (1993). RULA: a survey method for the investigation of work-related upper limb disorders. *Applied ergonomics, 24*(2), 91-99.

McGorry, R. W., DiDomenico, A., & Chang, C.-C. (2010). The anatomy of a slip: Kinetic and kinematic characteristics of slip and non-slip matched trials. *Applied ergonomics, 41*(1), 41-46.

Menant, J. C., Steele, J. R., Menz, H. B., Munro, B. J., & Lord, S. R. (2009). Effects of walking surfaces and footwear on temporo-spatial gait parameters in young and older people. *Gait & posture, 29*(3), 392-397.

Menz, H. B., Lord, S., & McIntosh, A. S. (2001). Slip resistance of casual footwear: implications for falls in older adults. *Gerontology, 47*(3), 145-149.

Moghaddam, S. R. M., Acharya, A., Redfern, M. S., & Beschorner, K. E. (2018). Predictive multiscale computational model of shoe-floor coefficient of friction. *Journal of biomechanics, 66*, 145-152.

Moghaddam, S. R. M., & Beschorner, K. E. (2017). *Sensitivity of a Multiscale Model of Shoe-Floor-Contaminant Friction to Normal Force and Shoe-Floor Contact Angle.* Paper presented at the 2017 STLE Annual Meeting & Exhibition.

Moghaddam, S. R. M., Redfern, M. S., & Beschorner, K. E. (2015). A microscopic finite element model of shoe–floor hysteresis and adhesion friction. *Tribology Letters, 59*(3), 42.

Montgomery, D. C., Peck, E. A., & Vining, G. G. (2006). *Introduction to linear regression analysis* (4th ed.). Hoboken, N.J: Wiley-Interscience.

Moore, C. T., Menezes, P. L., Lovell, M. R., & Beschorner, K. E. (2012). Analysis of shoe friction during sliding against floor material: role of fluid contaminant. *Journal of Tribology, 134*(4), 041104.

Moore, D. F. (1975). *Principles and applications of tribology* (1st ed. Vol. 14). Oxford;New York;: Pergamon Press.

Moyer, B., Chambers, A., Redfern, M. S., & Cham, R. (2006). Gait parameters as predictors of slip severity in younger and older adults. *Ergonomics, 49*(4), 329-343.

NIOSH. (1981). *Work Practices Guide for Manual Lifting*. Retrieved from Cincinnati, Ohio:

Perkins, P. (1978). Measurement of slip between the shoe and ground during walking. *American Society of Testing and Materials: Special Technical Publication, 649*, 71-87.

Perkins, P., & Wilson, M. (1983). Slip resistance testing of shoes—new developments. *Ergonomics, 26*(1), 73-82.

Powers, C. M., Brault, J. R., Stefanou, M. A., Tsai, Y. J., Flynn, J., & Siegmund, G. P. (2007). Assessment of Walkway Tribometer Readings in Evaluating Slip Resistance: A Gait-Based Approach. *Journal of forensic sciences, 52*(2), 400-405.

Powers, C. M., Burnfield, J. M., Lim, P., Brault, J. M., & Flynn, J. E. (2002). Utilized coefficient of friction during walking: static estimates exceed measured values. *Journal of Forensic Science, 47*(6), 1303-1308.

Proctor, T. D., & Coleman, V. (1988). Slipping, tripping and falling accidents in Great Britain—present and future. *Journal of Occupational Accidents, 9*(4), 269-285.

Redfern, M. S., & Bidanda, B. (1994). Slip resistance of the shoe-floor interface under biomechanically-relevant conditions. *Ergonomics, 37*(3), 511-524.

Redfern, M. S., Cham, R., Gielo-Perczak, K., Grönqvist, R., Hirvonen, M., Lanshammar, H., Marpet, M., Pai IV, C. Y.-C., & Powers, C. (2001). Biomechanics of slips. *Ergonomics, 44*(13), 1138-1166.

Redfern, M. S., & DiPasquale, J. (1997). Biomechanics of descending ramps. *Gait & posture, 6*(2), 119-125.

Shorrock, S. T., & Williams, C. A. (2016). Human factors and ergonomics methods in practice: three fundamental constraints. *Theoretical Issues in Ergonomics Science, 17*(5-6), 468-482.

Siegmund, G. P., Heiden, T. L., Sanderson, D. J., Inglis, J. T., & Brault, J. R. (2006). The effect of subject awareness and prior slip experience on tribometer-based predictions of slip probability. *Gait & posture, 24*(1), 110-119.

Singh, G., & Beschorner, K. E. (2014). A Method for Measuring Fluid Pressures in the Shoe–Floor–Fluid Interface: Application to Shoe Tread Evaluation. *IIE Transactions on Occupational Ergonomics and Human Factors, 2*(2), 53-59. doi:10.1080/21577323.2014.919367

Sridharan, K., & Sivaramakrishnan, R. (2012). Dynamic behavior of tyre tread block. *American Journal of Engineering and Applied Sciences, 5*(2).

Steven Moore, J., & Garg, A. (1995). The strain index: a proposed method to analyze jobs for risk of distal upper extremity disorders. *American Industrial Hygiene Association Journal, 56*(5), 443-458.

Strandberg, L., & Lanshammar, H. (1981). The dynamics of slipping accidents. *Journal of Occupational Accidents, 3*(3), 153-162.

Strobel, C. M., Menezes, P. L., Lovell, M. R., & Beschorner, K. E. (2012). Analysis of the contribution of adhesion and hysteresis to shoe–floor lubricated friction in the boundary lubrication regime. *Tribology Letters, 47*(3), 341-347.

Takala, E.-P., Pehkonen, I., Forsman, M., Hansson, G.-Å., Mathiassen, S. E., Neumann, W. P., Sjøgaard, G., Veiersted, K. B., Westgaard, R. H., & Winkel, J. (2010). Systematic evaluation of observational methods assessing biomechanical exposures at work. *Scandinavian journal of work, environment & health*, 3-24.

Tencer, A. F., Koepsell, T. D., Wolf, M. E., Frankenfeld, C. L., Buchner, D. M., Kukull, W. A., LaCroix, A. Z., Larson, E. B., & Tautvydas, M. (2004). Biomechanical properties of shoes and risk of falls in older adults. *Journal of the American Geriatrics Society, 52*(11), 1840-1846.

Tsai, Y. J., & Powers, C. M. (2008). The Influence of Footwear Sole Hardness on Slip Initiation in Young Adults*. *Journal of forensic sciences, 53*(4), 884-888.

U.S. Department of Labor- Bureau of Labor Statistics. (2016a). National Census of Fatal Occupational Injuires in 2015. Washington, D.C.

U.S. Department of Labor- Bureau of Labor Statistics. (2016b). Nonfatal Occupational Injuires and Illnesses Requiring Days Away From Work, 2015. Washington, D.C.

U.S. Department of Labor- Bureau of Labor Statistics. (2017). National Census of Fatal Occupational Injuires in 2016. Washington, D.C.

Verma, S. K., Chang, W. R., Courtney, T. K., Lombardi, D. A., Huang, Y.-H., Brennan, M. J., Mittleman, M. A., Ware, J. H., & Perry, M. J. (2011). A prospective study of floor surface, shoes, floor cleaning and slipping in US limited-service restaurant workers. *Occupational and environmental medicine, 68*(4), 279-285.

Waters, T. R., Putz-Anderson, V., Garg, A., & Fine, L. J. (1993). Revised NIOSH equation for the design and evaluation of manual lifting tasks. *Ergonomics, 36*(7), 749-776.

Wilson, M. P. (1990). Development of SATRA slip test and tread pattern design guidelines. *Slips, stumbles, and falls: pedestrian footwear and surfaces*, 113-123.

Winter, D. A. (1987). The biomechanics and motor control of human gait. Waterloo: University of Waterloo Press.

Yamaguchi, T., Hsu, J., Li, Y., & Maki, B. E. (2015). Efficacy of a rubber outsole with a hybrid surface pattern for preventing slips on icy surfaces. *Applied ergonomics, 51*, 9-17.

Yamaguchi, T., Katsurashima, Y., & Hokkirigawa, K. (2017). Effect of rubber block height and orientation on the coefficients of friction against smooth steel surface lubricated with glycerol solution. *Tribology International, 110*, 96-102.

Yamaguchi, T., & Masani, K. (2016). Contribution of center of mass–center of pressure angle tangent to the required coefficient of friction in the sagittal plane during straight walking. *Biotribology, 5*, 16-22.

Yeoh, H. T., Lockhart, T. E., & Wu, X. (2013). Non-fatal occupational falls on the same level. *Ergonomics, 56*(2), 153-165.